AN EXPLORATION OF AMYLOID-β SEEDING IN MOUSE MODELS OF DEMENTIA

SEAN GUY LACOURSIERE
Bachelor of Science, University of Lethbridge, 2016

A thesis submitted
in partial fulfilment of the requirements for the degree of

DOCTOR OF PHILOSOPHY

in

NEUROSCIENCE

Department of Neuroscience
University of Lethbridge
LETHBRIDGE, ALBERTA, CANADA

AN EXPLORATION OF AMYLOID-β SEEDING IN MOUSE MODELS OF DEMENTIA

STUDENT NAME: SEAN GUY LACOURSIERE

Date of Defence: August 31, 2022

Dr. R. J. Sutherland	Professor	Ph.D.
Dr. M.H. Mohajerani	Associate Professor	Ph.D.
Thesis Co-Supervisors		
Dr. A. Iwaniuk	Associate Professor	Ph.D.
Thesis Examination Committee Member		
Dr. M. Tatsuno	Professor	Ph.D.
Thesis Examination Committee Member		
Dr. B. Kolb	Professor	Ph.D.
Internal External Examiner		
Department of Neuroscience		
Faculty of Arts and Science		
Dr. K. Takehara	Associate Professor	Ph.D.
External Examiner		
University of Toronto		
Toronto, Ontario		
Dr. I.Q. Whishaw		
Chair, Thesis Examination Committee	Professor	Ph.D.

DEDICATION

To my family. I could not have done this without you.

ABSTRACT

Alzheimer's disease (AD) is characterized by the prion-like propagation of misfolded proteins that appears dependent on the initial accumulation of amyloid-β (Aβ). But the role of Aβ in cognitive impairment is still unclear. To determine the causal role of Aβ in AD, mouse models expressing pathological features of AD were intracerebrally seeded with Aβ to initiate Aβ deposition and the characteristic pathological process associated with AD. Spatial, object, context, and association memory were tested, along with aspects of sensory-motor ability, at multiple time points. Immunohistochemical and fluorescent microscopy techniques were used to assess the effects of seeding on Aβ plaque deposition, microgliosis, tau hyperphosphorylation and neurotransmitter levels. Thousands of Aβ plaques and microglia were measured throughout the brain using Ilastik, a kind of machine learning software used for high-throughput histological analysis. Seeding increased Aβ plaque deposition and microgliosis throughout the brain after a brief inoculation period. The type of Aβ seed and duration of inoculation altered the specific aggregation features of the Aβ plaque and the pattern of microgliosis but this effect was dependent on the presence of specific knocked-in genes. In the absence of these genes, neither Aβ pathology nor microgliosis developed. Seeding was found to increase the presence of tau hyperphosphorylation in isolated parts of the brain. Yet, no significant correlation between pathology and cognitive ability was found. In summary, large increases in Aβ plaque and microgliosis do not initially cause cognitive impairment. Suggesting other underlying disease processes may be driving cognitive decline in AD.

iv

ACKNOWLEDGEMENTS

TABLE OF CONTENTS

LIST OF TABLES

LIST OF FIGURES

LIST OF FIGURES

LIST OF ABBREVIATIONS

Aβ   Amyloid-β
AD   Alzheimer disease
amg   Amygdala
APP   Amyloid precursor protein
A/P   Anterior/posterior
App$^{-/-}$ App^{NL-G-F} mice; homozygous negative
App$^{+/+}$ App^{NL-G-F} mice; homozygous positive
App$^{+/-}$ App^{NL-G-F} mice; heterozygous
BB   Balance beam
cc   Corpus callosum.
ChAT   Choline acetyltransferase
CA   cornu Ammonis
DAPI   4′,6-diamidino-2-phenylindole
DG   Dentate gyrus
D/V   Dorsal/ventral
Iba1   Ionized calcium binding adaptor molecule 1
IR   Investigation ratio
EC   Entorhinal cortex
F   Artic mutation
FAD   Familial AD
FC   Fear conditioning
G   Beyreuther/Iberian mutation
HPC   Hippocampus
HPT   Hyper phosphorylated tau
Htau   Human tau mouse model
M/L   Medial/lateral
MEC   Medial entorhinal cortex
MSB   Medial septal band
MWT   Morris water task
NeuN   Hexaribonucleotide Binding Protein-3
NDP   Nanozoomer Digital Pathology
NFT   Neurofibrillary tangles
NL   Swedish mutation
NOR   Novel object recognition test
PBS   Phosphate buffered saline
PFA   Paraformaldehyde
ROI   Region of interest
rpAD   rapidly progressing Aβ seed isolated from HPC of patient with AD
RSc   Retrosplenial cortex
slAD   slowly progressing Aβ seed isolated from HPC of patient with AD
SNr   Substantia nigra reticular area
WT   Wildtype
82e1   Aβ N-terminal specific antibody

Chapter 1: General Introduction

The following introduction was adopted from McAllister and colleagues review on intracerebral seeding mechanisms with the relevant literature highlighted (McAllister et al., 2020). Please see the full review for greater details on this phenomenon.

Alzheimer's disease (AD) is a chronic neurodegenerative disorder and the most common cause of dementia. The course of the disease is associated with synaptic loss and brain atrophy, behavioural symptoms including cognitive decline, and – ultimately – death. Histologically, AD is characterized by the aggregation of proteins into insoluble deposits, resulting in two key pathological hallmarks: extracellular amyloid plaques and intracellular neurofibrillary tangles (NFTs). The severity of AD can be staged by the stereotyped progression of these plaques and tangles (Braak & Braak, 1991), the main components of which are the proteins amyloid-beta (Aβ) and tau, respectively. Broadly, cases of AD can be divided into two categories. The first, accounting for about 99% of all cases, is late-onset AD. Age is the major risk factor for developing late-onset AD, though there is also a strong genetic contribution; over 30 disease risk loci have been identified, with *APOE* and *TREM2* being the greatest genetic risk factors (Shi & Holtzman, 2018). The second category is familial AD (FAD), a rare, early-onset form of the disease exhibiting autosomal dominant inheritance. FAD has been linked to mutations in three genes: *APP*, *PSEN1*, and *PSEN2*. All three are critical for the production and processing of Aβ.

Aβ is a peptide that ranges in length, depending on how it is processed from the longer transmembrane amyloid precursor protein (APP) (Penke et al., 2019). The two variants that have garnered the most attention are $A\beta_{1-40}$ (Aβ40) and $A\beta_{1-42}$ (Aβ42), the latter of which is particularly prone to aggregation (Ahmed et al., 2010). However, many other Aβ proteoforms can also be found in the brains of AD patients, including a 43 amino

acid species ($A\beta_{1\text{-}43}$) (Welander et al., 2009), numerous examples of both N-terminal truncations ($A\beta_{x\text{-}40}$/$A\beta_{x\text{-}42}$) and C-terminal truncations ($A\beta_{1\text{-}x}$), as well as many post-translational modifications (e.g., N-terminal pyroglutamation) (Wildburger et al., 2017). APP is part of an evolutionarily ancient protein family. APP, and the $A\beta$ peptide, are expressed in all vertebrate species, with $A\beta$ exhibiting over 95% sequence homology in mammals (Tharp & Sarkar, 2013). While important properties of $A\beta$ differ even among mammalian species the presence of $A\beta$ throughout the vertebrate family suggests that it serves important functions, although its physiological roles are not fully understood. While $A\beta$ has been shown to possess neurotoxic properties (Liu et al., 2015; Lu et al., 2003; Pike et al., 1991; Seilheimer et al., 1997; Sengupta et al., 2016; Yankner et al., 1990), it has also been shown to have beneficial roles, including antimicrobial activity, tumor suppression, blood brain barrier repair, brain injury repair, and regulation of synaptic function (Brothers et al., 2018; Eimer et al., 2018; Kumar et al., 2016; Luna et al., 2013; Penke et al., 2019; Soscia et al., 2010). Whether $A\beta$ adopts supportive or neurotoxic functions depends on numerous factors, such as its concentration and quaternary structure (Liu et al., 2015), as well as properties (e.g., maturity) of the neuron being affected (Yankner et al., 1990).

$A\beta$ Seeding

Accumulation and aggregation of $A\beta$ peptides, a process that can be referred to as β-amyloidosis, has long been recognized as a hallmark of AD (Harper & Lansbury, 1997). The most prominent account of AD etiology, often referred to as the amyloid cascade theory, holds that $A\beta$ accumulation is the primary factor that spurs AD onset and progression (Hardy & Higgins, 1992; Hardy & Selkoe, 2002). Isolation of $A\beta$ from the brains of AD patients has shown that these peptides can exhibit a great deal of heterogeneity, including in terms of amino acid sequence, length, and post-translational

modification (De Strooper, 2010; Wildburger et al., 2017). *In vitro* experiments have further revealed that different varieties of Aβ can differ in their conformation and aggregate at different rates (Hatami et al., 2017; Vandersteen et al., 2012). Yet the factors that initiate and propagate the aggregation of Aβ are still not well understood – especially *in vivo*.

One way to study β-amyloidogenesis *in vivo* is to seed the aggregate-free brains of healthy host animals with exogenous, misfolded Aβ. It can then be observed whether this seeding is sufficient to trigger aggregation of endogenous Aβ and its deposition in the form of plaques. Many such *in vivo* Aβ seeding experiments have been performed, some using non-human primates (Gary et al., 2019; Ridley et al., 2006) or rats (Rosen et al., 2012) as hosts, but mostly using mice. One complication inherent to performing these experiments in mice is that wild type (WT) murine Aβ differs from human Aβ by three amino acids (Otvos Jr et al., 1993) and does not readily aggregate *in vivo* (Xu et al., 2015), even when seeded with misfolded protein (e.g., see (Kane et al., 2000; Meyer-Leuhmann et al., 2006). Fortunately, transgenic mice have been engineered that express either human APP or humanized murine APP (achieved by humanizing the three murine-specific amino acids). The inserted transgene usually bears mutations, identified from patients with FAD, that alter Aβ processing (e.g., the Swedish mutation, which increases total levels of Aβ). Such strains of APP transgenic mice exhibit spontaneous, age-related accumulation and aggregation of Aβ and deposition of amyloid plaques, often accompanied by cognitive decline and, in some cases, neurodegeneration (Jankowsky & Zheng, 2017). This makes them useful models for studying Alzheimer's disease (or, more precisely, cerebral β-amyloidosis, which represents a major component, though not the entirety, of Alzheimer's disease pathology). It is worth noting – given the finding, highlighted above, that WT murine Aβ does not readily aggregate on its own – that WT murine Aβ does co-deposit

3

with human Aβ in APP transgenic mice, forming mixed amyloid fibrils (Mahler et al., 2015). Murine Aβ also accumulates with age in APP transgenic mice, though much less preferentially than human Aβ.

In support of the prion theory, numerous experiments have clearly established that β-amyloidosis can be induced to develop prematurely in APP transgenic mice by intracerebral injection of amyloid-positive (amyloid +) brain tissue extracts (Table 1). These extracts can be derived from aged APP transgenic mice (Bachhuber et al., 2015; Burwinkel et al., 2018; Eisele et al., 2009; Hamaguchi et al., 2012; Heilbronner et al., 2013; Katzmarski et al., 2019; Langer et al., 2011; Mahler et al., 2015; Marzesco et al., 2016; Meyer-Leuhmann et al., 2006; Ruiz-Riquelme et al., 2018; Skachokova et al., 2015; Stöhr et al., 2012; Watts et al., 2011; Ye et al., 2017; Ye, Fritschi, et al., 2015; Ye, Hamaguchi, et al., 2015), from aged squirrel monkeys (Rosen et al., 2016) from AD patients (Di Fede et al., 2018; Duran-Aniotz et al., 2014; Fritschi, Langer, et al., 2014; Gary et al., 2019; Kane et al., 2000; Meyer-Leuhmann et al., 2006; Parhizkar et al., 2019; Rasmussen et al., 2017; Ruiz-Riquelme et al., 2018; L. C. Walker et al., 2002; Watts et al., 2014; Ziegler-Waldkirch et al., 2018), or even from individuals who show Aβ neuropathology but are non-demented or have only mild cognitive impairment (Duran-Aniotz et al., 2013). However, Aβ in cerebrospinal fluid (CSF), collected either from AD patients or APP transgenic mice, does not accelerate or enhance β-amyloidosis, for reasons that have yet to be fully understood (Fritschi, Langer, et al., 2014; Katzmarski et al., 2019; Skachokova et al., 2015). Interestingly, administration of brain extracts from aged individuals without AD to APP transgenic mice can induce Aβ deposition in some cases, though in a much more limited fashion relative to extracts from AD patients or APP transgenic mice (Kane et al., 2000; Meyer-Leuhmann et al., 2006). This supports the observation that some amount of

amyloid deposition is not uncommon at advanced ages even in cognitively normal people (Elobeid et al., 2016; Erten-Lyons et al., 2009; Robinson et al., 2018).

The Aβ seeding effect has most commonly been tested using APP23 transgenic mice as hosts, but experiments have also been conducted using the Tg2576, R1.40, APPPS1, and 5xFAD transgenic strains; all five overexpress human APP bearing the Swedish mutation(Hsiao et al., 1996; Lamb et al., 1997; Sturchler-Pierrat et al., 1997), with the APPPS1 mouse also expressing a human PSEN1 transgene bearing a mutation associated with FAD (Radde et al., 2006), and the 5xFAD mouse expressing four FAD-associated mutations, two of APP and two of PSEN1, in addition to the Swedish mutation (Oakley et al., 2006).

It is not strictly necessary for Aβ seeds to be administered directly to the brain in order to induce β-amyloidosis; peripheral administration by intraperitoneal injection is sufficient, though with a delayed onset compared to direct intracerebral administration, and requiring a much larger amount of amyloid + extract (Eisele et al., 2010, 2014).The efficacy of peripheral administration is reminiscent of prion diseases that can be transmitted through peripheral routes. However, relative to prion diseases, the transmissibility of β-amyloidosis in APP transgenic mice through peripheral administration of Aβ appears to be more limited in scope. An early study found that β-amyloidosis is not induced in APP23 mice by oral, intraocular, intranasal, or intravenous administration of Aβ (Eisele et al., 2009), although, more recently, successful induction of β-amyloidosis through the intravenous route has been reported using APPPS1 mice (Burwinkel et al., 2018).

Unlike the classic prion diseases, protein misfolding and amyloid formation in the periphery does not seem to be involved in the induction of cerebral β-amyloidosis by peripherally-administered Aβ (Eisele et al., 2010); this effect can be induced even in mice

that lack peripheral APP (Eisele et al., 2014). The exact mechanism by which the proteopathic seeds reach the brain and induce β-amyloidosis is not known, but it may involve uptake and transport by monocytes (Eisele et al., 2014). In support of a blood-borne mechanism, the pathology produced by intraperitoneal seeding is primarily CAA, which differs from the parenchymal pathology that is predominant in aged, non-seeded APP23 mice (Eisele et al., 2010), though this finding has been somewhat inconsistent (Eisele et al., 2014). Similarly, intravenous seeding results predominantly in CAA, including thalamic CAA that is not normally observed in APPPS1 mice (Burwinkel et al., 2018).

Seeding experiments in APP transgenic mice have shown that even when amyloid + extracts are administered directly into the brain, there is a considerable incubation period between the seeding event and the appearance of Aβ pathology. The incubation period can vary considerably depending on the host strain. In APP23 mice, the period is somewhere between 1 and 2 months (Meyer-Leuhmann et al., 2006). In contrast, R1.40 mice, which exhibit less APP overexpression, require a longer incubation period, as pathology in this strain develops more slowly following seeding than is observed in APP23 mice, even when the two strains are seeded with extracts from the same transgenic line (Hamaguchi et al., 2012; Meyer-Leuhmann et al., 2006; Ye, Hamaguchi, et al., 2015). The same has also been observed when amyloid + extracts are administered peripherally (Eisele et al., 2014). Conversely, in APPPS1 mice, which express two FAD-associated mutations, the incubation period is reduced to less than 1 month (Meyer-Leuhmann et al., 2006). Furthermore, the presence of mutations in genes other than APP can also affect the onset and rate of Aβ deposition. This has been seen in APPPS1 mice that either lack TREM2, a gene expressed by microglia, or express a neurodegenerative disease-associated loss-of-function mutation in this gene (Parhizkar et al., 2019). These mice exhibit more aggressive

Aβ deposition in response to seeding, relative to APPPS1 mice with WT TREM2, probably resulting from a reduced microglial response to β-amyloidosis and reduced microglial clearance of Aβ.

The findings presented above demonstrate the importance of factors endogenous to the host in shaping the response to seeding. Interestingly, the age at the time of seeding does not appear to be one such factor; mice seeded at 3 or 9 months show similar levels of β-amyloidosis after a 6-month incubation period (Hamaguchi et al., 2012). It should be noted, though, that it cannot be determined from this result whether age becomes an important factor closer to the end of the animal's lifespan.

The location of the intracerebral seeding is another factor that influences the nature of the resulting pathology. This was best demonstrated by Eisele et al. (2009), who injected amyloid + extracts into the hippocampus, parietal cortex, lateral entorhinal cortex, striatum, or olfactory bulb of APP23 mice. In contrast, other studies have used the dorsal hippocampus, or dorsal hippocampus and overlying neocortex, as target regions. Seeding a broader array of regions revealed that Aβ pathology was most pronounced, and included congophilic deposits, when the target was the hippocampus or cortex. These are also the regions that show the earliest endogenous (i.e., non-seed-induced) plaque deposition and develop the most prominent pathology with age in APP23 mice (Sturchler-Pierrat et al., 1997). In contrast, the striatum, which shows only "isolated" endogenous Aβ pathology even at very advanced ages, develops limited and diffuse deposits in response to seeding. Thus, it appears that the eventual pathology that develops in response to seeding of a given brain region depends on the underlying susceptibility of that region to form endogenous plaques. Some aspects of pathology are shared regardless of the location that is targeted for seeding, however, such as development of congophilic Aβ deposits along the pial and

thalamic vasculature (Eisele et al., 2009). This possibly results from the spread of seeds through the perivascular drainage pathway. It is also worth noting that peripheral seeding produces a distinct pattern of pathology, which is more widespread throughout the cortex than the pathology produced by intracerebral injection (Eisele et al., 2014).

While factors endogenous to the host are clearly important, the properties of the seeds, and the parameters of the seeding, are equally critical in shaping the outcome in these experiments. Most commonly, the concentration of Aβ in amyloid + extracts ranges from 1-20 ng/μl, and the volume of extract administered to the host is less than 5 μl, though larger volumes are sometimes used (Eisele et al., 2009; Hamaguchi et al., 2012; Heilbronner et al., 2013; Langer et al., 2011; Meyer-Leuhmann et al., 2006; Stöhr et al., 2012). Unsurprisingly, the concentration of amyloid + extract that is administered has a large effect on the severity of the resulting pathology (Fritschi, Cintron, et al., 2014; Meyer-Leuhmann et al., 2006; Morales et al., 2015; Stöhr et al., 2012; Ye et al., 2017). More interesting is that the resulting pathology also depends on the conformation of the Aβ aggregates used for seeding, which can differ depending on the genetics (and possibly other factors) of the source. Reflecting the great heterogeneity of AD, seeding with extracts from different AD patients can result in pathology that differs in severity and other characteristics (Di Fede et al., 2018; Rasmussen et al., 2017; Watts et al., 2014). This was shown in most detail through a set of experiments wherein APP transgenic mice were seeded with amyloid + extracts from either an FAD patient expressing the Arctic mutation – which occurs within the Aβ sequence of the APP gene, resulting in mutant Aβ – or from an FAD patient expressing the Swedish mutation – which occurs outside the Aβ sequence at the β-secretase cleavage site, increasing the production of WT Aβ (Watts et al., 2014). Mice seeded with the Artic Aβ had a shorter incubation time to the onset of astrocytosis and a lower Aβ40 to

Aβ42 ratio. They also developed CAA in the thalamus with a distinct "furry" morphology and exhibited deposition of Aβ38 around vessels – characteristics that were not observed in the mice seeded with Swedish extracts. Remarkably, these distinct properties were maintained following a second passage, in which brain extracts from the first-generation hosts were injected into a new set of mice. This indicates that it is the conformation of aggregated Aβ, templated by the misfolded Aβ seeds, that confers these differing properties, since the extracts – and therefore the Aβ – used for the second passage were all derived from APP transgenic mice expressing WT Aβ. These findings are reminiscent of the way in which the prion protein can self-replicate multiple different strains, which aggregate in distinct conformations with distinct pathogenic properties (Bessen et al., 1995).

Extracts from both AD patients and aged APP transgenic mice have been shown to contain Aβ monomers, oligomers, and larger multimers (Eisele et al., 2009; Meyer-Leuhmann et al., 2006). This raises the question of whether one form of aggregated Aβ in the extracts is more potent at seeding further aggregation. Following ultracentrifugation of amyloid + extracts, the amyloidogenic potency of the supernatant is about 30% that of the total extract, despite the supernatant possessing less than 0.1% as much Aβ (Langer et al., 2011). The soluble fraction of Aβ in the supernatant is also much more sensitive to degradation by proteinase K. Furthermore, fragmentation of the aggregates in the amyloid + extracts by extended sonication also increases amyloidogenic potential and sensitivity to proteinase K. These findings, and other similar results (Fritschi, Langer, et al., 2014), support the conclusion that small, soluble forms of Aβ are disproportionately potent at seeding β-amyloidosis. Aβ seeds associated with certain intracellular membranes may also be especially potent (Marzesco et al., 2016). Insoluble Aβ, while less potent than oligomeric

Aβ, is clearly also effective at seeding Aβ pathology when injected into the brain, though it is not known to what extent its seeding capacity is dependent on smaller, soluble fragments breaking off from the larger, insoluble fibrils. The high potency of soluble Aβ aggregates is consistent with the observation that the potency of amyloid + brain extracts (i.e., the concentration of extract required to induce amyloidosis, normalized to the total concentration of Aβ in the extract) is maximal when extracts are derived from APP transgenic mice around the age at which Aβ deposition begins (Ye et al., 2017), when the ratio of small, soluble aggregates to large, insoluble plaques should be high. Together, these findings form a pattern that fits with the increasingly well-supported conclusion from the AD literature that it is soluble oligomeric Aβ that is primarily responsible for impairing neuronal function and driving the progression of AD (Forner et al., 2017; Lue et al., 1999; McLean et al., 1999; Mucke & Selkoe, 2012).

To summarize the preceding paragraphs, a key point from the literature on *in vivo* Aβ seeding is that the nature of the pathology that eventually develops is dependent on factors relating to both the host and the seed. Finally, it is worth highlighting these factors can interact in complex ways. This host-agent interaction was first observed in an experiment by Meyer-Luehmann et al. (2006) and further characterized by Heilbronner et al. (2013). In these experiments, amyloid + extracts from APP23 mice were administered to APPPS1 hosts, and vice versa. In all cases, the extracts were taken from aged mice with significant amyloid deposition, and injected into younger, pre-depositing hosts. The resulting plaque deposition tended to reflect the endogenous pathology seen in the mice from which the extracts were sourced. Specifically, hosts injected with APP23-derived extracts exhibited plaques that featured a dense core surrounded by a diffuse, filamentous penumbra, whereas hosts injected with APPPS1-derived extracts developed plaques that

were smaller and more compact. Moreover, the plaques differed in their localization within the hippocampus depending on the source of the extracts. Interestingly, however, the differences in plaque morphology and localization were less pronounced when APPPS1 mice were used as hosts compared to when APP23 mice were hosts. The same pattern was also reflected in terms of plaque composition. In APP23 hosts, the relative levels of Aβ40 and Aβ42 in the plaques differed notably depending on the source of the extract. If the extract was from APP23 mice, whose endogenous plaques are predominantly composed of Aβ40, then the seeded plaques were also composed predominantly of Aβ40. If the extract was from APPPS1 mice, whose endogenous plaques are predominantly composed of Aβ42, then the ratio of Aβ40 to Aβ42 was much closer to 1:1 in the seeded plaques. In contrast, the plaques that developed in APPPS1 hosts were predominantly composed of Aβ42, regardless of the source of the seed material.

This contrasts with many previous Aβ seeding studies conducted using APP transgenic mice, in which congophilic or ThS-positive plaques were present and often accompanied by neuroinflammation and dystrophic neurites (Duran-Aniotz et al., 2014, p.; Eisele et al., 2009; Kane et al., 2000; Langer et al., 2011; Meyer-Leuhmann et al., 2006; Ye, Fritschi, et al., 2015; Ye, Hamaguchi, et al., 2015). It is possible, however, that ThS-positive plaques would emerge following a longer incubation period, as has been described in studies using other transgenic models in which the Aβ seeding effect is less aggressive than in the standard APP23 model (Hamaguchi et al., 2012; Morales et al., 2012).

Fortunately, a recent study by Ruiz-Requelme et al. (2018) has addressed this limitation by conducting Aβ seeding experiments using a knock-in mouse model. In this model (the App^{NL-F} mouse), a humanized APP gene containing the Swedish and Iberian mutations is expressed under the control of the endogenous murine APP promoter, resulting

in elevated levels of Aβ and an increased ratio of Aβ42 to Aβ40, but with normal murine expression of APP (Saito et al., 2014). The results of this study confirmed that Aβ deposition can indeed be induced to occur prematurely by intracerebral seeding in mice that do not overexpress APP. Notably, the parenchymal deposits that emerged in response to seeding were not labeled by thioflavin S (ThS) and were not accompanied by astrogliosis or microgliosis.

It is also worth noting here that intracerebral seeding has been shown to induce β-amyloidosis in primates that do not overexpress APP. This has been observed in at least two species: the marmoset (Ridley et al., 2006) and the mouse lemur (Gary et al., 2019). While both species can spontaneously develop Aβ pathology with age, intracerebral seeding with extracts from AD brains resulted in the formation of Aβ deposits (and, in the case of two mouse lemurs, tau deposits) at an age when such deposits were absent in controls. The deposits formed within 18 months in the mouse lemurs but required an incubation period of at least 3.5 years in the marmosets. Interestingly, as in the non-overexpressing mouse model, the deposits observed in mouse lemurs were not associated with astrogliosis or microgliosis, though significant cerebral atrophy and neuronal loss was noted, despite the sparseness of the Aβ and tau pathology.

One final limitation of the Aβ seeding literature is the lack, to date, of emphasis on brain function or behaviour. Little research has addressed whether accelerating the onset of β-amyloidosis by seeding translates into earlier onset of the functional network abnormalities and cognitive effects that are seen in many AD models (Palop & Mucke, 2016; Webster et al., 2014). Based on the theory that Aβ pathology is the primary driver of AD progression, one might reasonably hypothesize that such symptoms would emerge earlier in APP transgenic mice that have been seeded with misfolded Aβ. However, other

theories of AD etiology – including updated formulations of the amyloid cascade theory (De Strooper, 2010; Mucke & Selkoe, 2012) – have been posited, in which the deposition of Aβ in plaques is not the major cause of AD symptomology (Joseph et al., 2001). Instead, the accumulation of Aβ in insoluble plaques may serve a partially protective function, by reducing the load of neurotoxic soluble Aβ oligomers in the brain. If this is the case, then seeding of Aβ deposition might have little effect on brain function or cognitive behaviour. Either way, examining such outcomes in seeded APP transgenic mice would provide a useful test of these competing theories.

One study that has examined functional outcomes supports the conclusion that Aβ seeding can accelerate the onset of impairments (Ziegler-Waldkirch et al., 2018). Specifically, intracerebral Aβ seeding of 5xFAD mice decreased hippocampal neurogenesis, increased hippocampal cell death, reduced dendritic complexity in dentate granule cells, and – crucially – impaired spatial memory retention in the Morris water task, all at a relatively early age when these effects would not normally be seen in this strain. Housing in an enriched environment reduced the seeded Aβ pathology in the hippocampus, possibly by stimulating the phagocytic activity of microglia, and was protective against the impairments in neurogenesis and memory. Functional outcomes of Aβ seeding have also been examined in mouse lemurs (Gary et al., 2019). Within 6 months of seeding, the mouse lemurs exhibited impairments of learning and memory, as well as abnormalities in neuronal activity that could be detected by electroencephalography (EEG). The fact that these animals exhibited impaired cognition and neurodegeneration accompanied by only sparse Aβ (and, in some cases, tau) deposits provides evidence that the formation of deposits is not the cause of the neurodegeneration and functional impairments. More likely is that amyloid deposition and neurodegeneration are both downstream of a process (or, perhaps,

different processes) triggered by intracerebral seeding. Accumulation of soluble Aβ (or soluble tau) could be one such process.

Seeding with synthetic Aβ

If misfolded Aβ truly acts in a prion-like fashion, then administration of Aβ aggregates should be both necessary and sufficient to induce β-amyloidosis. Importantly, it was observed that the ability to induce β-amyloidosis is eliminated or substantially reduced when proteins in amyloid + extracts are denatured by heat or acid, when Aβ in the extracts is immunodepleted or targeted with Aβ-specific antibodies, or when the host mice are actively or passively immunized against Aβ (Meyer-Luehmann et al., 2006; Katzmarski et al., 2019). β-amyloidosis is also reduced when the extracts are treated with Aggregate Specific Reagent 1 (ASR1), a peptoid that binds aggregated proteins (Duran-Aniotz et al., 2014). This provides strong evidence that Aβ is indeed the active factor that is necessary for stimulating further amyloid deposition. However, it does not rule out the possibility that other cofactors present in the extracts play an important role – that is, the possibility that Aβ is, by itself, insufficient to seed β-amyloidosis.

Experiments in which synthetic Aβ fibrils are administered provide a less controvertible means of testing the sufficiency of Aβ. Early results found that seeding with synthetic Aβ40 or Aβ42 fibrils, or with Aβ oligomers, was insufficient to accelerate β-amyloidosis in APP transgenic mice, suggesting a critical role for cofactors (Meyer-Luehmann et al., 2006). However, more recent reports have overturned this conclusion. Seeding with synthetic Aβ40 peptides, polymerized into amyloid fibrils prior to administration, induces β-amyloidosis in APP transgenic mice, although a high concentration of synthetic Aβ is required to produce a considerable effect (Stöhr et al., 2012). The potency is affected by the method used to polymerize the Aβ into fibrils,

however, so reduced potency relative to endogenously formed Aβ aggregates may not be a necessary property of synthetic Aβ (Stöhr et al., 2014). Moreover, seeding with distinct strains of synthetic Aβ (differing in length or amino acid sequence) has been shown to result in differences in Aβ pathology, in terms of aggregate conformation as well as plaque morphology, distribution, Aβ40 versus Aβ42 composition, and Aβ38 content (Stöhr et al., 2014; Condello et al., 2018). This resembles the way in which Aβ seeds extracted from the brains of different AD patients can exhibit distinct conformations and strain-like properties that are maintained upon inoculation into an APP transgenic host (Watts et al., 2014; Rasmussen et al., 2017; Di Fede et al., 2018). To summarize, recent seeding experiments using synthetic Aβ do not rule out a role for cofactors in β-amyloidosis, but they do demonstrate that seeding with Aβ alone is sufficient to induce Aβ misfolding and aggregation in the living brain, with distinct synthetic strains producing differing pathological outcomes.

Spreading of seeded Aβ pathology

The Aβ pathology that occurs in the brains of AD patients progresses in a characteristic pattern, beginning in the neocortex and then involving, in succession, the hippocampal formation; the striatum, basal forebrain, and diencephalic nuclei; and, finally, the brainstem nuclei and cerebellum (Braak & Braak, 1991; Thal et al., 2002). This observation has led to the suggestion that Aβ pathology spreads anterogradely from affected brain regions into areas that receive synaptic connections from those regions (Thal et al., 2002). One possible mechanism underlying such spreading would be intracellular anterograde transport, in which an Aβ seed is internalized by a neuron, transported along the neuron's axon, and released – synaptically or otherwise – into a novel location, where it could begin templating the misfolding of normal Aβ protein (Aguzzi & Rajendran, 2009;

Nath et al., 2012, Domert et al., 2014). Mechanisms underlying intracellular transport and release of Aβ are discussed further in section 1.5. On the other hand, the temporal evolution of Aβ pathology is not inconsistent with a second possibility, which is that spreading propagates in a manner determined by proximity, rather than synaptic connectivity (Figure 3A). Indeed, a recent meta-analytic study, using observations from three previous studies examining the progression of spontaneous Aβ pathology in APP transgenic mice, concluded that a model based on spatial proximity was better able to account for the spread of pathology than was a model based on connectivity (Mezias & Raj, 2017). Here, the most likely mechanism would be extracellular diffusion of seeds.

A third possibility is that Aβ pathology is not spread by cellular transport or diffusion of existing Aβ seeds, but instead arises *de novo* across different regions. The stereotyped progression of Aβ pathology in AD could conceivably be explained by differences between brain regions in their susceptibility towards developing β-amyloidosis. Regional susceptibility could be influenced by differing rates of Aβ production and clearance. The latter may be particularly important, given that the rate of Aβ clearance is a key determinant of inter-individual variability in the clinical state of AD patients (Iturria-Medina et al., 2014).

Differences in regional susceptibility cannot fully explain, however, why the pathology induced by intracerebral Aβ injection spreads in different patterns depending on the region that is targeted, as is discussed below. Still, the explanation does not necessarily require the inter-regional transmission of prion-like Aβ seeds. Instead, the progression of Aβ pathology from an initial site to synaptically-connected regions could result indirectly via effects of Aβ on neuronal function. For instance, accumulation and aggregation of Aβ in a primary region (occurring naturally or because of intracerebral Aβ administration)

could affect the function of local neurons, causing them to produce and release more Aβ into synaptically-connected secondary regions (Eisele & Duyckaerts, 2016). If enough Aβ was to accumulate in a secondary region, this could trigger *de novo* Aβ aggregation, giving the appearance of spreading between connected regions without the actual transfer of a seed and without prion-like templated misfolding. As an example of a possible underlying mechanism, there is evidence that accumulation of Aβ pathology can trigger decreased α-secretase processing of APP in neurons, ultimately resulting in increased Aβ40 and Aβ42 production and release (Pietri et al., 2013). For another example, neurons near Aβ plaques have been found to exhibit hyperactivity due to impaired synaptic inhibition (Busche et al., 2008), which could quite plausibly increase the Aβ concentration in secondary regions, considering that Aβ release is enhanced by neuronal activity (Cirrito et al., 2005; Yamamoto et al., 2015). Increased Aβ release could then have a feed-forward effect on the local Aβ concentration by acting on pericytes and causing vasoconstriction, potentially reducing Aβ clearance and increasing Aβ production via β-secretase (Sun et al., 2006; Nortley et al., 2019) Given the possibilities outlined here, it is important to keep in mind that the spreading progression of Aβ pathology over time cannot merely be assumed, without additional evidence, to confirm the prion-like spread of Aβ seeds across regions.

Of course, the three mechanisms of spreading described above (i.e., intraneuronal transport and release of prion-like seeds, extracellular diffusion of seeds, and *de novo* aggregation of Aβ across regions without inter-regional transmission of seeds) are not mutually-exclusive (nor exhaustive – e.g., glial cells could be involved in transport); the interesting question may be the extent to which each dominates under different conditions. It should also be noted that even if Aβ pathology spreads preferentially to synaptically-connected regions it does not necessarily follow that the spreading occurs through a

mechanism of intracellular transport and release. It could instead be the case that Aβ spreads extracellularly along fiber tracts, leading to a blended proximity- and connectivity-based pattern of spreading.

One of the primary advantages of the intracerebral seeding method is that the progression of Aβ deposition can be measured from a spatially-restricted location and from a defined point in time – a useful feature for testing hypotheses about spreading. Unfortunately, detailed observations on the spread of Aβ pathology are lacking in many seeding experiments, and there are methodological limitations that pose a challenge for accurately assessing how seeded Aβ pathology spreads. For one, as APP transgenic mice age, they spontaneously develop β-amyloidosis. Thus, at advanced ages, it can be difficult to ascertain what pathology stems from the exogenous seeds and what pathology would have developed independently of seeding. This is particularly problematic since the regions that are almost always targeted for seeding – the hippocampus and/or neocortex – are generally the first areas to develop spontaneous pathology in APP transgenic mice. For another, it is difficult to rule out the possibility that the apparent spread of Aβ pathology results from diffusion of the exogenous seeds, with the delayed development of pathology at areas distal to the injection site reflecting the reduced concentration of exogenous seeds that reach these areas (Eisele et al., 2009). In support of this possibility, Walker et al. (2002) injected India ink into the same site as was used for intracerebral Aβ seeding and found that the areas the ink had dispersed to within 1 week were roughly the same as the areas that developed Aβ deposition following a 5-month incubation period.

Accepting these caveats, seeding experiments have provided some useful information regarding the spread of Aβ pathology. Experiments in which mice were examined across multiple time points clearly show that the extent and severity of pathology

is strongly dependent on the length of the post-seeding incubation period (Walker et al., 2002; Meyer-Luehmann et al., 2006; Eisele et al., 2009; Hamaguchi et al., 2012; Morales et al., 2012; Ye et al., 2015a; Ye et al., 2015b; Ruiz-Riquelme et al., 2018; Katzmarski et al., 2019). With prolonged incubation, Aβ deposits can be found in regions quite distant from the injection site, such as distal regions of the neocortex when the hippocampus is targeted (Morales et al., 2012), or in the thalamus, septum, and distal regions of neocortex when the hippocampus and dorsal neocortex are seeded (Hamaguchi et al., 2012). Moreover, the regional distribution and temporal progression of seeded Aβ pathology differs from the distribution and progression of spontaneous, age dependent Aβ pathology. The fact that the progression of Aβ pathology differs based on where and when the pathology begins confirms that this progression is not due solely to regional differences in the susceptibility towards spontaneously developing β-amyloidosis (though differences in regional susceptibility to β-amyloidosis seem to play a part).

The Aβ seeding literature does provide a few hints that Aβ pathology spreads preferentially to synaptically-connected regions, though the matter is not conclusively settled. Spreading has been described from the entorhinal cortex into the dentate gyrus and from the striatum into overlying neocortex (Eisele et al., 2009), as well as from the hippocampus into the entorhinal cortex and subiculum (Katzmarski et al., 2019). The most detailed characterization of the spread of seeded Aβ pathology was provided by Ye et al. (2015b), who injected amyloid + extracts into the hippocampi of APP transgenic mice (both the R1.40 and APP23 strains) and, following an incubation period, observed preferential deposition in synaptically-connected regions, including the entorhinal cortex, retrosplenial cortex, septum, nucleus accumbens, mammillary bodies, and anterior thalamus. These results provide solid evidence for the connectivity-based spread of Aβ, although they leave

unresolved the question of whether Aβ spreads in an anterograde or retrograde fashion, since the connections between the hippocampus and many of the regions to which pathology spreads are bidirectional.

Mouse models of AD

One of the main methods of inquiry to understand AD is using non-human animal models of disease. These models are genetically modified to express certain pathological markers of AD, such as Aβ, presenilin, and tau. These models are excellent tools to isolate the effects of each type of pathological marker. As genetic techniques are becoming more sophisticated, crossing different strains yields models combining both Aβ and tau pathology, or several types of pathology. However, until a model is available that can express the full range of AD pathology, it is difficult to fully understand the etiology of AD (Gidyk et al., 2015). Additionally, these models, specifically the Aβ models, are developed based on the underlying amyloid hypothesis and are more akin to the familial form of AD, which accounts for ~5% of all AD cases, whereas the sporadic form, one that is not entirely dependent on genetic risk factors, accounts for the remaining cases.

While these models have provided insight into understanding AD, they leave an incomplete or inaccurate picture of how or what AD pathology is causing cognitive impairment. Attempting to determine the true etiology of AD from these models may lead to false conclusions. For example, earlier models promoted the production of APP to induce greater Aβ deposition. The conclusions of these studies suggested that it was the deposition of Aβ causing impairment but in fact was the overproduction of APP (Sasaguri et al., 2022). It would be difficult to argue that overexpression of any protein in the brain would not cause some disruption.

One major limitation to this, and other mouse models of disease, is that the onset of plaque is almost directly correlated with age, and it is therefore not possible to rule out age being a factor in the development of memory loss when plaque saturation occurs. And while the App^{NL-G-F} mice were compared to wild type C57Bl/6J mice in the characterization by Mehla et al. (2019), it is unknown how the knock in genes effect aging and general disuse syndrome (Bortz II, 1984) or how the knock-in genes affects the general development of these mice. As aging is the greatest risk factor for AD, and an irreversible process that leads to a reduction in brain volume and loss of synapses (Breijyeh & Karaman, 2020), to conclude that Aβ deposition is causing the memory impairment found in these mice might be premature. It could simply be the over production of any protein causes impairment or that knocking in the genes alters development of the mice, resulting in greater vulnerability of neurons to any insult.

To address this concern, a recently developed mouse model of AD, the App^{NL-G-F} model, is a single knock-in mouse model with three mutations. These mutations function to increase the development of Aβ 40 and 42 and increases the ratio of Aβ 42 to 40 without over expressing APP. When characterized, it was found that this model began developing Aβ plaque and astrocytosis around six months of age with full saturation around 10 – 12 months (Saito et al., 2014) along with a reduction in cholinergic cells in the medial septum band and a loss of norepinephrine cells in the locus coeruleus. At the onset of the initial pathology, memory impairment was also found (Mehla et al., 2019).

Overview

The main results of this dissertation each have a dedicated chapter in which the specific questions, hypothesis, and justifications for methods used will be provided for the

experiment. At the end of each chapter, the results will be discussed in relation to the current literature. Supplementary data may be supplied at the end of each chapter. In the appendix, detailed methods can be found describing the mouse models used, the Aβ seeds, the intracerebral injection surgery, the cognitive tests used, immunohistochemical protocols and reagents, imaging and stereology methods, and experimental design and statistics used.

Summary of literature

In vivo studies of protein aggregation mechanism use transgenic and knock-in mouse models and intracerebral injections of Aβ seeds (Friesen & Meyer-Leuhmann, 2019). Several mouse models of AD have been seeded with many types of Aβ seeds and multiple locations in the brain, with varying concentrations and volumes of seed (McAllister et al., 2020). Overall, intracerebral administration of exogenous proteins consistently seeds the formation of AD – like pathology in mice and humans. The pathogenic proteins associated with AD, tau, and Aβ, have been shown to have unique effects on pathology formation which is altered by the absence or presence of endogenous protein.

Unknowns and problems

1. Reconsideration of the cause for cognitive deficits in earlier generations of AD mouse models (Sasaguri et al., 2022) suggests that the data from these studies may not accurately model what is occurring in human AD. Few studies assessing protein aggregation following seeding have used the *App* knock-in mouse model – engineered to model AD pathology without the artifacts found in previous models (Mehla et al., 2019; Saito et al., 2014; Sasaguri et al., 2022).

2. Of the studies that used the *App* knock-in model, 30 µL of human Aβ seed was intracerebrally injected in the cerebral hemisphere (Purro et al., 2018; Ruiz-Riquelme et al., 2018). Both studies focused on Aβ pathology but neither study assessed how intracerebral seeding altered cognition, or other disease markers.

3. There is a paucity of literature on seeding Aβ into tau mouse models and the effects of Aβ on tau pathology remain unclear (McAllister et al., 2020).

Theory

Abnormal protein aggregation is the major pathogenic mechanism in AD.

Central question

How does Aβ seeding and its resultant pathology in multiple mouse models alter protein aggregation, AD-like pathology, and learning and memory?

General methods

Two-month-old mice engineered to model specific features of AD pathology were intracerebrally seeded with unique human derived Aβ seeds. Afterwards, the cognitive abilities of the mice were tested. Protein aggregation and related AD pathology were assessed using immunohistochemical and stereological techniques. See Appendix 1 for detailed methods.

Major findings

- Aβ seeding effects are dependent on the presence of knock-in genes in the $App^{NL\text{-}G\text{-}F}$ mice (Chapter 2)

- Aβ plaque deposition and microgliosis following seeding in $App^{NL\text{-}G\text{-}F}$ mice is unique to type of Aβ seed (Chapter 3)

- Seeding human Aβ into Htau mice induces transient tau hyperphosphorylation (Chapter 4).

Summary

The effects of Aβ seeding show that the genetic background of the host is a determining factor in the induction of the types of AD pathology (Meyer-Leuhmann et al., 2006). Seeding human Aβ into the $App^{NL\text{-}G\text{-}F}$ mouse model caused rapid induction of Aβ immunoreactivity throughout the brain. Microgliosis was found to be significantly correlated with Aβ immunoreactivity in synaptically connected regions, suggesting the seeding accelerated *de novo* amyloidosis. The characteristics of Aβ plaque and the activation profile of microglia was unique to each type of seed and was dependent on inoculation time. Despite Aβ immunoreactivity and microgliosis in HPC, cortex and other subcortical regions, and loss of cholinergic cells in the forebrain of the Aβ seeded mice, no significant impairment in cognitive abilities were found. In the Htau mice, Aβ seeding resulted in no Aβ immunoreactivity but hyperphosphorylated tau was found in the EC one- and four-months following seeding but, in the SNr, only one month following seeding with Aβ.

CHAPTER 2

ABSTRACT

Alzheimer's disease (AD) is characterized by the prion-like propagation of amyloid-β (Aβ). However, the role of Aβ in cognitive impairment is still unclear. To determine the causal role of Aβ in AD, we intracerebrally seeded the entorhinal cortex of two-month-old App^{NL-G-F} mouse model with an Aβ peptide derived from patients who died from rapidly progressing AD. When the mice were three months of age or one month following seeding, spatial learning and memory were tested using the Morris water task. Immunohistochemical labeling showed seeding with the Aβ was found accelerate Aβ plaque deposition and microgliosis in the App^{NL-G-F} mice but this was dependent on the presence of the knocked-in genes. However, we found no correlation between pathology and spatial performance. The results of the present study show that the seeding effects in the App^{NL-G-F} knock-in model, and these are dependent on the presence of a humanized App gene. But these pathological changes were not initially causal in memory impairment.

The effect of Aβ seeding is dependent on the presence of knock-in genes in the

App^{NL-G-F} mice.

2.1 Introduction

The following chapter was previously published. See Lacoursiere et al. (2022) for final published version. Alzheimer disease (AD) is the most common form of dementia, affects millions of people and has a high social and monetary cost (Alzheimer's Association, 2019). It is characterized by stereotypical pathological stages of amyloid-β (Aβ) aggregation and neurofibrillary tangle formation that are progressive (Braak & Braak, 1991; Ettcheto et al., 2018) - this protein aggregation is assumed to be central to AD pathogenesis (Friesen & Meyer-Luehmann, 2019; B. B. McAllister et al., 2020). As pathology progresses it is thought that an associated with memory loss, impaired thinking skills, and eventually impairments in all facets of life will occur (de Vugt et al., 2005; Ferri et al., 2004; Matteson et al., 1996). The cause of AD may be a prion-like spread of Aβ resulting in neuroinflammation, plaque deposition, and hyperphosphorylation of tau, ultimately causing synapse loss and brain atrophy (Bloom, 2014; Harper & Lansbury, 1997; Walker et al., 2018).

Intracerebral seeding has become an effective tool to understand the role of protein aggregation in neurodegenerative diseases as it allows the control over the spatial and temporal onset of amyloidosis (Friesen & Meyer-Luehmann, 2019) as seeding Aβ accelerates the deposition of Aβ plaque *in vivo* in a prion-like manner (Olsson et al., 2018; Walker et al., 2016). In which native Aβ species are misfolded following the template and conformational properties of the seeded Aβ (Come et al., 1993; Eisele, 2013). The effects of seeding, are also dependent on the genotype of the host: mice without mutations in *App*

or only possessing murine *App*, do not show this effect, or if they do, the required incubation time increases significantly before effects are seen (Eisele et al., 2009; Friesen & Meyer-Luehmann, 2019; Meyer-Leuhmann et al., 2006).

Much of the intracerebral seeding work has been done using first generation mouse models using synthetic or murine Aβ (McAllister et al., 2020); however, due to the presence of APP artifacts in the first generation mouse models, the conclusions drawn about the correlation between Aβ pathology, the effects of seeding, and the behavioural outcomes are in question (Sasaguri et al., 2017, 2022). Recently, the single knock-in App^{NL-G-F} mouse model was developed (Saito et al., 2014). To develop this second generation, knock in model, the murine Aβ sequence was first humanized and Swedish, Beyreuther/Iberian, and Arctic mutations were inserted. The Swedish (NL) mutation (KM670/671NL) increases the production of APPβ and the C-terminal fragment containing the entire Aβ sequence in neuronal cells (Shin et al., 2010). The Beyreuther/Iberian (F) mutation (I716F) increases the ratio of $Aβ_{42}$ to $Aβ_{40}$ and APP C-terminal fragments but also decreases the APP intracellular domain production; this is thought to be due to a reduction in APP proteolysis by γ-secretase due to the mutation leading to a protein that is poorly processed by γ-secretase (Guardia-Laguarta et al., 2010). The Arctic mutation (G) alters binding properties of various antibodies to Aβ for immunohistochemistry (Saito et al., 2014).

Several studies have characterized the development of pathology, functional connectivity, and behavioural phenotypes of these mice under multiple conditions (Jafari et al., 2018; Latif-Hernandez et al., 2019, 2020; Mehla et al., 2019; Upīte et al., 2020). Of the studies using this for Aβ seeding, both studies found seeding accelerated Aβ deposition but neither tested behaviour of the mice following seeding (Purro et al., 2018; Ruiz-

Riquelme et al., 2018). To address the paucity of behavioural testing immediately following seeding, we seeded human Aβ into the *App^{NL-G-F}* mouse model.

Here we wanted to determine whether seeding Aβ would cause immediate impairment in spatial learning and memory in the single *App* knock in mouse model and to further understand how the presence of mutations influenced the effects of seeding on Aβ deposition but also on the response of microglia. We used young mice to determine if the initial Aβ deposition caused cognitive impairment without any other endogenously generated pathology and cognitive impairment.

First, we predicted that the mice seeded with Aβ would show a reduction in spatial learning and memory; second, it is predicted that the presence and absence of the knocked in mutations would determine the seeding effects and the level of cognitive impairment. Finally, we predicted that the Aβ seeding would increase activated microglia. Overall, we found that the effects of seeding human HPC tissue and Aβ containing tissue was dependent on the presence of the NL G F knock-in genes.

2.2. Methods

Institutional Review Board Statement. The animal study protocol was approved by the Animal Ethics Committee of the University of Lethbridge (protocol code 1810 and date of approval May 28, 2019). All Aβ seeding was done in a Biosafety Level 2+ surgical suite following approved protocols from the University of Lethbridge Biosafety Offices (protocol code BC2019-06, approved May 28, 2021).

Subjects.

Fifty-three single knock-in *App* mice were seeded in this study. Similar number of male and female mice were used (31 males, 22 females) as no difference between sexes was found in previous characterization (Mehla et al., 2019). The mice were caged in standard housing, 2-5 mice per cage, and kept on a 12 h light/dark cycle. The mice were given *ad libitum* food and water. The mice were handled prior to behavioural testing - which was completed at approximately the same time during the light cycle by an experimenter blinded to the conditions.

The mice were created by crossing mice from the RIKEN institute and *C57Bl/6J* mice. The mice were grouped based on genotype and seed. The mice were either homozygous negative ($App^{-/-}$), carrying no mutations; heterozygous ($App^{+/-}$) carrying only one copy of the Swedish, Beyreuther/Iberian, and Arctic mutations; and homozygous positive ($App^{+/+}$) carrying two copies of the knocked-in mutations. The mice were then randomly assigned to be seeded with the control or rpAD seed. See Table 1.1 for final grouping.

Table 1.1 Grouping of genotype and seed used for behavioural testing (and immunohistochemical analysis).

Genotype	Control	rpAD
$App^{-/-}$	15 (3)	15 (3)
$App^{+/-}$	7 (3)	3 (3)
$App^{+/+}$	4 (2)	9 (3)

Genotyping

Punched mouse ear tissue was subjected to DNA extraction and PCR cycling using Millipore-Sigma's RedExtract-N-Amp Tissue PCR kit (XNAT-100RXN). PCR cycler condition: 94℃ for 3min, 94℃ for 30sec 57℃ for 45sec 72℃ for 1min x 35 cycles. Stored at 4℃. Primer sequences were obtained from the Riken Institute: E16WT: 5'- ATC TCg gAA gTg AAg ATg - 3'; E16MT: 5'- ATC TCg gAA gTg AAT CTA - 3'; WT: 5'- TgT AgA TgA gAA CTT AAC - 3'; loxP: 5'- CgT ATA ATg TATgCT ATA CgA Ag - 3'. PCR products were loaded onto agarose gel electrophoresis for visualization, with wild type band at 700bp and mutant band at 400bp.

Aβ Seed.

The Aβ seeds were obtained from human hippocampal tissue (The National Prion Disease Pathology Surveillance Center at Case Western Reserve University Medical School), assessed for purity, and stereotaxically injected. The University Hospitals Institutional Review Board (IRB) approval is for all autopsied ("discarded") human tissues and all samples are anonymized (coded) and handled in compliance with NIH policy to protect privacy. The type of seed was determined by the rate of AD progression. The biochemical analysis for the control tissue showed effectively zero $A\beta(D/N)$ ratio $A\beta_{40}$ or $A\beta_{42}$ but Aβ% according to sedimentation velocity in calibrated sucrose ingredient showed between ~8 – 12% $A\beta_{40}$ and $A\beta_{42}$ for the controls (Cohen et al., 2015). All brain tissue homogenate was buffered with phosphate buffered saline (PBS) at a pH of 7.4 and kept at

-80°C. The seed was 10% w/v. Prior to possession of the tissue, the tissue underwent several selection criteria steps.

1.   Referral to the National Prion Disease Pathology Surveillance Centre to classify any prion disease.

2.   Six or more MMSE points of decline per year.

3.   Absence of autosomal dominant AD patterns

4.   Absence of mutations in human prion protein.

5.   Aβ and tau proteins resembling sporadic Alzheimer's Disease.

6.   No other neuropathological comorbidity.

7.   All results within 85% confidence interval.

Another five inclusion criteria for the classical Alzheimer's Disease tissue were used, they are as follows:

1.   Clear clinical diagnosis of Alzheimer's disease

2.   No autosomal dominant patterns of dementia.

3.   Alzheimer's Disease based on tau and Aβ proteins.

4.   No comorbidity with other neuropathological diseases.

5.   Results within 95% confidence interval.

Stereotaxic intracerebral seeding surgery.

The mice were subcutaneously injected with buprenorphine (Vetergesic; 0.05 mg/kg; concentration = 0.03 mg/ml) 30 min prior to anaesthesia induction (Isoflurane). Oxygen flow rate for induction was between 4-5 L/min and isoflurane was increased in a stepwise manner to a maximum of 5 L/min. Oxygen and anaesthesia flow rate were reduced

to 0.9 L/min and 1.5-3 L/min, respectively for the duration of the surgery. After the head was shaved, the scalp was cleaned with 4% stanhexadine (Omegalab) followed by 70% isopropyl alcohol. Lidocaine (0.1 mL of 0.2%; Rafter8) was subcutaneously injected under the scalp. Bregma was used to find the stereotaxic coordinates for the medial entorhinal cortex (Allen Institute for Brain Science, 2016). The coordinates used for injection were AP: -4.48, ML: 3.00, DV: 3.44 to target the medial entorhinal cortex. A 0.5 mm diameter hole was drilled through the skull to the brain at the coordinates.

The tissue homogenate was vortexed for 30 s before being loaded into the micropipette. Each mouse received 2 µL (1 µL/hemisphere) of the Aβ or control tissue homogenates. Seeding was performed with a Nanoject II (Drummond Scientific Company, PA) set to slowly inject 50.6 nL. Prior to seeding, a test injection was done to ensure proper flow and the micropipette was cleaned with 70% isopropyl. The micropipette was inserted into the brain at the locations described and allowed to rest for 2 min before the first injection, with all following injections 20 seconds apart for a total of 20 injections. The micropipette stayed in place for 2 minutes after the final injection before being removed. A test injection was done again once the micropipette was removed, and the micropipette was cleaned with 70% isopropyl alcohol before the next hemisphere injection. The mice were kept on the same 12 h light/dark cycle throughout recovery.

Perfusions and sectioning

Following the behavioral testing, the mice were overdosed with an intraperitoneal injection of sodium pentobarbital and transcardially perfused with 1X phosphate buffered saline (PBS) and 4% paraformaldehyde (PFA). The brains were fixed for 24 hrs. in 4%

PFA before being transferred to a solution of 30% sucrose solution for at least three days.

The brains were sectioned on a frozen sliding microtome at 40 μm in a 1:6 series and stored

in 1X PBS + 0.02% sodium azide solution until staining. Prior to staining, the brain sections

were mounted on super frost positively charged slides, allowed to dry up right for 30 mins

and stored over night at 4ºC.

Aβ deposition and microglia immunohistochemistry

Slides were rinsed in 4% PFA for four minutes, washed with 1X Tris Buffer Saline

(TBS), and underwent a 70% Formic Acid wash. Slides were rinsed in 1X TBS, TBS-A

(1X TBS+ 0.1% Triton X), and TBS-B (TBS + 0.1% Triton X + 2% bovine serum albumin

(BSA)). The primaries used were: Anti-82E1 (Anti-β-amyloid (N), IBL,10323, mouse)

1:1000 and Anti-Iba1 (Rabbit, 019-19741, Wako) -20C 1:1000, 1ml/slide in TBS-B for 2

days at RT in a dark humid chamber, sealed in plastic wrap on the rotator at 50RPM.

Following primary incubation TBS, TBS-A, and TBS-B washes were repeated.

Secondaries used: Anti-mouse-alexa-488 (IgG (H+ L) goat, Abcam, ab150113) 1:1000 and

anti-rabbit-alexa-594 (IgG (H+L) goat, Invitrogen, A11037) 1:1000 (1ml/slide) in TBS-B

overnight in a dark humid chamber sealed in plastic wrap on the rotator at 50RPM.

Secondary was washed with 1X TBS and cover slipped with Vectashield + DAPI.

Imaging

Full slide imaging was completed on a digital slide scanner (NanoZoomer 2.0-RS,

HAMAMATSU, JAPAN) at 20X magnification. Slide images were exported using

NDP.View 2. Quantification of Aβ plaques and microgliosis was done by pixel and object

classification using iLastik (version 1.3.0-OSX) (Berg et al., 2019) and ImageJ (version 1.51 s). ILastik was trained to segment both plaque and activated microglia separately. Threshold values were between 0.3-0.4, with a size filter minimum of 10 pixels. Sections were processed from ~AP 1.7 to -4.77 and the count for each section was averaged within groups.

Apparatus.

The MWT pool was 1.55 m in diameter with water temperature maintained at 21°C ± 1°C with a white, 12.5 cm submerged target platform and unobstructed distal cues surrounding the edges. A camera fixed to the ceiling connected to a laptop with HVS Image 2100 which was used to track the swim patterns of the mice.

Procedure.

At two months of age, the mice were intracerebrally injected with a human tissue or the rpAD seed. One month following seeding, the mice were tested using the MWT to determine if this seeding resulted in an impairment in spatial learning and memory. The mice were given four, 30 sec trials each day for six days. Starting position for each day was pseudo-randomized based on the cardinal starting locations, with each sequence of starting locations being different each day. On day seven the mice were tested using a no platform probe. Following the testing, tissue was collected to assess the extent of Aβ deposition and microgliosis.

Statistics

Four parameters were measured during MWT training: the proximity of the mouse to the hidden platform, the time to find the platform, the pathlength, and swim speed. Following training, the mice were tested on a no-platform probe trial and the amount of time spent in the target quadrant was compared to the opposing quadrant, and to the average of the two adjacent quadrants. For the pathology analysis, the number and size of Aβ plaque throughout the brain was measured along with the number of microglia cells.

A two-way repeated measures ANOVA with a Dunnett's multiple comparison test was used to determine whether the mice significantly reduced their swim parameters from the first to last day of training and to determine whether the time spent in the target quadrant was influenced by the seed and genotype, using the time in the target quadrant as the dependent variable. Probe test performance was also compared to chance performance (25%) using a single tailed paired sample t-test as we only wanted to know if performance was better than chance.

As the effects of seeding the rpAD seed were unknown it is difficult specifying the effect size of interest. Furthermore, we were testing whether seeding would have an effect or not, and not necessarily the size of the effect. Therefore, the resource equation method was used to determine if the sample size was sufficient. The error degrees of freedom were determined to be 47: six treatment groups subtracted from the total number of experimental units, 53, putting the error degrees of freedom far above the necessary amount to detect a specified effect (Festing et al., 2002). All statistics were done using Prism 9 (mac OS).

2.3. Results

No amyloid or microglia pathology was found in the App$^{-/-}$ mice up to seven months post seeding (Fig 2.6). Seeding either the control or rpAD seed into the *App*$^{+/+}$ mice resulted in significant increase of plaque count [$F(2, 11) = 136.1, p < 0.0001$], plaque size [$F(2, 11) = 150.4, p < 0.0001$] and activated microglia cells [$F(2, 11) = 18.19, p = 0.0003$] compared to both the *App*$^{-/-}$ and *App*$^{+/-}$; both of which showed no Aβ plaque pathology or activated microglia (Fig 2.1 B). The seed was found to have no significant effect on plaque count [$F(1, 11) = 0.303, p = 0.593$], plaque size [$F(1, 11) = 1.64, p = 0.227$], or activated microglia [$F(1, 11) = 0.472, p = 0.507$].

While no difference in plaque count or size was found between the *App*$^{+/+}$ C and rpAD seeded mice the rpAD seeded mice showed a significant correlation between the number of microglia and the number of plaque whereas the *App*$^{+/+}$ C mice did not show a significant correlation (Fig. 2.2). A significant negative correlation was found for the number of activated microglia and the size of the plaque in the *App*$^{+/+}$ C mice, but this correlation was not found in the rpAD mice.
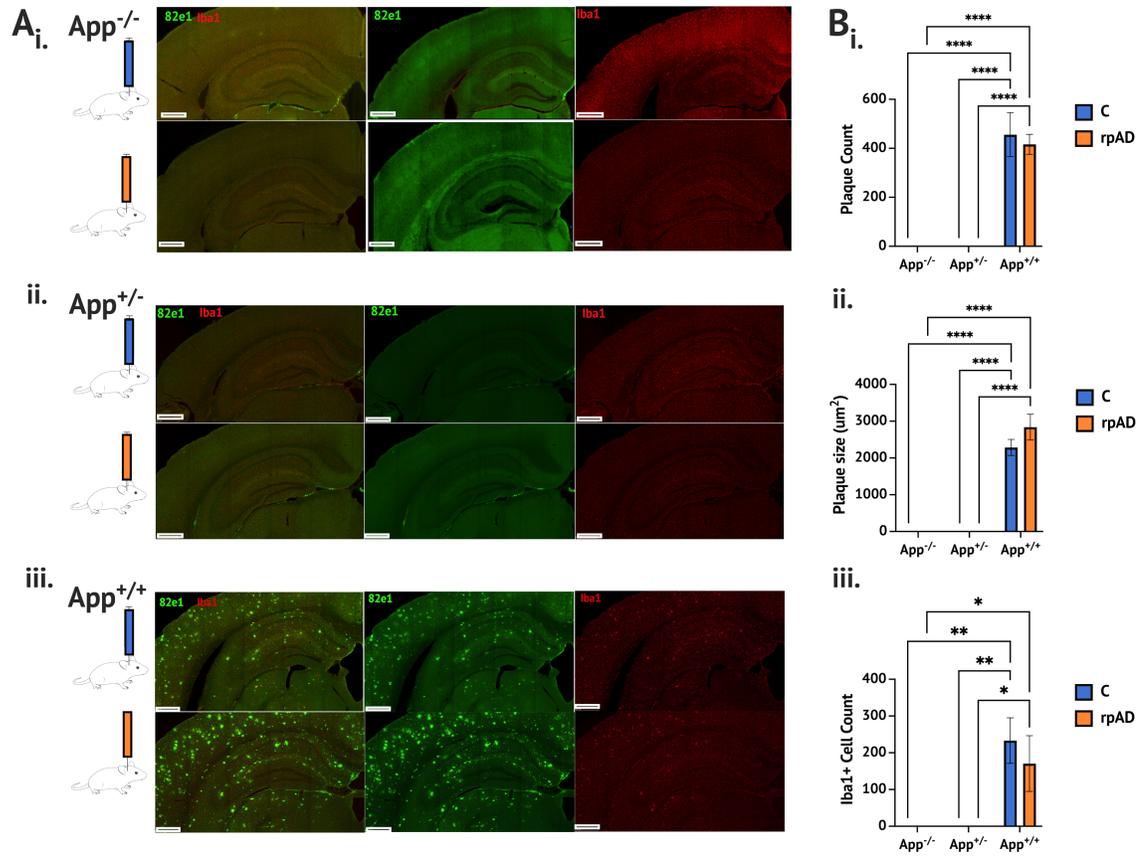
Fig. 2.1 Aβ and microglia pathology analysis one month following seeding. **(A.)** Photomicrographs of representative immunohistochemical staining of Aβ plaque (82e1, green) and microglia (Iba1, red) following seeding of the control HPC tissue (blue) and rpAD seed (orange). **(B).** Quantification of plaque and microglia showing **(i.)** plaque count **(ii.)** plaque size, and **(iii.)**. microglia were significantly increased in the $App^{+/+}$ mice following seeding with the C and rpAD seed. Scale bar = 1 mm.
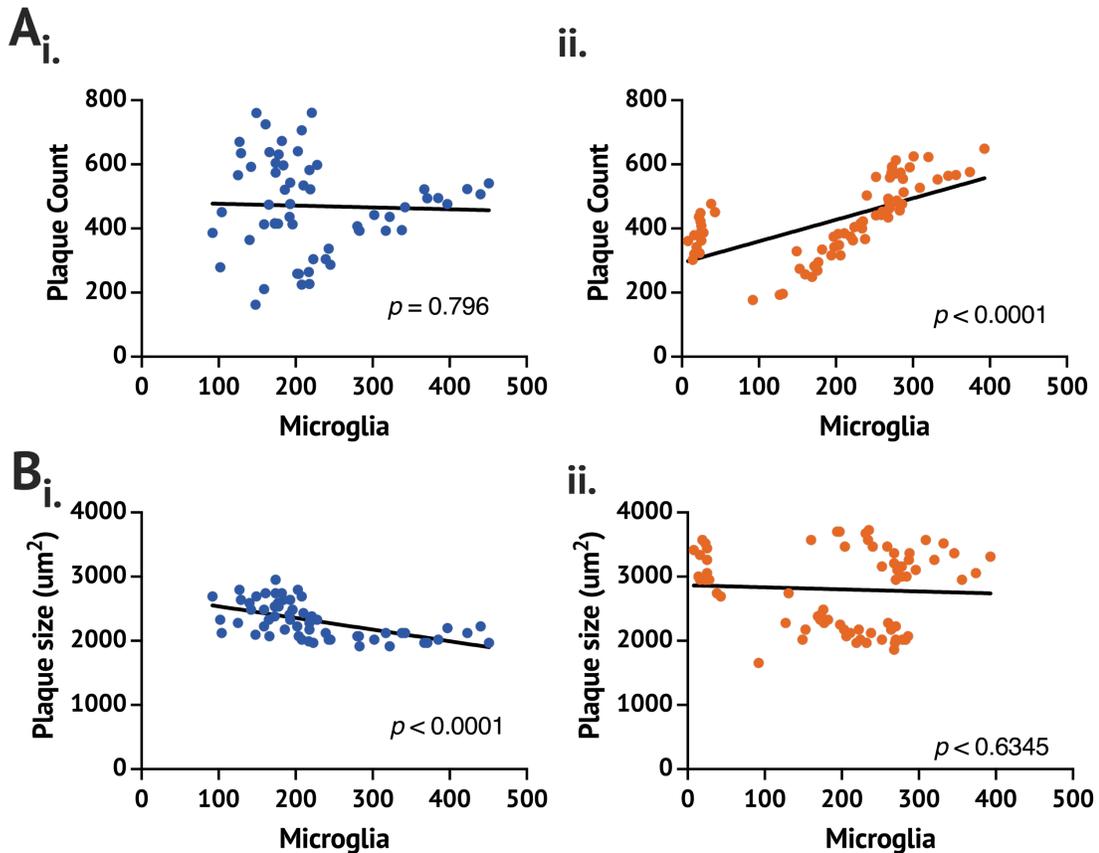
Fig. 2.2. Correlation of plaque and microglia count one month following seeding in the *App^{+/+}* mice seeded with the (**A.**) control (n = 2 brains,) and (**B.**) rpAD seed (n = 3). Correlation is between the mean plaque count (**i.**) or plaque size (**ii.**) and the number of counted microglia on full brain sections sampled from 1:6 sectioning series.

When trained and tested on the MWT, the mice showed a significant reduction in proximity across training [$F_{(5, 235)} = 14.41$, $p < 0.0001$]. While no group differences were found [$F_{(5, 47)} = 0.901$, $p = 0.489$], a significant group x day interaction was found [$F_{(25, 235)} = 1.690$, $p = 0.025$]. The *App^{-/-}* C and *App^{-/-}* rpAD mice showed a significant reduction in proximity between the first and last day of training ($p < 0.01$) and so did the *App^{+/-}* rpAD ($p < 0.05$) and *App^{+/+}* rpAD mice ($p < 0.0001$) – the *App^{+/+}* rpAD seeded mice showed a

significant reduction in proximity after one day of training ($p = 0.01$). The $App^{+/-}$ C mice did not show a significant reduction between the first and last day but did show a significant reduction by the fifth day; the $App^{+/+}$ C mice did not show any significant reduction (Fig 2.3. Ai).

The mice also showed a significant reduction in latency to escape across training [$F(5, 235) = 15.19$, $p < 0.0001$] but no group differences [$F(5, 47) = 1.190$, $p = 0.329$] or group x day interaction [$F(25, 235) = 0.969$, $p = 0.510$] was found. All groups of mice showed significant reduction in latency to escape. The $App^{-/-}$ C, $App^{-/-}$ rpAD, $App^{+/-}$ C, $App^{+/+}$ C, and $App^{+/+}$ rpAD all showed significant reduction in latency to escape by the final day ($p < 0.05$), but the $App^{+/-}$ rpAD only showed significant reduction by the fifth day (Fig 1.3. Aii).

The swim speed was found to increase significantly over training [$F(5, 235) = 20.32$, $p < 0.0001$] and significant differences between groups were found [$F(5, 47) = 3.84$, $p = 0.005$]; no group x day interaction was found [$F(25, 235) = 1.23$, $p = 0.218$]. All groups, except for the App$^{+/-}$ rpAD, and $App^{+/+}$ C, significantly increased their swim from the first to last day of training ($p < 0.05$). The $App^{+/-}$ C and rpAD mice were both found to have an overall significantly faster swim speed than the $App^{+/+}$ rpAD mice ($p < 0.05$; Fig 1.3. Aiii).

The overall pathlength of the mice significantly shortened over training [$F(5, 235) = 3.85$, $p = 0.0023$]; with the pathlength significantly shortening by the fifth day ($p = 0.0006$) but no group individually showed a significant reduction in pathlength (Fig. 3Aiv.). No group differences [$F(5, 47) = 2.31$, $p = 0.059$] or group x day interaction [$F(25, 235) = 1.147$, $p = 0.292$] were found (Fig 2.3.Aiv.).

In the no-platform probe trial within genotype comparisons were used to determine if the mice spent significantly more time in the target quadrant compared to the average of

the two adjacent quadrants and the opposing quadrant (the opposing quadrant was the starting quadrant). Both the $App^{-/-}$ C and rpAD mice spent significantly more time in the target quadrant compared to the non-target quadrants [$F(2, 56) = 10.83$, $p = 0.0001$] but the seed had no effect [$F(1, 28) = 0.0003$, $p = 0.985$]. Neither the $App^{+/-}$ C or rpAD mice spent significantly more time in the target quadrant [$F(2, 16) = 1.98$ $p = 0.170$] but again the seed had no significant effect on performance [$F(1, 8) = 0.556$, $p = 0.477$]. Within the $App^{+/+}$ mice, a significant preference for the target was found [$F(2, 22) = 5.59$, $p = 0.012$] with an overall preference for the target quadrant compared to the opposing ($p = 0.0479$) and adjacent ($p = 0.0150$) quadrants. The $App^{+/+}$ rpAD mice showed significant preference to the target quadrant compared to the adjacent quadrants ($p < 0.05$) but not the opposing quadrant. The $App^{+/+}$ C mice showed no significant preference for the target quadrant (Fig 2.3. Bi).

No effect of sex was found on time in target quadrant [$F(1, 41) = 0.345$, $p = 0.560$]. Despite not all mice showing preference for the target quadrant compared to the non-target quadrants, no significant effect of seed [$F(1, 47) = 0.0141$, $p = 0.906$] or genotype [$F(2, 47) = 0.692$, $p = 0.506$] was found on the time in the target quadrant. When comparing the time spent in the target quadrant to chance performance, the $App^{-/-}$ C [$t(14) = 2.144$, $p = 0.025$], $App^{-/-}$ rpAD [$t(14) = 3.191$, $p = 0.003$], $App^{+/-}$ rpAD [$t(2) = 2.925$, $p = 0.0498$], $App^{+/+}$ C [$t(3) = 2.769$, $p = 0.035$], and $App^{+/+}$ rpAD [$t(8) = 2.732$, $p = 0.0129$] seeded mice spent significantly more time in the target quadrant compared to what would be predicted by chance. The $App^{+/-}$ C mice did not show performance above chance [$t(6) = 1.244$, $p = 0.130$; Fig. 2.3C). Furthermore, when looking at whether the mice crossed the platform location during the probe trial, 83% of the $App^{-/-}$ C mice, 92% of the $App^{-/-}$ rpAD, 83% of the $App^{+/-}$ C, 100% of the $App^{+/-}$ rpAD, 50% of the $App^{+/+}$ C, and 57% of the $App^{+/+}$ rpAD

mice showed at least one platform crossing. The swim pattern also shows that the *App*^{-/-} and *App*^{+/+} paths were much more directed in the target quadrant whereas the *App*^{+/-} mice showed a much more diffuse pattern of swimming, with the path following the edge of the pool.
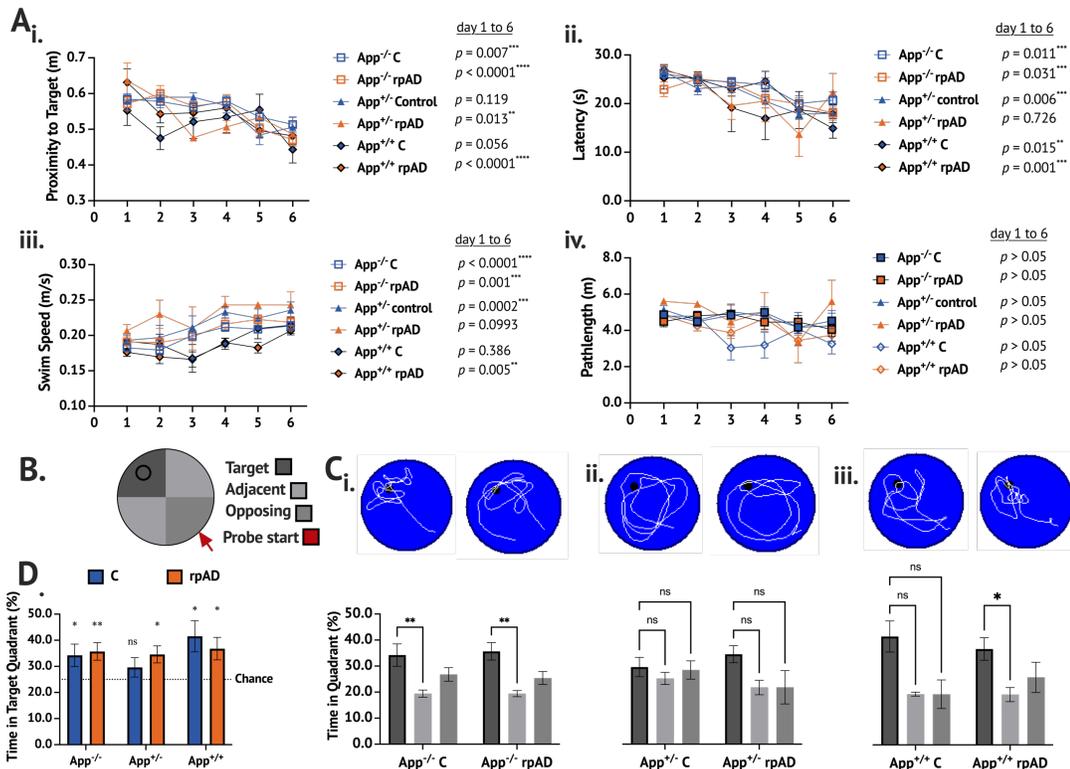
Fig 2.3. MWT performance. (**A.**) Acquisition phase showing (**i.**) proximity to the target, (**ii.**) latency to escape, (**iii.**) swim speed, and (**iv.**) pathlength over the six days of training. (**B.**) representative pool quadrant breakdown and probe start location. (**C.**) Representative swim paths and immediately below, the time in quadrant break down for (**i.**) *App*^{-/-}, (**ii.**) *App*^{+/-}, and (**iii.**) *App*^{+/+} seeded mice. (**D.**) Time in target quadrant compared to chance showed all groups of mice except the *App*^{+/-} C mice performed greater than chance.

41

The results presented show that one month following seeding both human tissue and Aβ protein increased Aβ plaque pathology and this was dependent on the presence of the NL G F mutations on the *App* gene. When tested on the MWT, the mice showed they were able to learn and remember the location of the hidden platform except for the *App*$^{+/-}$ C mice. Despite the most extensive pathology, the *App*$^{+/+}$ mice were able to successfully learn the task. However, the *App*$^{+/+}$ mice showed the smallest proportion of mice showing at least one platform crossing, whereas the *App*$^{+/-}$ mice, showed a relatively high occurrences of the mice crossing the platform at least once.

2.4. Discussion

Here we show that the initial pathology of AD – microglia activation and Aβ plaque deposition – is dependent on the combination of knocked in genes and the seed. Each combination resulted in unique phenotypic expression of behaviour, Aβ deposition, and microglia activation pattern in young *App*$^{NL-G-F}$ mice. One month following intracerebral seeding, prior to when the natural endogenous development of Aβ plaque deposition and microgliosis occurred, we found that Aβ plaque deposition and microgliosis increased in the *App*$^{+/+}$ mice but not in the *App*$^{-/-}$ and *App*$^{+/-}$ mice. The difference in Aβ plaque deposition and microgliosis in these mice in which more copies of the genes either promotes Aβ deposition or perhaps reduces the ability to slow Aβ deposition. Here we provide evidence that suggests this is due to the reduction in the ability to slow Aβ deposition and this is due to the prion-like properties of Aβ and the role microglia play to control their growth.

In the test of spatial learning and memory used, both the $App^{-/-}$ and $App^{+/+}$ mice showed evidence of learning the location of the hidden target. Due to only using 30 second trials, the learning curves were not as strong as those seen using 60 second trials but the performance of the mice by the sixth day of training was similar to tasks using longer trials; however, the increased days of training does result in better probe test performance (Mehla et al., 2019). Suggesting that the task parameters resulted in similar patterns of learning compared to age matched, non – seeded controls but due to the reduced training volume before testing, the no-platform probe trial becomes more difficult. However, no significant difference was found in the time spent in the target quadrant between the different groups in our study despite the $App^{+/-}$ C mice showing no preference for the target quadrant – this may be due to the small sample size, but the swim path suggests these mice did not learn the task. The impairment found in the $App^{+/-}$ C mice is an effect that will have to be further investigated as well as an in-depth characterization of the of the $App^{+/-}$ mice.

The App knock in mice have humanized Aβ, but if one allele was producing murine Aβ, a disruption in the processing and function of Aβ during development may occur, specifically impairing the cerebrovascular system (Luna et al., 2013). This may not be occurring when only murine Aβ is present ($App^{-/-}$) or when only human Aβ is present ($App^{+/+}$). Unfortunately we did not assess cerebrovascular health in these mice but other work has shown that cerebrovascular dysfunction is a risk factor AD (Esiri et al., 1999; Zhai et al., 2016). But understanding how the cerebrovascular system changes in the brain during AD progression is important for understanding AD pathobiology.

One facet of AD that is still not well understood the pathogenetic mechanisms leading to the difference in progression and phenotypic expression of AD (Cohen et al.,

2015; Schellenberg & Montine, 2012). Our results, and others, suggest that two general factors influence the difference in phenotypic expression: the type of Aβ and the underlying genetics. The underlying mechanism leading to these phenotypic differences may be the activation pattern of microglia in the brain.

Here we showed that the relationship of microglia to Aβ plaque pathology was influenced by the type of seed and the presence of the three knock-in genes described. For example, in the $App^{+/+}$ C mice, no significant correlation was found between plaque count and activated microglia but as the number of microglia increased, there was a concomitant decrease in the average size of the plaque. In the $App^{+/+}$ rpAD mice, as the plaque count increased so did the microglia; however, the plaque size did not correlate with the number of activated microglia. Despite the differences in correlation between size of plaque and number of microglia cells, the overall number of microglia was not found to be significantly different between the control and rpAD seeded $App^{+/+}$ mice.

The $App^{-/-}$ mice did not develop plaque or microgliosis up to seven months following seeding – or nine months of age. The $App^{+/-}$ mice did develop plaque four months following seeding but to a significantly lesser degree than the $App^{+/+}$ mice at the same age.

Despite finding that microglia and plaque size and count were significantly related we were not able to directly discern the direction of this relationship. But, from the work of others, the elimination of microglia results in a reduction of Aβ plaque production early in the disease but not in the later portions of the disease (Saucken et al., 2020; Spangenberg et al., 2019). Microglia are thought to internalize neuronally derived Aβ and begin the initial aggregating phase of Aβ before being deposited into the extracellular space (Spangenberg et al., 2019). Suggesting that the activation of microglia may initially be

causing the plaque deposition to protect the brain from the exogenously introduced agent such as bacteria, viruses, such as the currently relevant SARS-COV2 virus, and exogenous Aβ (Dominy et al., 2019; Eimer et al., 2018; Montalvan et al., 2020; Wu et al., 2020); however, Aβ deposition could also occur due to an autoimmune response (Meier-Stephenson et al., 2022). We show that this plaque/microglia response is dependent specifically on the brain environment and the genetics underlying this phenotype as we found no microglia activation in the control or rpAD seeded $App^{-/-}$ mice.

Microglia are known as the resident immune cells of the CNS and are known to interact with plaque to create a barrier. These innate immune cells (Webers et al., 2020) interact with plaque to control growth, development, and plaque morphology (Baik et al., 2016; Bolmont et al., 2008; Casali et al., 2020) and to prevent the toxic effects of Aβ$_{42}$ (Condello et al., 2015a). However, excessive uptake of Aβ can result in microglial death, resulting in the release of accumulated Aβ into the extracellular space and contributing to plaque growth (Baik et al., 2016). The activation of microglia cells with Aβ plaque pathology may explain why the $App^{+/+}$ mice did not show impairment. Microglia may be playing a role in the hyper synchrony and what is thought to be a compensatory mechanism that is found in the early stages of AD (Latif-Hernandez et al., 2019; Shah et al., 2016).

It is not uncommon for a peripheral inflammatory response to have effects on CNS function (Block, 2019). A poor microbiome, which is associated with inflammation, is associated with lower cognitive scores (Fröhlich et al., 2016; Gareau, 2016; Komanduri et al., 2021) can also lead to AD (Lin et al., 2018; N. Shi et al., 2017; Thaiss et al., 2016). One potential mechanism that could explain why a poor microbiome is associated with lower cognitive could be due to disruption in tryptophan metabolism. Tryptophan metabolism is

a key regulator of brain innate immunity (Meier-Stephenson et al., 2022) and a poor microbiota can lead to impaired tryptophan metabolism and serotonin signalling (Dinan & Cryan, 2017; Jenkins et al., 2016).

Further evidence that the etiology may be an immune response arises from fecal microbiota transplant experiments. The microbiota of six-month-old App^{NL-G-F} mice when transplanted into wild type controls resulted in a disease phenotype – this effect was also sex and genotype specific (Kundu et al., 2022). APP/PS1 mice transplanted with healthy fecal microbiota were found to have alleviated AD symptoms, such as a reduction in Aβ production and increased short chain fatty acid butyrate (Sun et al., 2019). Aged microbiota when transplanted was found to accelerate age and drive a pathological phenotype in young mice (Parker et al., 2022).

Lipid metabolism of microglia appears central to the functioning of microglia (Chausse et al., 2021), suggesting that disruption of these processes may impair microglia function and therefore their influence on plaque morphology and the innate immune system. As described above, the microbiota influences the immune system and this appears to be through the maturation, function, and lipid metabolism of microglia in the CNS (Erny et al., 2015). Therefore, an impairment of the gut microbiome may be a central point in which AD begins. Its disruption leads increased inflammation, disrupts microglia function and maturation, and potentially the metabolic processes of microglia – such as the processes related to managing Aβ plaque growth and toxicity (Baik et al., 2016; Bolmont et al., 2008; Condello et al., 2015a).

We do acknowledge the limitations to this study. First, we focused only on spatial navigation learning and memory. In only testing spatial navigation, we are unable to make

conclusions on the effects of seeding, or genotype in different cognitive domains. However, the MWT was originally designed to test the function of the HPC in memory and one of the earliest impairments in AD is found in HPC memory. In future studies additional behavioural tests should be included or a novel home cage-based assessment of rodent's behaviour (Contreras et al., 2022; Singh et al., 2019) may offer insights into phenotypical expression of mouse genotypes and seeding and across time not found in traditional rodent behavioural testing. Furthermore, we did not measure soluble Aβ and instead focused on Aβ plaque load and characteristics throughout the brain and how this was associated with microglia. We therefore cannot make any conclusions on how seeding affected soluble Aβ. Lastly, while the control tissue had no rpAD Aβ, Aβ from the HPC where the tissue was collected could have induced the seeding response, which could explain the lack of difference in Aβ pathology one month following seeding.

Given the recent failures of Aβ targeted therapies to treat AD (Kurkinen, 2021), it is clear the etiology of AD is not understood. The role of the immune system in the etiology of AD has been gaining interest (Jevtic et al., 2017). Recent hypotheses put forth have described that the initial Aβ plaque deposition that ultimately leads to AD occurs as a means to protect the brain from infection (Eimer et al., 2018; Kumar et al., 2016; Moir et al., 2018). While still speculative, our results along with others, suggest that the underlying genetic factors that contribute to AD may be closely related to the innate immune response and specifically the role of microglia. This immune response is determined by genetic and potentially epigenetic predisposition to the development of $A\beta_{42}$ and the ratio of $A\beta_{42}$ and $A\beta_{40}$, but also the type of Aβ present in the brain, whether endogenous (Cohen et al., 2015, 2016) or exogenously introduced. It is well known that both genetic and environmental

factors influence the etiology of AD (McDonald et al., 2010) but specifically, factors involving the immune system may be a novel approach to treat AD and age related cognitive decline. Future studies should focus on microglia metabolism in health and disease and how this is influenced by the microbiome and the immune system.

Chapter 3

ABSTRACT

Alzheimer's disease (AD) is characterized by the prion-like propagation of amyloid-β (Aβ). However, the role of Aβ in cognitive impairment is still unclear. Two-month-old App^{NL-G-F} were intracerebrally seeded with three conformationally distinct Aβ seeds. The mice were trained in a multi-model paradigm using multiple behavioural tests. Immunohistochemical techniques were used to assess Aβ deposition, microgliosis, and cholinergic tone. Seeding accelerated AD pathology throughout the brain in a region dependent manner. Cholinergic tone was found to be significantly reduced in the medial septal band. No impairment in learning and memory was found. Microgliosis was elevated in the substantia nigra reticular area. Here we show that the effects of intracerebral Aβ seeding in the App^{NL-G-F} mice are determined by the properties of the Aβ seed and is unique to each region. No cognitive decline was found. These results suggest that other underlying causal factor for cognitive decline in the initial stages of AD are not Aβ or microgliosis.

Aβ plaque deposition and microgliosis following seeding in *App*^{NL-G-F} mice is

regionally distinct

3.1. Introduction

The amyloid hypothesis of AD is based on the correlation of abnormal Aβ deposition in the central system with dementia (Breijyeh & Karaman, 2020; Hardy & Higgins, 1992). It is clear that Aβ oligomers and plaque can damage synapses and disrupt networks supporting cognitive function (Harper & Lansbury, 1997; Selkoe, 2000). However, abnormal amyloid plaque deposition did not correlate with cognitive decline even though the level of disease pathology was abundant (Jack Jr et al., 2014). This raises the question as to whether Aβ plaque deposition is a causal factor in the initiation of AD related cognitive decline or if other age-related factors are the cause.

To address this question, the aging process and deposition of Aβ plaque need to be separated. As the nucleation phase is the rate limiting step of Aβ plaque deposition, seeding exogenous seeding of Aβ can greatly accelerate the deposition of Aβ (Come et al., 1993; Friesen & Meyer-Luehmann, 2019; McAllister et al., 2020; Meyer-Leuhmann et al., 2006; Rosen et al., 2012). Aβ has several prion-like properties, such as conformation and dose dependent propagation and some evidence demonstrates that misfolded Aβ aggregates propagate different structural motifs in appropriate mouse models which is thought to resemble strain-specific prion transmission (Duran-Aniotz et al., 2021; Meyer-Leuhmann et al., 2006). Meaning that not only will the Aβ deposition be accelerated in the location of seeding but the Aβ deposition should occur throughout the brain. Using this technique, the deposition of Aβ can begin months before it would naturally in mouse models of AD,

allowing the separation of age and Aβ deposition and determining the effects of Aβ on learning and memory and the systems supporting these functions.

To accelerate the deposition of Aβ, the App^{NL-G-F} mice were seeded at two months of age with one of three human HPC derived seeds. The control, the rpAD and an Aβ seed isolated from a patient with slowly progressing AD (slAD) (Cohen et al., 2015). As Aβ pathology is thought to begin in the entorhinal area of this mouse model, the MEC was targeted as the seeding location. As a behavioural control, a non-seeded group of App^{NL-F} mice were tested alongside the seeded mice. The mice underwent cognitive testing at approximately one, three-, and five-months following seeding following a previously used test battery with slight modifications (Mehla et al., 2019). Following cognitive testing, the brains were collected for pathology analysis.

It was hypothesized that accelerating Aβ nucleation in the MEC through Aβ seeding of different strains would result in 1) impairment of memory one month after seeding in the rpAD mice and not until later time points in the in the slAD mice; 2) At one month following seeding the rpAD mice would have significantly greater number of plaques in MEC and HPC regions compared to slAD and control seeded mice; 3) As the control seed had no Aβ we expected no significant increase in the Aβ plaque load in the HPC and MEC; 4) increased microgliosis is expected throughout the brain, clustering around plaques; 5) the number of cholinergic cells in the basal forebrain will be reduced relative the Aβ deposition in the area.

Seeding Aβ accelerated Aβ plaque deposition and caused microgliosis. Furthermore, a reduction in cholinergic cells in the MSB was found in the Aβ seeded mice compared to control seeded mice. Despite the increase in pathology and reduction in

cholinergic cells, no obvious cognitive decline was found in these mice. These results show that increased Aβ deposition, even with a reduction in cholinergic cells did not cause learning and memory impairment.

3.2. Methods

Experimental design. A randomized block design was used to test the factors of incubation time, genotype of mouse, and seed. The mice were grouped into cohorts based on date of birth, genotyped, and then randomly assigned to intracerebral seeding groups. Only homozygous positive App^{NL-G-F} mice were used The sample size was calculated using the Resource Equation (Festing et al., 2002). Alpha = 0.05.

At two months of age, the mice were seeded with a control (n = 14), rpAD (n = 14), or slAD (n = 14) seed. One, three- and five-months following seeding, learning and memory was assessed using the MWT, NOR, BB, and FC. The behavioural testing lasted twenty-three days for each time point and the order of the tests was randomized for each block of mice. FC was always tested last FC. Following the testing, brains were collected immunohistochemical analyses. See Table 3.1. for final grouping.

Table 3.1. Grouping of genotype and seed used for behavioural testing (and immunohistochemical analysis).

	Time post seeding		
Seed	**1**	**3**	**5**
Non-seeded	6 (0)	6 (0)	6 (3)
Control	14 (3)	11 (2)	8 (4)
rpAD	14 (2)	12 (4)	7 (4)
slAD	14 (1)	11 (2)	8 (3)

Subjects. Forty-five *App^{NL-G-F}* mice (19 males/24 females) were used in this study. The

App^{NL-G-F} mice (Saito et al., 2014) and their derivative littermates are a knock-in mouse

model expressing three unique Aβ genes in the *App* gene without overexpressing amyloid

precursor protein were previously characterized (Mehla et al., 2019) and used in this

study. The mice were caged in standard housing, 2-5 mice per cage, and kept on a 12 h

light/dark cycle. All testing was completed during the light cycle and done at

approximately the same time each day by an experimenter blinded to the conditions. Mice

were given *ad libitum* food and water. All animals were handled prior to behavioural

testing.

Aβ Seed. The Aβ seeds were obtained from human hippocampal tissue (The National Prion

Disease Pathology Surveillance Center at Case Western Reserve University Medical

School), assessed for purity, and stereotaxically injected. The University Hospitals

Institutional Review Board (IRB) approval is for all autopsied ("discarded") human tissues

and all samples are anonymized (coded) and handled in compliance with NIH policy to

protect privacy. The type of seed was determined by the rate of AD progression (Cohen et

al., 2015). All brain tissue homogenate was buffered with phosphate buffered saline (PBS)

at a pH of 7.4 and kept at -80ºC. The seed was 10% w/v. Prior to possession of the tissue,

the tissue underwent several selection criteria steps. See Supplementary methods for

inclusion criteria.

Stereotaxic intracerebral seeding surgery. The mice were intracerebrally injected with the

Aβ seeds at two months of age with a Nanoject II (Drummond Scientific Company, PA).

The coordinates used for injection were AP: -4.48, ML: 3.00, DV: 3.44 to target the medial

entorhinal cortex. Bregma was used to find the stereotaxic coordinates for the medial entorhinal cortex (Allen Institute for Brain Science, 2016). A 0.5 mm diameter hole was drilled through the skull to the brain at the coordinates. The tissue homogenate was vortexed for 30 s before being loaded into the micropipette. Each mouse received 2 μL (1 μL/hemisphere) of the Aβ or control tissue homogenates. Prior to seeding, the micropipette was cleaned with 70% isopropyl. The mice were kept on the same 12 h light/dark cycle throughout recovery.

Perfusions and Immunohistochemistry. The mice were overdosed with an intraperitoneal injection of sodium pentobarbital and transcardially perfused with 1X phosphate buffered saline (PBS) and 4% paraformaldehyde (PFA). The brains were fixed for 24 hrs. in 4% PFA before being transferred to a solution of 30% sucrose solution for at least three days. The brains were sectioned on a frozen sliding microtome at 40 μm in a 1:6 series and stored in 1X PBS + 0.02% sodium azide solution until immunohistochemical labelling of Aβ plaque, microglia, and cholinergic cells was completed.

Imaging and pathology analysis. Full slide imaging was completed on a digital slide scanner (NanoZoomer 2.0-RS, HAMAMATSU, JAPAN) at 20X magnification. The size, number, and convexity of pathology was measured using Ilastik (Berg et al., 2019). Convexity is a ratio of the area of the object measured and the area of its convex hull. This ratio represents a measure of how deviated the object is from a circle. Sections were assessed from ~AP 1.7 to -4.77 and the count for each section was averaged within groups. Ten sections of HPC, including dorsal and ventral HPC, three sections of Substantia nigra, medial septal complex, and entorhinal cortex at 240 μm intervals were assessed. Percent area was calculated following methods outlined previously (Schenk et al., 1999). Briefly,

the region of interest (ROI) was outlined using ImageJ and total pixel area was calculated. The percent of the brain region occupied by the labelled pixels was calculated. ChAT+ cells were quantified through the medial septal complex using NeuroInfo Suite.

Procedure.

MWT. Spatial learning and memory was tested by measuring the Gallagher proximity index (Gallagher et al., 1993; Maei et al., 2009; Vorhees & Williams, 2006). As the mouse learns the location of the hidden platform, the average proximity the mouse is to the target reduces. The proximity is independent of swim speed and can account for smaller changes in performance. The swim speed was also measured. The mice were given 8, 30 sec trials each day for 10 days. On the 11th the mice were tested using a no platform probe trial.

NOR. The mice were habituated to an open field (10 min x 3 days). On the fourth day two identical objects were placed in the open field and the mice were allowed to explore for 10 minutes. On the fifth day one object was replaced with a novel object and the mice were allowed to investigate for 5 minutes. The investigation ratio is the total investigation time of the novel object divided by the sum of total investigation time mouse investigates a pair of objects was used to determine if the mouse able to distinguish the novel to familiar object.

Statistics. All statistics were done using Prism (Mac OS Version 9). Sidak's multiple comparison following when appropriate. Two-way ANOVA and mixed effect models were used to analyze behavioural and histology data.

3.3. Results

Aβ and microglia analysis revealed unique regional patterns of pathology.

Characteristics of microglia and Aβ plaque pathology was quantified using Ilastik in the EC, HPC, SNr, RSc, and MSB (Figure 3.1A and B). At one, three-, and five-months post seeding the immunohistochemical staining revealed a unique pattern of expression (Fig 1 C – H). Overall, the percent area covered by 82e1+ [$F(2, 17) = 0.625, p = 0.547$] and Iba1+ [$F(2, 16) = 0.8688, p = 0.438$] immunoreactivity was not significantly different between seeds (Fig 3.1F.). Compared to earlier time points, the later time points showed a significant increase in the percent area covered by 82e1+ immunoreactivity [$F(2, 17) = 4.415, p = 0.0286$] but Iba1+ immunoreactivity [$F(2, 16) = 3.435, p = 0.057$].
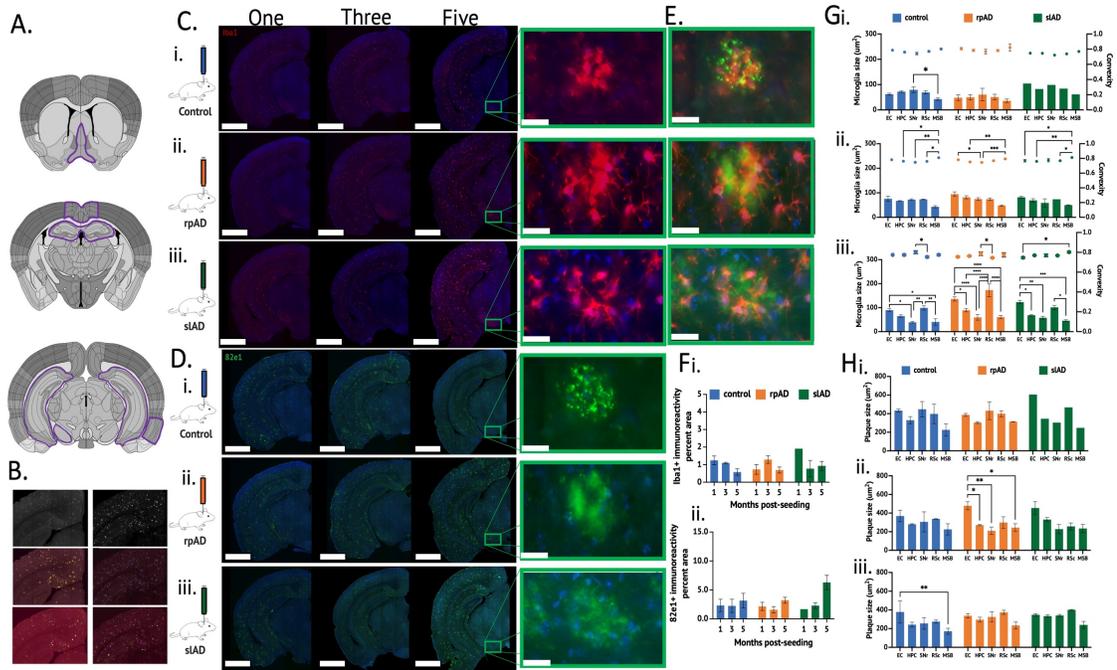
Fig 3.1. Immunohistochemical analysis revealed unique regional patterns of microglia and plaque pathology following seeding. **A.** Schematic representation of the EC, HPC, SNr, RSc, and MSB areas sampled throughout the brain (outlined in purple). **B.** Representation of Ilastik segmentation of pathology. **C.** Photomicrographs of microglia immunohistochemistry (Iba1 in red; DAPI in blue) at one, three-, and five-months post seeding in the (**i.**) control, (**ii.**) rpAD, and (**iii.**) slAD seeded mice. Insert shows magnified microglia pathology sampled from the SNr. **D.** Photomicrographs of Aβ plaque immunohistochemistry (82e1 in green; DAPI in blue) at one, three-, and five-months post seeding in the (**i.**) control, (**ii.**) rpAD, and (**iii.**) slAD seeded mice. **E.** Photomicrographs of merged microglia and plaque pathology of insert in **C.** and **D. F.** Percent area of (**i.**) iba1+ immunoreactivity and (**ii.**) 82e1+ immunoreactivity at each month post seeding. **G.** Quantitative measurements of microglia size (left axis; bar) and convexity (right axis; dot) at (**i.**) one, (**ii.**) three, and (**iii.**) five months post seeding. **H.**

Quantitative measurements of plaque size (**i.**) one, (**ii.**) three, and (**iii.**) five months post seeding. Schematic atlas modified from those provided by (Jin et al., 2022). Scale bar for **C. and D** set to 2.5 mm; insert and merged scale bar = 25 μm. *, $p < 0.05$; **, $p < 0.01$; ***, $p < 0.005$, ****, $p < 0.0001$.

Iba1+ immunoreactivity was found to be significantly different between regions of the brain sampled with immunoreactivity changing over time.One month post seeding the region sampled had a significant effect on Iba1+ immunoreactivity percent area [$F(4, 12) = 7.39$, $p = 0.0030$]. Overall, the SNr had significantly greater immunoreactivity compared to the EC, HPC, and MSB ($p < 0.05$). Three months post seeding, the region had significant effect on Iba1+ immunoreactivity [$F(4, 20) = 21.08$, $p < 0.0001$] and a significant region x seed interaction was found [$F(8, 20) = 2.460$, $p = 0.049$]. Overall, the SNr had significantly greater Iba1+ immunoreactivity compared to the EC, HPC, and MSB ($p < 0.01$). The HPC and RSc also had significantly greater Iba+ immunoreactivity compared to the MSB ($p < 0.05$).

The interaction is due to the control and rpAD seeded mice showing significant differences between regions whereas the slAD seeded mice showed no regional differences. Consistently, the SNr had significantly greater Iba1+ immunoreactivity compared to all other regions in the control and rpAD seeded mice three months following seeding. In the rpAD seeded mice, the RSc, HPC, and SNr had significantly higher percent area covered compared to the MSB. Five months following seeding the effect of the region sampled had a significant effect on Ib1+ immunoreactivity [$F(4, 32) = 4.83$, $p = 0.004$]; Overall, the EC, SNr, and RSc all had significantly greater Iba1+ immunoreactivity compared to the MSB.

Analysis one month following seeding showed that the region sampled had a significant effect on 82e1+ immunoreactivity [$F_{(4, 12)}$ = 8.29, p = 0.002] but the seed did not [$F_{(2, 3)}$ = 0.0561, p = 0.946]. The EC had significantly greater immunoreactivity compared to the HPC, SNr, and MSB (p < 0.05). The RSc was also found to have significantly greater immunoreactivity compared to the MSB. Three months following seeding the region was also found to have a significant effect on 82e1+ immunoreactivity [$F_{(4, 17)}$ = 6.917, p = 0.002; mixed-effects analysis[1]]. The EC had significantly higher immunoreactivity compared to the SNr, and MSB (p < 0.05). Five months post seeding regional 82e1+ immunoreactivity differences were found [$F_{(4, 31)}$ = 17.74, p < 0.0001; mixed effects analysis for missing values]. The EC had significantly greater immunoreactivity compared to the HPC, SNr, and MSB (p < 0.001). The RSc had significantly greater immunoreactivity compared to the HPC, SNr, and MSB (p < 0.0005). The EC, the location targeted for seeding, had the highest overall 82e1+ immunoreactivity compared to all other regions. Consistently the cortical regions, EC and RSc had the highest levels of 82e1+ immunoreactivity – the MSB consistently had the least 82e1+ immunoreactivity.

Reduction in cholinergic tone in MSB following Aβ seeding.

The number of ChAT+ neurons was reduced significantly in Aβ seeded compared to the control tissue seeded mice [$t_{(9)}$ = 3.355, p = 0.0042] and the non-seeded controls (non-seeded controls: 404.0 ± 134.4 cells vs. Aβ seeded: 152.6 ± 46.06; [$t_{(8)}$ = 2.319, p =0.0245]. The number of ChAT+ cells in the MSB was significantly reduced in the Aβ

---

[1] Due to poor staining or damage of tissue, inconsistent sampling occurred for some regions resulting in missing values.

seeded mice compared to control seeded mice (152.6 ± 46.06 vs. 416.8 ± 66.4,

respectively). In the control compared to the Aβ seeded mice, respectively; this represents

a 273% reduction in cholinergic cells, with the Aβ seeded mice having only 36% of

cholinergic cells compared to the control seeded mice (Fig. 3.2C)
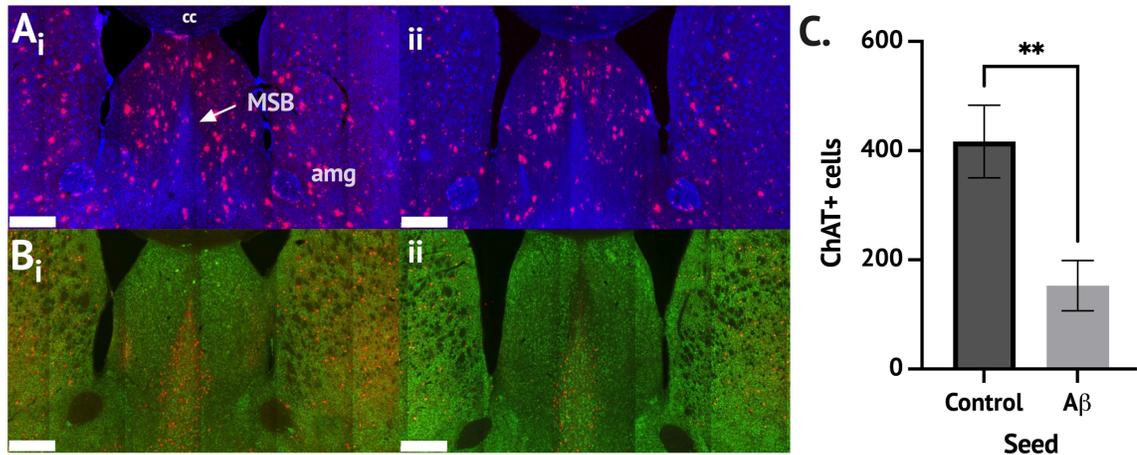
Fig. 3.2. Seeding Aβ caused a significant reduction in ChAT+ cells in the MSB. A.

Aβ deposition (red; counterstained with DAPI, blue) and **B.** ChAT+ cells (red,

counterstained with NeuN, green) in the MSB. Control tissue seeded mice (**i.**) showed

significantly more ChAT+ cells compared to the (**ii.**) Aβ seeded mice five months post

seeding. Abbreviations cc: corpus callosum; amg: amygdala. Scale bars set to 500μm.

*, $p < 0.05$; **, $p < 0.01$; ***, $p < 0.005$, ****, $p < 0.0001$.

Seeding did not impair spatial learning and memory.

The mice significantly reduced their average proximity to the target across training

with no significant differences between groups, showing they were able to learn the

location of target platform (one month (Fig 3Ai): training effect [$F(3, 44) = 0.556$, $p =$

0.647] and no day x group interaction [$F(27, 396) = 0.714$, $p = 0.855$]; three months (Fig

3Aiv): training effect [$F_{(9, 324)} = 17.82$, $p < 0.0001$] between group [$F_{(3, 36)} = 2.03$, $p = 0.128$], day x group interaction [$F_{(27, 324)} = 0.817$, $p = 0.730$]; five months (Fig 3Avii): training effect [$F_{(9, 225)} = 14.3$, $p < 0.0001$], between groups [$F_{(3, 25)} = 0.579$, $p = 0.635$], day x group interaction [$F_{(27, 225)} = 0.293$, $p = 0.999$].

Training caused a significant increase in swim speed, but no group differences were found (one month (Fig 3Aii): training effect [$F_{(9, 396)} = 6.37$, $p < 0.0001$] between group [$F_{(3, 44)} = 1.49$, $p = 0.231$], day x group interaction [$F_{(27, 396)} = 0.714$, $p = 0.855$]; three month (Fig 3Av): training effect [$F_{(9, 279)} = 4.59$, $p < 0.0001$], group differences [$F_{(2, 31)} = 2.92$, $p = 0.069$], day x group interaction [$F_{(18, 279)} = 0.996$, $p = 0.464$]; five months (Fig 3 viii): training effect [$F_{(9, 225)} = 0.93$, $p = 0.496$], group differences [$F_{(3, 25)} = 0.546$, $p = 0.655$] day x group interaction [$F_{(27, 225)} = 0.149$, $p > 0.9999$]). In the probe trial, no significant difference was found between groups at each time point tested.

The mice all had similar swim speeds at each time point (one month (Fig 3Aii): between group [$F_{(3, 44)} = 0.571$, $p = 0.637$]; three months (Fig 3Av): between group [$F_{(3, 36)} = 1.56$, $p = 0.216$]; five months (Fig 3Aviii): between group [$F_{(3, 25)} = 0.254$, $p = 0.858$]). The mice also had similar proximity to the target (data not shown) (one month: between group [$F_{(3, 44)} = 0.207$, $p = 0.891$]; three months: between group [$F_{(3, 36)} = 0.08$, $p = 0.971$]; five months: between group [$F_{(3.00, 19.59)} = 0.497$, $p = 0.689$; Brown-Forsythe ANOVA used due to significantly different standard deviations ($p = 0.011$)].

The mice all spent similar time in the target quadrant (one month (Fig 3 Aiii): between group [$F_{(3, 44)} = 0.178$, $p = 0.911$]; three months (Fig 3Avi): between group [$F_{(3, 36)} = 0.095$, $p = 0.962$]; five months (Fig 3Avi) between group [$F_{(3, 25)} = 0.41$, $p = 0.7495$]).   When comparing the percentage of time spent in the target quadrant compared to chance all groups showed significant preference for the target quadrant. One month: non-

seeded [$t(5) = 5.56$, $p = 0.001$], control [$t(13) = 5.04$, $p = 0.0001$], rpAD [$t(13) = 5.39$, $p <$ 0.0001], and slAD [$t(13) = 5.77$, $p < 0.0001$]. Three months: non-seeded [$t(5) = 3.59$, $p = $ 0.008], control [$t(10) = 5.73$, $p < 0.0001$], rpAD [$t(11) = 3.86$, $p = 0.001$], and slAD [$t(10)$ $= 4.36$, $p = 0.0007$]. Five months: non-seeded [$t(5) = 8.39$, $p = 0.0002$], control [$t(7)=5.81$, $p = 0.0003$], rpAD [$t(6) = 5.20$, $p = 0.001$], and slAD [$t(7) = 7.94$, $p < 0.0001$]

The measures of the MWT were compared across the three time points tested and the seed had no significant effect on proximity [$F(2, 39) = 1.14$, $p = 0.332$], swim speed [$F(2, 39) = 1.74$, $p > 0.05$], or time in target quadrant [$F(2, 90) = 0.088$, $p > 0.05$]. Proximity significantly decreased across time [$F(2, 51) = 8.25$, $p = 0.0008$]. Swim speed significantly increased over time [$F(2, 51) = 7.75$, $p < 0.05$], between one and three months ($p = 0.0006$). Time following seeding had no significant effect on the time spent in the target quadrant [$F(2, 90) = 1.050$, $p > 0.05$].

The mice in this study were able to sufficiently learn the location of target platform at each time point tested. Significant changes in swim speed occurred across training and between testing time points. The seed had no significant effect on spatial memory or swim speed.

NOR revealed unique behaviour towards objects used but discrimination between the novel and familiar object was not impaired.

At one and five months following seeding the mice had a significant preference for the novel object but spent equal time investigating the novel and familiar objects three months following seeding (one month (Fig 2A): novel vs familiar [$F(1, 35) = 40.2$, $p <$ 0.0001]; three month (Fig 2B): [$F(1, 29) = 0.69$, $p = 0.413$]; five month (Fig 2C): novel vs familiar [$F(1, 25) = 57.2$, $p < 0.0001$]). The mice spent equal time investigating the objects during the NOR at each time point tested (one month: [$F(3, 35) = 1.36$, $p = 0.270$]; three

62

months: between groups [$F(3, 29) = 0.742$, $p = 0.536$]; five months: between groups [$F(3, 25) = 0.71$, $p = 0.553$]). The IR for the novel object was similar between groups at each time point (one month: between group [$F(3, 35) = 1.26$, $p = 0.303$]; three months: between groups [$F(3, 29) = 0.124$, $p = 0.945$]; five months: between groups [$F(3, 25) = 0.71$, $p = 0.553$]).
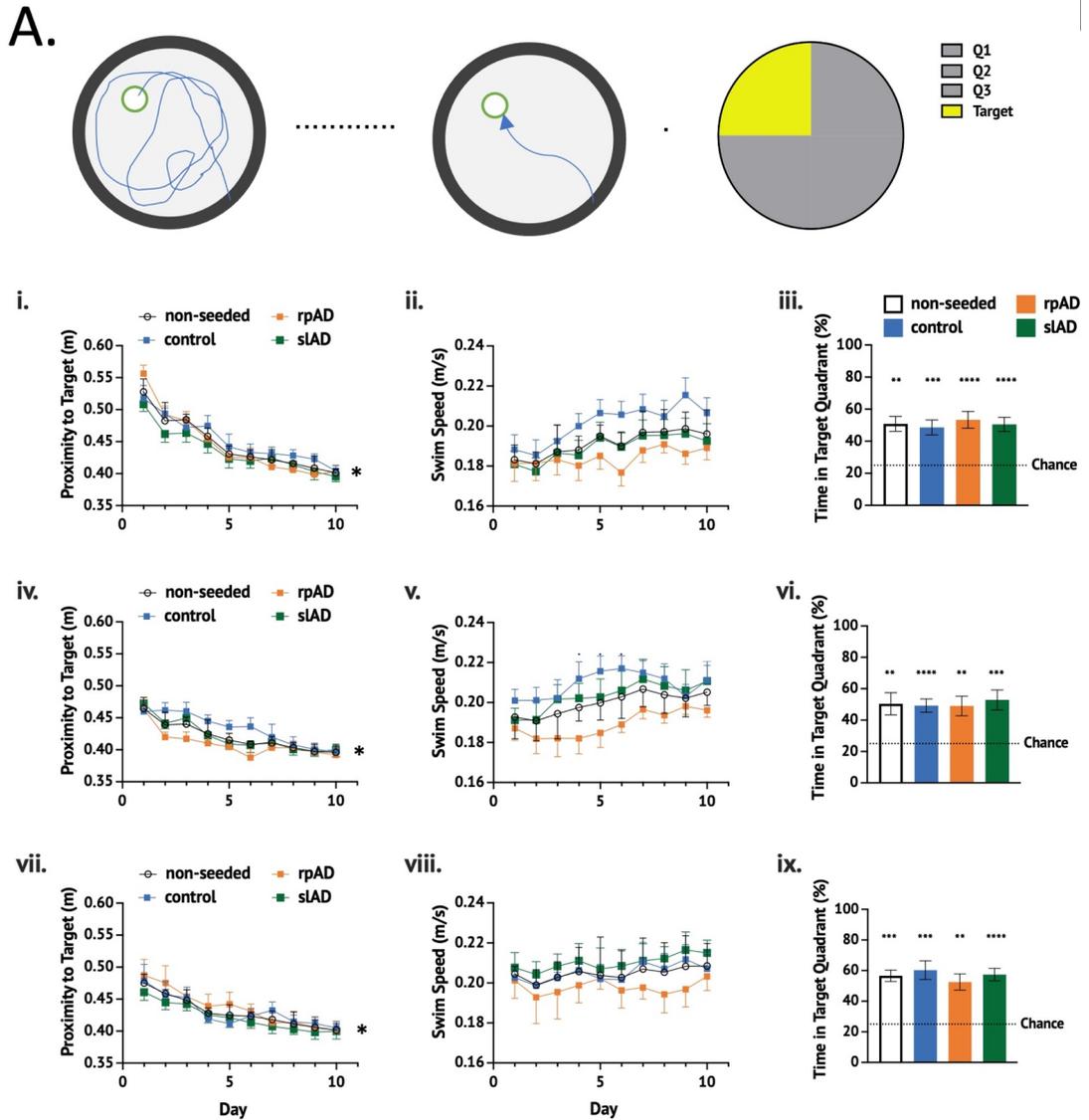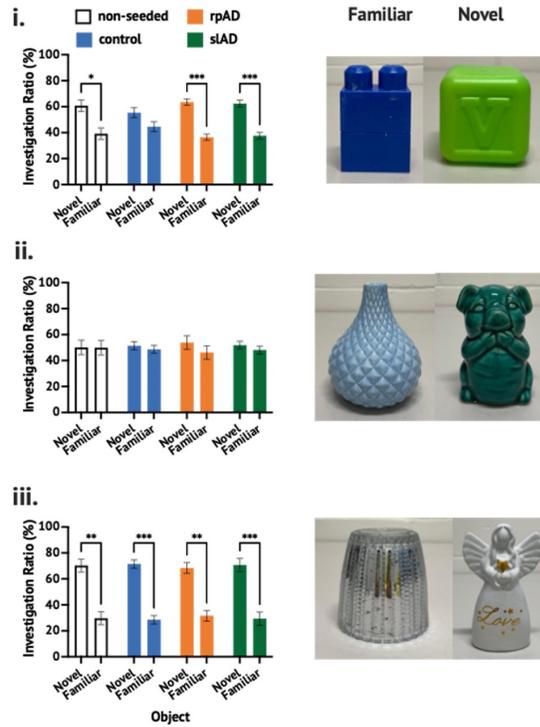
Fig 3.3. Behavioural assessment following seeding showed no obvious deficit in spatial, or object memory. A. Schematic of MWT paradigm and predicted outcome. (**i – iii.**) Proximity to target, swim speed, and time in target quadrant, respectively one month following seeding. (**iv – vi**) Proximity to target, swim speed, and time in target quadrant, respectively three months following seeding. (**vii - ix**) Proximity to target, swim speed, and time in target quadrant, respectively five months following seeding. **B.** Schematic of NOR paradigm. Investigation percent and object pairing (**i.**) one month, (**ii.**) three months, and (**iii.**) five months following seeding. *, $p < 0.05$; **, $p < 0.01$; ***, $p < 0.005$, ****, $p < 0.0001$.

3.4. Discussion

In this study, *App^NL-G-F* mice were intracerebrally seeded with three different seeds isolated from unique forms of disease or health in the human brain to determine what effects Aβ deposition absent of advanced age does to learning and memory. The major finding is that the seeded mice all developed extensive Aβ plaque throughout the brain, from the most posterior sections of deep nuclei to the olfactory bulb only one month following seeding. Previous work has shown plaque as early as four months in the *App^NL-G-F* mouse model with cognitive decline appearing initially at six months despite minimal plaque (Jafari et al., 2018; Mehla et al., 2019). Despite the significant increase in plaque and loss of cholinergic cells in the MSB, no impairment in learning and memory impairment in the seeded mice was found.

It may be that the younger mice used were resistant to Aβ as age is a significant factor in Aβ toxicity (Joseph et al., 2001). Or the inflammation may have not been sustained long enough to induce TNF-α-mediated necroptosis (Salvadores et al., 2022) which would only show up in older mice. Furthermore, due to the mice in this study being young and trained at multiple times throughout their life, this cognitive testing becomes more cognitive training, increasing resiliency to the disease state (Soldan et al., 2017; Stern, 2009).

Aβ and cholinergic tone

Previous reports in rodents have shown that lesion of forebrain cholinergic cells results in cognitive deficits (Bennett et al., 2007) and chronic optogenetic stimulation of these cells prevents cognitive decline in aged *App^NL-G-F* mice (unpublished data). The

cholinergic hypothesis of AD has been central in attempting to understand disease etiology and progression (Craig et al., 2011; Frölich, 2002; Hachisu et al., 2015). Here we found a reduction in cholinergic neurons in the MSB five months following seeding in the Aβ seeded mice yet, these mice showed no significant impairment in cognition. The reduction resulted in the Aβ seeded mice having only 36% of the cholinergic cells in the MSB compared to control seeded mice. In AD, an overall 55% of cortical cholinergic fiber are lost but the loss was dependent on the cortical area, where the loss of cholinergic fibres was greatest in the temporal lobe and temporal association areas (Geula & Mesulam, 1996). As Aβ deposition does not alone appear sufficient to cause learning and memory impairment, it also appears that a reduction in cholinergic cells along with an increase in Aβ plaque deposition, and microgliosis is not sufficient to cause impairment.

Microglia

Like others, we have found a strong correlation between Aβ pathology and microglia activation (Baik et al., 2016; Bisht et al., 2016; Condello et al., 2015b) that cannot be overlooked. However, the role of microglia in plaque removal is still unclear (Garcia-Alloza et al., 2007). It is understood that microglia can limit plaque expansion by phagocytising amyloid fibrils that extend from the plaque core; in doing so, the plaque becomes compact (Casali et al., 2020). Microglia also surround plaque, creating a physical barrier and preventing the accumulation of the toxic soluble Aβ42 (Casali et al., 2020).

As microglia are the resident immune cells of the brain, the immune system is clearly involved in the etiology of AD – how it is involved is still not fully understood. However, AD has been proposed to be an autoimmune disorder in which the adaptive

immune system permits chronic immunological memory (Meier-Stephenson et al., 2022) and therefore the chronic involvement of the immune system in AD.

Aβ aggregation kinetics

The type of seed affected the aggregation kinetics in a region dependent manner. The kinetic signature from Aβ aggregation may be significantly different between specific seeds, such as Aβ as shown here, but could arise from other proteins, and potentially viruses, bacteria, and fungus – all of which cause amyloidosis. Furthermore, the plaque size was not constant, nor did it consistently get larger following the initiation of the aggregation as the average size of plaque fluctuated at each time point.

Due to finding Aβ plaque in the olfactory bulb which is only one connection from the EC (Vanderwolf, 2001) only one month following seeding suggests the seed spread along neural connections (Harris et al., 2010; Pignataro & Middei, 2017). However, the HPC had consistently lower levels of 82e1+ immunoreactivity whereas cortical regions showed higher levels. As much less seed was used compared to previous studies, the proximity or diffusion-based spread should have been reduced. Yet, it cannot be ruled out that *de novo* amyloidosis is occurring (McAllister et al., 2020; Morales et al., 2012).

3.5. Conclusion

The described seeding experiment here had three major findings. 1) The specific seed used was found to alter the aggregation kinetics of amyloid plaque and microglia activation pattern. However, it is not clear as to what specific property of the seed alters the aggregation of Aβ or changes the activation of microglia. Assessing whole brain regions following seeding should be completed to further understand the regional microglia/Aβ

interaction. 2) The Aβ seed of diseased patients was found to significantly reduce cholinergic cells in the MSB; and 3) seeding did not significantly impair learning and memory at the time points tested. Cognitive training artifacts may have prevented decline despite early Aβ deposition and microgliosis.

Chapter 4.

Abstract

The amyloid cascade theory of AD etiology is that Aβ pathology precedes tau pathology in the brain and, moreover, that the accumulation of Aβ acts upstream of tau aggregation, but tau being responsible for most of the neurotoxic effects and disease progression, at least in mouse models. The Htau mouse model expresses six isoforms of human tau but does not express mouse tau was seeded with either the control or the rpAD amyloid seed. The immunohistochemical analysis showed sparse and inconsistent immunoreactivity of hyperphosphorylated tau (HPT) in the HPC and cortex. Some mice showed relatively high levels of HPT was found in the cortex and HPC but nearly entirely absent in others. Seeding with an rpAD Aβ seed can induce acute HPT in the EC, where Aβ was seeded, and SNr, a location indirectly connected. AT8 immunoreactivity was greater in the three-month-old mice compared to the six-month-old mice, suggesting that amyloid increases hyperphosphorylation of tau immediately following but, if the environment is not suitable for Aβ proliferation hyperphosphorylation does not progress.

Seeding human Aβ into mice with humanized tau induces transient tau hyperphosphorylation dependent on Aβ conformation.

4.1. Introduction

A central tenet of the amyloid cascade theory of AD etiology is that Aβ pathology precedes tau pathology in the brain and, moreover, that the accumulation of Aβ precipitates tau pathology (Hardy & Selkoe, 2002; Selkoe & Hardy, 2016). Indeed, tau has been described as the "bullet" to Aβ's "trigger" (Bloom, 2014), with Aβ acting upstream of tau aggregation, but tau being responsible for most of the neurotoxic effects and behavioural deficits associated with disease progression, at least in mouse models (Roberson et al., 2007). The importance of tau for the cytotoxic, dystrophic, and functional effects of Aβ is supported by many *in vitro* and *in vivo* experiments (Bloom, 2014; Chabrier et al., 2014; Jin et al., 2011; Nussbaum et al., 2013; Shipton et al., 2011). Moreover, enhancement of pathological tau accumulation and propagation, as well as neurodegeneration, by the presence of APP mutations that cause Aβ pathology is supported by numerous experiments on double-transgenic mice (Bennett et al., 2017; Héraud et al., 2014; Hurtado et al., 2010; Lewis et al., 2001; Oddo et al., 2003; Pooler et al., 2015; Saul et al., 2013), and augmentation of tau pathology propagation by regional Aβ burden is also supported by computational modeling (Vogel et al., 2019). The presence of Aβ pathology in the human brain also appears to enhance the seeding potential of tau; when tested in an *in vitro* seeding assay, tissue homogenate from human brains with tauopathy but no plaques was less efficacious at seeding tau aggregation than was homogenate from brains with both tauopathy and plaques (Bennett et al., 2017). It should be noted, though, that there is also evidence that the presence of tau pathology can exacerbate Aβ deposition in transgenic

mice (Leroy et al., 2012; Ribé et al., 2005); in this way, Aβ and tau may form a positive feedback loop, versus Aβ acting exclusively upstream of tau.

Following from the amyloid cascade and trigger/bullet theories, a clear prediction is that the seeding of Aβ pathology should induce or enhance the formation of tau pathology, either by a direct "cross-seeding" effect of misfolded Aβ on soluble tau or, perhaps, through an indirect pathway, in which Aβ pathology impairs the function of neurons or alters the regional environment of the brain in some way that promotes tau aggregation. There is no robust effect of Aβ seeding on tau pathology in APP transgenic or knock-in mice. Of the studies that have successfully induced β-amyloidosis by seeding APP transgenic mice with amyloid + brain extracts or synthetic Aβ, only two report the presence of any form of tau pathology. In the first case, seeding the hippocampus and overlying neocortex with amyloid + extracts was found to induce tau hyperphosphorylation in callosal axons around the injection site (Walker et al., 2002). Some degree of hyperphosphorylation was even noted in non-transgenic mice. In the other case, peripheral injection of amyloid + extracts resulted in the detection of neurites containing hyperphosphorylated tau (Eisele et al., 2010). The remaining studies have found no sign of tau pathology (Kane et al., 2000; Morales et al., 2012, 2015; Ruiz-Riquelme et al., 2018) or make no mention of tau pathology.

While there is minimal evidence for the cross-seeding of tau pathology by Aβ in APP transgenic or knock-in mice, intracerebral injections of Aβ have been shown to induce tau pathology in certain tau transgenic strains (Bolmont et al., 2008; Götz et al., 2001). In one of the earliest successful intracerebral seeding experiments, Götz et al. (2001) showed that seeding with synthetic Aβ42 fibrils led to rapid development of tau pathology in transgenic mice expressing human P301L mutant tau. Within 3 weeks, substantial tau

pathology had formed, including silver-stained and ThS-positive NFTs. This pathology further increased in severity up to at least 2-months post-seeding. The burden of pathology was most appreciable in the amygdala, an area distal to, but synaptically connected with, the injection site. Active immunization against Aβ42 was not capable of preventing the induction of tau pathology (Kulic et al., 2006). It has also been demonstrated that intracerebral injection of brain homogenate, collected from aged APP23 mice that exhibit abundant Aβ pathology but no tau pathology, is capable of inducing hyperphosphorylated tau pathology, which spreads to several brain regions within 6 months (Bolmont et al., 2008). These experiments used a different strain of tau P301L transgenic mice that show less aggressive development of endogenous tau pathology relative to the mice used by Götz et al. (2001). The injectate also contained a much lower concentration of Aβ, which did not aggregate around the injection site, unlike in the experiments by Götz et al. (2001) or induce endogenous Aβ aggregation. In contrast to these studies that used mice expressing mutant human tau, seeding with brain extract from aged APP23 mice does not induce tau pathology (or Aβ pathology) in transgenic mice that express WT human tau (Clavaguera et al., 2013).

The experiments described above indicate that intracerebral Aβ seeding can induce tau pathology, but they do not address whether the effect is due to direct cross-seeding or through an indirect pathway. In a cell-free *in vitro* assay, it has been conclusively demonstrated that synthetic Aβ aggregates can cross-seed the formation of tau fibrils (Vasconcellos et al., 2016). These heterotypic tau seeds, formed *in vitro*, can induce tau aggregation when injected into PS19 mice, in much the same way as standard homotypic tau PFFs, though possibly with greater potency. However, this still does not address the question of *in vivo* cross-seeding.

It is not known exactly how Aβ interacts with tau to shift the nature of tau pathology, but the evidence is consistent with a model wherein Aβ plaques disrupt axonal function, causing soluble tau to mislocalize and accumulate in dystrophic axons around the Aβ plaques, where this tau can then be readily seeded into fibrillar NP-like pathology when tau seeds are administered (He et al., 2018). Over time, this axonal tau pathology may serve as a further source of tau seeds that are retrogradely transported to the somatodendritic compartment, exacerbating the formation of NFT- and NT-like pathology.

To expand on the Aβ seeding into tau mouse models, two-month-old Htau mice were intracerebrally injected with human HPC tissue containing an Aβ seed. The mice were allowed to age for either one- or four-months following seeding before their brains were collected for immunohistochemical analysis of Aβ deposition and hyperphosphorylated tau (HPT).

4.2. Methods

Six Htau mice (3 male, 3 female) were seeded with either the control (n = 2) or the rpAD seed (n = 4). The Htau mouse model (B6.Cg-*Mapt^{tm1(EGFP)Klt}* Tg(MAPT)8cPdav/J) expresses six isoforms of human tau, but does not express mouse tau (Andorfer et al., 2003) The Htau mice develop age-associated tau pathology, which is most severe in the neocortex and hippocampus at nine to 15 months. Pathology includes redistribution of tau to cell bodies and dendrites, phosphorylated tau, accumulation of aggregated paired helical filaments, and thioflavin-S-positive neurofibrillary tangles.

Following seeding, the mice were left undisturbed until their brains were collected. The brains were sectioned and stained for Aβ plaque deposition and HPT using AT8.

73

Immunoreactivity of the pathology markers were assessed throughout the septo-hippocampal formation, cortex, and SNr.

4.3. Results

Following seeding, no immediate effects on phenotype were found and all the mice seeded were healthy at the time of death. We predicted that the seeded Aβ would cause an increase in HPT throughout the septo-hippocampal area as the Aβ seed was introduced into the entorhinal cortex (EC) and this would spread throughout the septo-hippocampal area and disrupting function (Guo & Lee, 2014; Harris et al., 2010). Aβ immunoreactivity was not expected following seeding, as both the host and seed need to be compatible for this seeding effect to occur (Meyer-Leuhmann et al., 2006). An increase in HPT was predicted.
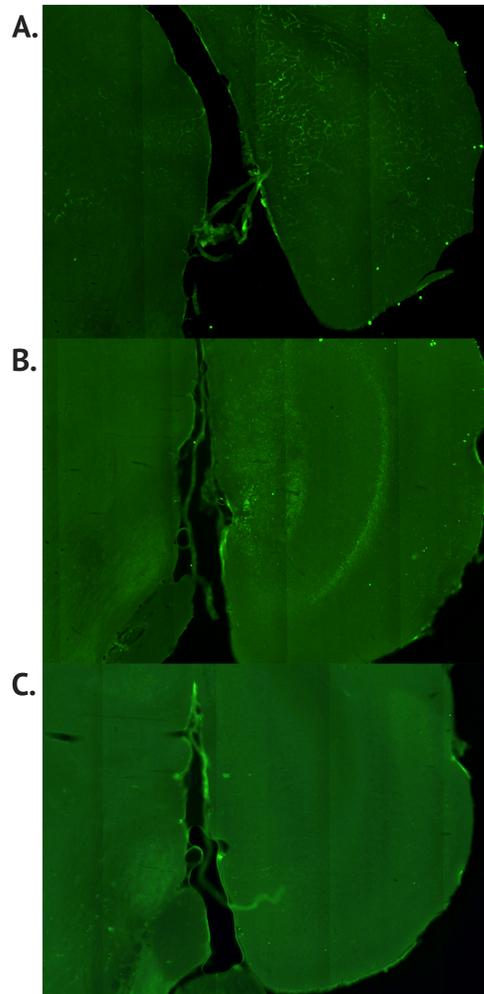
Fig. 4.1. AT8 immunoreactivity following Aβ seeding. AT8 immunoreactivity was found in the EC of both (**A.**) three and (**B.**) six-month-old rpAD seeded mice. AT8 immunoreactivity was never found in the six-month control seeded mice (**C.**).

The immunohistochemical analysis showed sparse immunoreactivity of HPT in the HPC and cortex (Fig 4.1). The immunoreactivity was also inconsistent – in some mice, relatively high levels of HPT was found in the cortex and HPC but nearly entirely absent in others. We found that the AT8 immunoreactivity was greater in the three-month-old mice compared to the six-month-old mice, suggesting that seeding increases hyperphosphorylation of tau immediately following but, if the environment is not suitable

for Aβ proliferation (which is expected in the Htau model as no Aβ pathology is produced naturally), hyperphosphorylation is reduced. Furthermore, these results suggest that hyperphosphorylation of tau can occur without the presence of Aβ plaque but we cannot rule out the effects of soluble Aβ on tau hyperphosphorylation. Due to the lack of Aβ plaque, it is suspected that the injected Aβ remained soluble and it may be the reason increased hyperphosphorylation occurred. In the EC, AT8 immunoreactivity was found at both three and six months in the rpAD seeded mice but it was inconsistent, with only half of the rpAD seeded mice showing AT8 immunoreactivity at both three and six months. However, no AT8 immunoreactivity was found in the control seeded mice at six months.
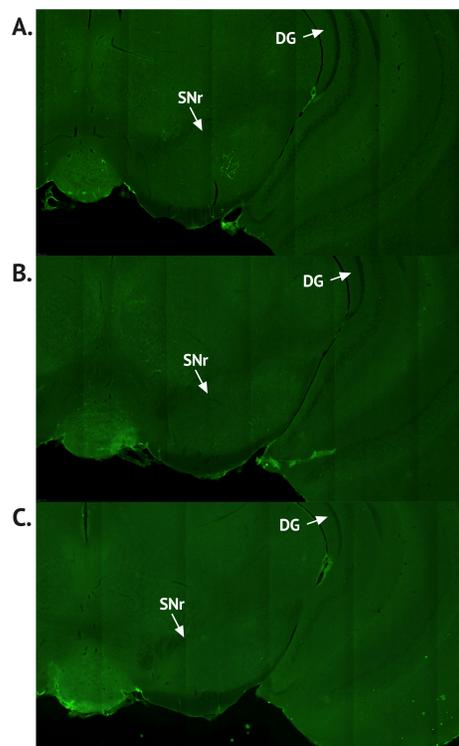
Fig. 4.2. AT8 immunoreactivity was found in the SNr following seeding. (**A.**) One month following seeding with an rpAD seed but not four months following seeding with either the rpAD (**B.**) or control seed (**C.**).

AT8 immunoreactivity was found in the Substantia Nigra reticular area (SNr) in the three-month-old rpAD seeded mice but not found in the six-month rpAD or control seeded mice (Fig 4.2). Previously we have found that increased microglial cell density is found in the SNr compared to other regions, despite no Aβ pathology in the App^{NL-G-F} mice. It was suspected that microglia reside in the SNr or migrate there before obvious plaque deposition occurs. The presence of HPT in the SNr suggests that the SNr may be a vulnerable hub to initial AD pathology.

4.4. Discussion

In this study Htau mice were intracerebrally seeded with a human Aβ seed and allowed the seed to inoculate for one or four months. Immunohistochemical assessment of HPT showed tau expression at the location of injection one at one and four months. Initially the HPT appears to be extracellularly expressed with the AT8 immunoreactivity appearing in the cellular layer at four months. The control seeded mice never showed AT8 immunoreactivity four months following seeding. Interestingly, AT8 immunoreactivity was found in the SNr

Hyperphosphorylation of tau results in the destabilization of tau – tubulin associated unit. Tubulin functions to maintain synapses and its destabilization would disrupt synapses, resulting in long term or permanent reduction in activity in the region of disconnected synapses. It has been previously proposed that the phosphorylation of tau is a mechanism to avoid Aβ mediated toxicity (Ittner Arne et al., 2016). Phosphorylation of tau and its subsequent targeting to subsynaptic sites may regulate NMDA receptor-mediated synaptic

gain in neuronal networks, ultimately reducing activity in the network as phosphorylation of tau (Arendt & Bullmann, 2013).

These studies suggest that Aβ induces increased excitation in neurons and as means to suppress this activity, tau is phosphorylated. While initially this can be beneficial in reducing unwarranted neuronal firing and hyper excitability, prolonged tau phosphorylation would lead to destabilization of networks and the onset of cognitive decline. Under this view, it would suggest that increased HPT in the EC following Aβ seeding was causing the hyperphosphorylation of tau in the SNr, suggesting that SNr disruption could be a node that is disrupted early in the disease process of AD. It is not clear as to whether the Aβ spread from the injection site from the EC towards the SNr through proximal diffusion, or, if the Aβ resulted in local phosphorylated tau which, along with the Aβ seeded, disrupted the EC signalling and its output ultimately resulting in disruption of the SNr and tau hyperphosphorylation.

4.5. Conclusion

Here we show that seeding with an rpAD Aβ seed can induce acute HPT in the EC, where Aβ was seeded, and SNr, a location indirectly connected. However, after four months, the HPT was no longer found in the SNr and was reduced in the EC. This change suggests that tau can be unphosphorylated given that Aβ plaque is not present in the brain.

Chapter 5. General Discussion

AD is characterized by the aggregation of amyloid plaque throughout the brain. Yet a discrepancy exists between individual pathology examinations. Specifically, the extent of aggregation of plaque does not correlate with cognitive decline uniformly. This heterogeneity of disease is of interest. The specific question then is: why does this heterogeneity exist? While AD is a multifaceted disease with both genetic and lifestyle factors influencing the disease (Eisele et al., 2014; Gardener et al., 2015; McDonald, 2002) it has been previously hypothesized that the specific conformational properties of amyloid dictate the severity of the disease itself (Cohen et al., 2015, 2016). The unique conformations of amyloid were predicted to cause a corresponding phenotype of disease - as determined by the rate of and extent of disease spread. Here, using three conformationally distinct amyloid homogenates intracerebrally seeded into the medial entorhinal cortex of the App^{NL-G-F} mouse model three unique pathological states in the brain can be determined through regional plaque aggregation and microglial response. It should be noted that the specific seed did not create significantly different disease states in terms of cognitive decline and extent of pathology as measured through number of sizes of the plaque, the microglia morphology, but time at which regional responses to seed progression was unique to the seed.

These results suggest that the heterogeneity of AD may be in part due to the type of amyloid expression in brain. The question that arises is why are their distinct amyloid conformations in the brain? A theory of AD has been put forth in previous years placing AD as an immune disease (Jevtic et al., 2017; Meier-Stephenson et al., 2022; Webers et al., 2020) due to the striking similarities between the immune response in the brain and the traditional pathologies of AD – the presence of Aβ plaque and hyperphosphorylated tau.

79

Under this new perspective it is not unreasonable to suggest that specific infectious agents may be dictating the conformational properties of amyloid as it is produced in brain. For example, it is known that not only does amyloid seed pathology, but herpes virus (Eimer et al., 2018), bacteria (Dominy et al., 2019; Ryder, 2020), and fungus (Alonso et al., 2014) can all accelerate amyloid deposition and diagnosis of AD. Each of these agents may be in turn creating a unique conformational property of amyloid that results in unique phenotypes of disease much the same that specific infectious agents are known to cause unique adaptive immune responses throughout the body. As the brain is no longer considered an immune privileged region, it is necessary to understand disease pathology as it relates to the immune system and potentially a holistic view of brain diseases. In this view, while removing $A\beta$ later in the course of the disease may prove useful to stop the progression of the disease, preventing $A\beta$ aggregation may increase the damage due to invading pathogens. Removing $A\beta$ for the sake of removing $A\beta$, removing the pathogen causing $A\beta$ deposition may serve as a much more functional means to treat AD (Dominy et al., 2019). $A\beta$ may serve a fundamental role in the innate immune response of the brain (Eimer et al., 2018; Kumar et al., 2016; Moir et al., 2018; Soscia et al., 2010).

The lack of effect of $A\beta$ seeding on learning and memory behaviour is inconsistent with other published work (Ziegler-Waldkirch et al., 2018). The lack of behavioural effect may be largely in part due to the repetitive testing of the mice across age which has been found to drastically reduce pathological and behavioural problems in this mouse model (Mehla et al., 2022), specifically multi model training with physical exercise components e.g. swimming in the MWT. In non-trained mice but who swam in the MWT showed reduced pathology load (Mehla et al., 2022). Behaviours that promote cognitive reserve

80

could be a mechanism to improve resiliency to disease and age related neurodegeneration (Alexander et al., 1997; Premi et al., 2013; Soldan et al., 2017; Stern, 2002, 2009). Cognitive reserve is an explanation for the heterogeneity of AD. If one individual has high pathology burden but no cognitive impairment, whereas another individual had low pathology burden and noticeable cognitive impairment, it would be concluded that the first individual has greater cognitive reserve. The brain of the first individual is said to have higher cognitive reserve. The behaviours that promote cognitive reserve, such as exercise, diet, circadian rhythm and sleep patterns, and education or career attainment, overlap significantly with reducing the risk factors associated with the onset of AD. Here, exercise and what is arguably environmental enrichment through time, were the two risk factors modulated and this may have blunted the seeding's effect on cognitive decline.

Limitations of seeding experiments

Though intracerebral seeding provides many strengths as an experimental model, there are limitations that may affect the extent to which it provides results that accurately reflect the spreading that occurs in AD patients (Vogel et al., 2019). Most notably, there are considerable differences in the genetics, and resulting neural environment, of mice and humans, including genes likely involved in AD (Miller et al., 2010). In addition, the amount of misfolded protein injected in most seeding experiments vastly exceeds the concentration of protein endogenously produced in the human brain. To overcome this, small volume of amyloid homogenate was injected in each hemisphere to better understand the mechanisms and pattern by which AD pathology spreads. Iturria-Medina et al. (2014) developed an epidemic spreading model – in which a signal spreads from an epicenter through a set of interconnected nodes – to simulate the regional spread of AD pathology through the human brain (Iturria-Medina et al., 2014). They then compared the output of this model with real

Aβ deposition patterns, measured by positron emission tomography (PET), in healthy and diseased brains. The model best predicted regional Aβ load (accounting for 46-56% of variance) when connectivity between nodes was defined based on structural connectivity between brain regions, measured by diffusion-weighted magnetic resonance imaging in a separate set of healthy participants. It also identified the anterior and posterior cingulate cortices as the most likely epicenters from which Aβ pathology spreads. More recently, Weickenmeier et al. (2019) developed a physics-based model to simulate the prion-like spreading of misfolded proteins – including Aβ, tau, and α-synuclein – in neurodegenerative disorders. The simulation provided a good approximation of the real spread of pathology (based on post-mortem analysis) when it included parameters reflecting both anisotropic spreading (i.e., connectivity-based axonal transport or spreading along axons) and isotropic diffusion (i.e., extracellular proximity-based spreading) from the initial seed region, with a rate of diffusion favouring anisotropic over isotropic diffusion by a 2:1 ratio. Increasing or decreasing this ratio resulted in patterns of spreading that appeared non-physiological. Together, these models of pathological spread in AD support the same conclusion as do seeding experiments in mice: the spread of Aβ pathology is dictated primarily by neuronal connectivity – though spatial proximity also plays a role.

One particularly relevant limitation to seeding experiments and the prion theory of β-amyloidosis, is that APP transgenic mice eventually develop Aβ pathology spontaneously, even without seeding. One can conclude from these studies that seeding accelerates the development of amyloid pathology, but this differs from prion diseases, in which misfolded prion proteins induce pathology that would be extremely unlikely to emerge spontaneously within the host organism's lifetime. Two relevant studies reviewed by McAllister and colleagues (2020) highlight that seeding amyloid + extracts can

accelerate β-amyloidosis in both rats and mice with humanized APP which do not develop Aβ until very late life. As shown in the current work, when seeded with amyloid + extracts, the App$^{-/-}$ mice did not show Aβ aggregation even at nine months of age. This emphasises the requirement of a proper, compatible seed/host interact to studying amyloid seeding. Caution should also be taken when using transgenic mice with seeding as an incorrect genotype error of the mouse could result in large differences in seeding effect.

limitations to the use of APP transgenic mice (and rats) apply more broadly across preclinical AD research. One such limitation is that these animals provide a better model of FAD – where etiology can be directly linked to a known mutation that is highly predictive of developing the disease – than of late-onset AD, in which the factors that initiate disease onset are complex, multivariate, and often unknown. Yet FAD is a very rare condition relative to late-onset AD, with an earlier onset that clearly reflects differences in etiology between the two forms.

A previous limitation to intracerebral studies was the APP transgenic model's insertion of the APP transgene under a non-endogenous promoter leading to ectopic expression, and often overexpression, of APP. Yet, the overexpression of APP does not occur in AD. APP and its products have numerous physiological effects on brain function, which could be altered by overexpression (Frautschy et al., 1996). APP has been shown to result in abnormal accumulation of APP products other than just Aβ, such as C-terminal fragment β. Accumulation of these products may account for many of the pathological effects, previously erroneously attributed to Aβ and β-amyloidosis, that have been observed in APP transgenic mice (Saito et al., 2014, 2016). In short, effects observed in the brains

of these mice may not translate to brains (murine or human) in which APP is expressed at endogenous levels.

The current study and other recent studies have addressed this limitation by conducting Aβ seeding experiments using knock-in mouse models. In these models, a humanized APP gene containing the Swedish and Iberian mutations (APP^{NL-F} strain), or the Swedish, Arctic, and Iberian mutations (APP^{NL-G-F} strain), is expressed under the control of the endogenous murine APP promoter, resulting in elevated levels of Aβ and an increased ratio of Aβ42 to Aβ40, but with normal murine expression of APP (Saito et al., 2014). The results of these studies confirmed that Aβ deposition can indeed be induced to occur prematurely by intracerebral seeding in mice that do not overexpress APP (Purro et al., 2018; Ruiz-Riquelme et al., 2018; Saito et al., 2019). Ruiz-Requelme et al. (2018) observed that the parenchymal deposits in the brains of *App^{NL-F}* mice that emerged in response to seeding were not labeled by thioflavin S (ThS) and were not accompanied by astrogliosis or microgliosis.

Here, it was found that the plaque in *App^{NL-G-F}* mice seeded with human Aβ were consistently surrounded by microglia cells. Suggesting that the plaque found was not directly resultant of the seeding but the acceleration of *de novo* amyloidosis or β - amyloidosis that is accompanied by microglia - Aβ aggregation made of toxic Aβ. Regardless, Aβ aggregation occurred sooner in the seeded mice compared to age matched controls in other studies. Following the same transmission mechanism of the PrP protein, in which single amino acid changes can impede transmission (Barron et al., 2001), it would be expected that the sequence of amino acids between the human seed used and the

humanized sequence of the APP gene produced in the rodent was more inline (Ruiz-Riquelme et al., 2018).

Future directions

A general shortcoming of the Aβ seeding literature are the lack of *in vivo* seeding studies attempting to experimentally disentangle the contributions of anterograde versus retrograde mechanisms of spreading, or even of intracellular versus extracellular mechanisms. The greater level of experimental control provided by the intracerebral seeding method in animal models would allow to answer these questions. To test whether the spreading of Aβ seeds is dependent on activity-dependent synaptic release, one could microinject the sodium channel blocker tetrodotoxin, or chronically supress neuronal activity using a chemogenetic approach, and observe whether this reduces or eliminates spreading. However, if it did not, this approach would not rule out the possibility of non-activity-dependent mechanisms of intracellular transport and release. A complementary approach, then, would be to block microtubule polymerization by administering a tubulin inhibitor, such as colchicine, which would test whether axonal transport is required for the spreading of Aβ seeds. For such experiments, a host that shows a rapid pathological response to seeding and a strain of Aβ that spreads aggressively would be highly useful to observe how various experimental interventions alter the spread of Aβ seeds on as short a timescale as possible, minimizing the potentially confounding effects of neuronal dysfunction caused by the intervention. Alternatively, a chronic microdialysis approach could be used to detect the spread of seeds into a given region, ideally using seeds that can be easily distinguished from endogenous protein (e.g., human-derived seeds in a mouse expressing only WT murine protein) or identified by a tag (e.g., myc). The results of such experiments would aid in drawing more definitive conclusions about the mechanisms by

which Aβ seeds propagate throughout the brain, ultimately informing understanding of how AD pathology spreads and, perhaps, how best its spread can be prevented.

Another direction of understanding the disease is through the modulation of microglia. The spread of Aβ and its deposition throughout the brain is a critical factor in the progression of AD (Aguzzi & Rajendran, 2009; Domert et al., 2014; McAllister et al., 2020) and stopping the spread of Aβ could be a means to slow or stop the disease. If $Aβ_{1-42}$ oligomers are not degraded or cleared, they will begin to accumulate and transported throughout the brain through connected neural networks (Domert et al., 2014). As Aβ spreads through the brain in a prion-like manner (Aguzzi & Rajendran, 2009; McAllister et al., 2020), microglia would become activated as the highly neurotoxic Aβ oligomers (oAβ) formed at an early disease stage and Aβ fibrils induce pro-inflammatory microglia activation and releasing neurotoxic mediators that contribute to neurodegeneration (Schlachetzki & Hull, 2009). As the inflammation becomes global and chronic as Aβ plaque deposition increases, both neuroinflammation and Aβ plaque become damaging. This damage furthers activation of microglia and increases neuroinflammation (Prokop et al., 2013).

Targeting inflammation early on, or when Aβ is first present could act as a prophylaxis for AD. Minocycline is a tetracycline antibiotic that inhibits microglia activation, reduces the pro-inflammatory phenotype of microglia when challenged with oAβ, enhances phagocytosis of fibril Aβ, and has been found to be neuroprotective in global brain ischemia (El-Shimy et al., 2015, p.; Fan et al., 2007; Ferretti et al., 2012; Malm et al., 2008; Yrjänheikki et al., 1998) Minocycline has also been found to reverse memory impairment caused by $Aβ_{1-42}$ (Garcez et al., 2017). These results suggest minocycline could

be novel strategy for AD treatment by attenuating microglia-induced inflammation while maintaining efficient Aβ clearance (El-Shimy et al., 2015; Norins, 2021) and inhibiting the spread of Aβ. However, more research is necessary to understand whether this is an efficacious treatment but clinical trials in humans do not seem promising as minocycline did not appear to reduce the onset of AD (Howard et al., 2020).

References

Aguzzi, A., & Rajendran, L. (2009). The transcellular spread of cytosolic amyloids, prions, and prionoids. *Neuron*, *64*(6), 783–790.

Ahmed, M., Davis, J., Aucoin, D., Sato, T., Ahuja, S., Aimoto, S., Elliott, J. I., Van Nostrand, W. E., & Smith, S. O. (2010). Structural conversion of neurotoxic amyloid-β1–42 oligomers to fibrils. *Nature Structural & Molecular Biology*, *17*(5), 561–567. https://doi.org/10.1038/nsmb.1799

Alexander, G., Furey, M., Grady, C., & Pietrini, P. (1997). Association of premorbid intellectual function with cerebral metabolism in Alzhiemer's disease: Implications for the cognitive reserve hypothesis. *The American Journal of Psychiatry*, *154*(2), 165.

Alonso, R., Pisa, D., Marina, A., Morato, E., Rábano, A., & Carrasco, L. (2014). Fungal Infection in Patients with Alzheimer's Disease. *Journal of Alzheimer's Disease*, *41*(1), 301–311. https://doi.org/10.3233/JAD-132681

Alzheimer's Association. (2019). 2019 Alzheimer's Disease Facts and Figures. *Alzheimer's & Dementia*, *15*(3), 321–387.

Arendt, T., & Bullmann, T. (2013). Neuronal plasticity in hibernation and the proposed role of the microtubule-associated protein tau as a "master switch" regulating synaptic gain in neuronal networks. *American Journal of Physiology. Regulatory, Integrative and Comparative Physiology*, *305*(5), R478-489. https://doi.org/10.1152/ajpregu.00117.2013

Bachhuber, T., Katzmarski, N., McCarter, J. F., Loreth, D., Tahirovic, S., Kamp, F., Abou-Ajram, C., Nuscher, B., Serrano-Pozo, A., Müller, A., Prinz, M., Steiner, H., Hyman, B. T., Haass, C., & Meyer-Luehmann, M. (2015). Inhibition of

amyloid-β plaque formation by α-synuclein. *Nature Medicine*, *21*(7), 802–807.

https://doi.org/10.1038/nm.3885

Baik, S., Kang, S., Son, S., & Mook-Jung, I. (2016). Microglia contributes to plaque

growth by cell death due to uptake of amyloid β in the brain of Alzheimer's

disease mouse model. *Glia*, *64*(12), 2274–2290.

https://doi.org/10.1002/glia.23074

Barron, R. M., Thomson, V., Jamieson, E., Melton, D. W., Ironside, J., Will, R., &

Manson, J. C. (2001). Changing a single amino acid in the N-terminus of murine

PrP alters TSE incubation time across three species barriers. *The EMBO Journal*,

20(18), 5070–5078. https://doi.org/10.1093/emboj/20.18.5070

Bennett, B. M., Reynolds, J. N., Prusky, G. T., Douglas, R. M., Sutherland, R. J., &

Thatcher, G. R. J. (2007). Cognitive Deficits in Rats after Forebrain Cholinergic

Depletion are Reversed by a Novel NO Mimetic Nitrate Ester.

Neuropsychopharmacology, *32*(3), 505–513.

https://doi.org/10.1038/sj.npp.1301054

Bennett, R., DeVos, S., Dujardin, S., Corjuc, B., Gor, R., Gonzalez, J., Roe, A., Frosch,

M., Pitstick, R., Carlson, G., & Hyman, B. (2017). Enhanced Tau Aggregation in

the Presence of Amyloid β. *The American Journal of Pathology*, *187*(7), 1601–

1612.

Berg, S., Kutra, D., Kroeger, T., Straehle, C., Kausler, B., Haubold, C., Schiegg, M.,

Ales, J., Beier, T., Rudy, M., Eren, K., Cervantes, J., Xu, B., Beuttenmueller, F.,

Wolny, A., Zhang, C., Koethe, U., Hamprecht, F., & Kreshuk, A. (2019). ilastik:

Interactive machine learning for (bio)image analysis. *Nature Methods*.

Bessen, R. A., Kocisko, D. A., Raymond, G. J., Nandan, S., Lansbury, P. T., & Caughey, B. (1995). Non-genetic propagation of strain-specific properties of scrapie prion protein. *Nature*, *375*(6533), 698–700. https://doi.org/10.1038/375698a0

Bisht, K., Hajj, H., Savage, J., Sánchez, M., & Tremblay, M. (2016). Correlative Light and Electron Microscopy to Study Microglial Interactions with β-Amyloid Plaques. *Journal of Visualized Experiments*, *112*, e54060.

Block, J. (2019). Alzheimer's disease might depend on enabling pathogens which do not necessarily cross the blood-brain barrier. *Medical Hypotheses*, *125*, 129–136.

Bloom, G. (2014). Amyloid-β and tau: The trigger and bullet in Alzheimer disease pathogenesis. *JAMA Neurology*, *71*(4), 505–508.

Bolmont, T., Haiss, F., Eicke, D., Radde, R., Mathis, C. A., Klunk, W. E., Kohsaka, S., Jucker, M., & Calhoun, M. E. (2008). Dynamics of the Microglial/Amyloid Interaction Indicate a Role in Plaque Maintenance. *The Journal of Neuroscience*, *28*, 4283–4292. https://doi.org/10.1523/JNEUROSCI.4814-07.2008

Bortz II, W. (1984). The Disuse Syndrome. *Western Journal of Medicine*, *141*, 691–694.

Braak, H., & Braak, E. (1991). Neuropathological stageing of Alzheimer-related changes. *Acta Neuropathologica*, *82*(4), 239–259. https://doi.org/10.1007/BF00308809

Breijyeh, Z., & Karaman, R. (2020). Comprehensive Review on Alzheimer's Disease: Causes and Treatment. *Molecules (Basel, Switzerland)*, *25*(24). https://doi.org/10.3390/molecules25245789

Brothers, H., Gosztyla, M., & Robinson, S. (2018). The Physiological Roles of Amyloid-β Peptide Hint at New Ways to Treat Alzheimer's Disease. *Frontiers in Aging Neuroscience*, *10*(118).

Burwinkel, M., Lutzenberger, M., Heppner, F., Schulz-Schaeffer, W., & Baier, M. (2018). Intravenous injection of beta-amyloid seeds promotes cerebral amyloid angiopathy (CAA). *Acta Neuropathologica Communications*, *6*(23). https://doi.org/10.1186/s40478-018-0511-7

Casali, B. T., MacPherson, K. P., Reed-Geaghan, E. G., & Landreth, G. E. (2020). Microglia depletion rapidly and reversibly alters amyloid pathology by modification of plaque compaction and morphologies. *Neurobiology of Disease*, *142*. https://doi.org/10.1016/j.nbd.2020.104956

Chabrier, M. A., Cheng, D., Castello, N. A., Green, K. N., & LaFerla, F. M. (2014). Synergistic effects of amyloid-beta and wild-type human tau on dendritic spine loss in a floxed double transgenic model of Alzheimer's disease. *Neurobiology of Disease*, *64*, 107–117.

Chausse, B., Kakimoto, P. A., & Kann, O. (2021). Microglia and lipids: How metabolism controls brain innate immunity. *Seminars in Cell & Developmental Biology*, *112*, 137–144. https://doi.org/10.1016/j.semcdb.2020.08.001

Clavaguera, F., Akatsu, H., Fraser, G., Crowther, R. A., Frank, S., Hench, J., Probst, A., Winkler, D. T., Reichwald, J., Staufenbiel, M., Ghetti, B., Goedert, M., & Tolnay, M. (2013). Brain homogenates from human tauopathies induce tau inclusions in mouse brain. *Proceedings of the National Academy of Sciences*, *110*(23), 9535. https://doi.org/10.1073/pnas.1301175110

Cohen, M., Appleby, B., & Safar, J. G. (2016). Distinct prion-like strains of amyloid beta implicated in phenotypic diversity of Alzheimer's disease. *Prion*, *10*(1), 9–17. https://doi.org/10.1080/19336896.2015.1123371

Cohen, M., Kim, C., Haldiman, T., ElHag, M., Mehndiratta, P., Pichet, T., Lissemore, F., Shea, M., Cohen, Y., Chen, W., Blevins, J., Appleby, B., Surewicz, K., Surewicz, W., Sajatovic, M., Tatsuoka, C., Zhang, S., Mayo, P., Butkiewicz, M., … Safar, J. (2015). Rapidly progressive Alzheimer's disease features distinct structures of amyloid-β. *Brain*, *138*(4), 1009–1022.

Come, J., Fraser, P., & Lansbury, Jr, P. (1993). A kinetic model for amyloid formation in the prion diseases: Importance of seeding. *Proceedings of the National Academy of Sciences*, *90*(13), 5959–5963.

Condello, C., Yuan, P., Schain, A., & Grutzendler, J. (2015a). Microglia constitute a barrier that prevents neurotoxic protofibrillar Aβ42 hotspots around plaques. *Nature Communication*, *6*, 6176.

Condello, C., Yuan, P., Schain, A. J., & Grutzendler, J. (2015b). Microglia constitute a barrier that prevents neurotoxic protofibrillar Aβ42 hotspots around plaques. *Nature Communications*, *6*(1). https://doi.org/10.1038/ncomms7176

Contreras, E. B., Sutherland, R. J., Mohajerani, M. H., & Whishaw, I. Q. (2022). Challenges of a small world analysis for the continuous monitoring of behavior in mice. *Neuroscience & Biobehavioral Reviews*, *136*, 104621. https://doi.org/10.1016/j.neubiorev.2022.104621

Craig, L., Hong, N., & McDonald, R. (2011). Revisiting the cholinergic hypothesis in the development of Alzheimer's disease. *Neuroscience & Biobehavioral Reviews*, *35*, 1397–1409.

De Strooper, B. (2010). Proteases and proteolysis in Alzheimer disease: A multifactorial view on the disease process. *Physiological Reviews*, *90*(2), 465–494. https://doi.org/10.1152/physrev.00023.2009

de Vugt, M., Stevens, F., Aalten, P., Lousberg, R., Jaspers, N., & Verhey, F. (2005). A

    prospective study of the effects of behavioral symptoms on the institutionalization

    of patients with dementia. *International Psychogeriatrics*, *17*(4), 577–589.

Di Fede, G., Catania, M., Maderna, E., Ghidoni, R., Benussi, L., Tonoli, E., Giaccone, G.,

    Moda, F., Paterlini, A., Campagnani, I., Sorrentino, S., Colombo, L., Kubis, A.,

    Bistaffa, E., Ghetti, B., & Tagliavini, F. (2018). Molecular subtypes of

    Alzheimer's disease. *Scientific Reports*, *8*(1), 3269.

    https://doi.org/10.1038/s41598-018-21641-1

Dinan, T. G., & Cryan, J. F. (2017). The Microbiome-Gut-Brain Axis in Health and

    Disease. *Gastroenterology Clinics of North America*, *46*(1), 77–89.

    https://doi.org/10.1016/j.gtc.2016.09.007

Domert, J., Rao, S., Agholme, L., Brorsson, A., Marcusson, J., Hallbeck, M., & Nath, S.

    (2014). Spreading of amyloid-β peptides via neuritic cell-to-cell transfer is

    dependent on insufficient cellular clearance. *Neurobiology of Disease*, *65*, 82–92.

Dominy, S., Lynch, C., Ermini, F., Benedyk, M., Marczyk, A., Kondradi, A., Nguyen,

    M., Haditsch, U., Raha, D., Griffin, C., Holsinger, J., Arastu-Kapur, S., Kaba, S.,

    Lee, A., Ryder, M., Potempa, B., Mydel, P., Hellvard, A., Adamowicz, K., …

    Potempa, J. (2019). Porphyromonas gingivalis in Alzheimer's disease brains:

    Evidence for disease causation and treatment with small-molecule inhibitors.

    Science Advances, *5*(1), eaau3333.

Duran-Aniotz, C., Morales, R., Moreno-Gonzalez, I., Hu, P. P., Fedynyshyn, J., & Soto,

    C. (2014). Aggregate-depleted brain fails to induce Aβ deposition in a mouse

    model of Alzheimer's disease. *PloS One*, *9*(2), e89014.

    https://doi.org/10.1371/journal.pone.0089014

Duran-Aniotz, C., Morales, R., Moreno-Gonzalez, I., Hu, P. P., & Soto, C. (2013). Brains from non-Alzheimer's individuals containing amyloid deposits accelerate Aβ deposition in vivo. *Acta Neuropathologica Communications*, *1*(1), 76. https://doi.org/10.1186/2051-5960-1-76

Duran-Aniotz, C., Moreno-Gonzales, I., Gamez, N., Perez-Urrutia, N., Vegas-Gomez, L., Soto, C., & Morales, R. (2021). Amyloid pathology arrangements in Alzheimer's disease brains modulate in vivo seeding capability. *Acta Neuropathologica*, *9*(1), 56. https://doi.org/10.1186/s40478-021-01155-0

Eimer, W., Kumar, D., Shanmugam, N., Rodriguez, A., Mitchell, T., Washicosky, K., György, B., Breakefield, X., Tanzi, R., & Moir, R. (2018). Alzheimer's Disease-Associated β-Amyloid Is Rapidly Seeded by Herpesviridae to Protect against Brain Infection. *Neuron*, *99*, 56–63. https://doi.org/10.1016/j.neuron.2018.06.030

Eisele, Y. (2013). From Soluble Aβ to Progressive Aβ Aggregation: Could Prion-Like Templated Misfolding Play a Role? *Brain Pathology*, *23*, 333–341.

Eisele, Y., Bolmont, T., Heikenwalder, M., Langer, F., Jacobson, L., Yan, Z., Roth, K., Aguzzi, A., Staufenbiel, M., Walker, L., & Jucker, M. (2009). Induction of cerebral β-amyloidosis: Intracerebral versus systemic Aβ inoculation. *Proceedings of the National Academy of Sciences*, *106*(31), 12926–12931.

Eisele, Y., Obermüller, U., Heilbronner, G., Baumann, F., Kaeser, S., Wolburg, H., Walker, L., Staufenbiel, M., Heikenwalder, M., & Jucker, M. (2010). Peripherally Applied Aβ-Containing Inoculates Induce Cerebral β-Amyloidosis. *Science*, *330*(6006), 980–982.

Eisele, YS., Fritschi, SK., Hamaguchi, T., Obermüller, U., Füger, P., Skodras, A., Schäfer, C., Odenthal, J., Heikenwalder, M., Staufenbiel, M., & Jucker, M.

(2014). Multiple factors contribute to the peripheral induction of cerebral β-amyloidosis. *The Journal of Neuroscience : The Official Journal of the Society for Neuroscience*, *34*(31), 10264–10273. https://doi.org/10.1523/JNEUROSCI.1608-14.2014

Elobeid, A., Libard, S., Leino, M., Popova, S. N., & Alafuzoff, I. (2016). Altered Proteins in the Aging Brain. *Journal of Neuropathology & Experimental Neurology*, *75*(4), 316–325. https://doi.org/10.1093/jnen/nlw002

El-Shimy, I. A., Heikal, O. A., & Hamdi, N. (2015). Minocycline attenuates Aβ oligomers-induced pro-inflammatory phenotype in primary microglia while enhancing Aβ fibrils phagocytosis. *Neuroscience Letters*, *609*, 36–41. https://doi.org/10.1016/j.neulet.2015.10.024

Erny, D., Hrabě de Angelis, A. L., Jaitin, D., Wieghofer, P., Staszewski, O., David, E., Keren-Shaul, H., Mahlakoiv, T., Jakobshagen, K., Buch, T., Schwierzeck, V., Utermöhlen, O., Chun, E., Garrett, W. S., McCoy, K. D., Diefenbach, A., Staeheli, P., Stecher, B., Amit, I., & Prinz, M. (2015). Host microbiota constantly control maturation and function of microglia in the CNS. *Nature Neuroscience*, *18*(7), 965–977. https://doi.org/10.1038/nn.4030

Erten-Lyons, D., Woltjer, R. L., Dodge, H., Nixon, R., Vorobik, R., Calvert, J. F., Leahy, M., Montine, T., & Kaye, J. (2009). Factors associated with resistance to dementia despite high Alzheimer disease pathology. *Neurology*, *72*(4), 354. https://doi.org/10.1212/01.wnl.0000341273.18141.64

Esiri, M., Nagy, Z., Smith, M., Barnetson, L., & Smith, A. (1999). Cerebrovascular disease and threshold for dementia in the early stages of Alzheimer's disease. *Lancet*, *354*(9182), 919–920. https://doi.org/10.1016/S0140-6736(99)02355-7

Ettcheto, M., Abad, S., Petrov, D., Pedrós, I., Busquets, O., Sánchez-López, E.,
Casadesús, G., Beas-Zarate, C., Carro, E., Auladell, C., Olloquequi, M., Pallàs,
M., Folch, J., & Camins, A. (2018). Early preclinical changes in hippocampal
CREB-Binding protein expression in a mouse model of familial Alzheimer's
disease. *Molecular Neurobiology*, *55*, 4885–4895.

Fan, R., Xu, F., Previti, M., Davis, J., Grande, A., Robinson, J., & Van Nostrand, W.
(2007). Minocycline Reduces Microglial Activation and Improves Behavioral
Deficits in a Transgenic Model of Cerebral Microvascular Amyloid. *The Journal
of Neuroscience*, *27*(12), 3057–3063. https://doi.org/10.1523/JNEUROSCI.4371-
06.2007

Ferretti, M., Allard, S., Partridge, V., Ducatenzeiler, A., & Cuello, A. (2012).
Minocycline corrects early, pre-plaque neuroinflammation and inhibits BACE-1
in a transgenic model of Alzheimer's disease-like amyloid pathology. *Journal of
Neuroinflammation*, *9*(62), 1–16.
http://www.jneuroinflammation.com/content/9/1/62

Ferri, C., Ames, D., Prince, M., & 10/66 Dementia Research Group. (2004). Behavioral
and psychological symptoms of dementia in developing countries. *International
Psychogeriatrics*, *16*, 441–459.

Festing, M., Overend, P., Gaines Das, R., Borja, M., & Berdoy, M. (2002). *The Design of
Animal Experiments: Reducing the use of animals in research through better
experimental design: Vol. No. 14*. The Royal Society of Medicine Press.

Forner, S., Baglietto-Vargas, D., Martini, A., Trujillo-Estrada, L., & LaFerla, F. (2017).
Synaptic Impairment in Alzheimer's Disease: A Dysregulated Symphony. *Trends
in Neurosciences*, *40*(6), 347–357.

Frautschy, S. A., Yang, F., Calderón, L., & Cole, G. M. (1996). Rodent models of

    Alzheimer's disease: Rat aβ infusion approaches to amyloid deposits.

    Development of Animal Models of Alzheimer's Disease: Status of the Field, *17*(2),

    311–321. https://doi.org/10.1016/0197-4580(95)02073-X

Friesen, M., & Meyer-Luehmann, M. (2019). Aβ Seeding as a Tool to Study Cerebral

    Amyloidosis and Associated Pathology. *Frontiers in Molecular Neuroscience*,

    12(233). https://doi.org/10.3389/fnmol.2019.00233

Fritschi, S. K., Cintron, A., Ye, L., Mahler, J., Bühler, A., Baumann, F., Neumann, M.,

    Nilsson, K. P. R., Hammarström, P., Walker, L. C., & Jucker, M. (2014). Aβ

    seeds resist inactivation by formaldehyde. *Acta Neuropathologica*, *128*(4), 477–

    484. https://doi.org/10.1007/s00401-014-1339-2

Fritschi, S. K., Langer, F., Kaeser, S. A., Maia, L. F., Portelius, E., Pinotsi, D., Kaminski,

    C. F., Winkler, D. T., Maetzler, W., Keyvani, K., Spitzer, P., Wiltfang, J.,

    Kaminski Schierle, G. S., Zetterberg, H., Staufenbiel, M., & Jucker, M. (2014).

    Highly potent soluble amyloid-β seeds in human Alzheimer brain but not

    cerebrospinal fluid. *Brain*, *137*(11), 2909–2915.

    https://doi.org/10.1093/brain/awu255

Fröhlich, E. E., Farzi, A., Mayerhofer, R., Reichmann, F., Jačan, A., Wagner, B., Zinser,

    E., Bordag, N., Magnes, C., Fröhlich, E., Kashofer, K., Gorkiewicz, G., & Holzer,

    P. (2016). Cognitive impairment by antibiotic-induced gut dysbiosis: Analysis of

    gut microbiota-brain communication. *Brain, Behavior, and Immunity*, *56*, 140–

    155. https://doi.org/10.1016/j.bbi.2016.02.020

Frölich, L. (2002). The cholinergic pathology in Alzheimer's disease—Discrepancies

between clinical experience and pathophysiological findings. *Journal of Neural*

Transmission, *109*, 1003–1013.

Gallagher, M., Burwell, R., & Burchinal, M. (1993). Severity of Spatial Learning

Impairment in Aging: Development of a Learning Index for Performance in the

Morris Water Maze. *Behavioral Neuroscience*, *107*(4), 618–626.

https://doi.org/10.1037/0735-7044.107.4.618

Garcez, M. L., Mina, F., Bellettini-Santos, T., Carneiro, F. G., Luz, A. P., Schiavo, G. L.,

Andrighetti, M. S., Scheid, M. G., Bolfe, R. P., & Budni, J. (2017). Minocycline

reduces inflammatory parameters in the brain structures and serum and reverses

memory impairment caused by the administration of amyloid β (1-42) in mice.

Progress in Neuro-Psychopharmacology and Biological Psychiatry, *77*, 23–31.

https://doi.org/10.1016/j.pnpbp.2017.03.010

Garcia-Alloza, M., Ferrara, B. J., Dodwell, S. A., Hickey, G. A., Hyman, B. T., &

Bacskai, B. J. (2007). A limited role for microglia in antibody mediated plaque

clearance in APP mice. *Neurobiology of Disease*, *28*, 286–292.

https://doi.org/10.1016/j.nbd.2007.07.019

Gardener, H., Wright, C., Rundek, T., & Sacco, R. (2015). Brain health and shared risk

factors for dementia and stroke. *Nature Reviews Neurology*, *11*(11), 651.

Gareau, M. G. (2016). Cognitive Function and the Microbiome. *International Review of*

Neurobiology, *131*, 227–246. https://doi.org/10.1016/bs.irn.2016.08.001

Gary, C., Lam, S., Hérard, A.-S., Koch, J., Petit, F., Gipchtein, P., Sawiak, S., Caillierez,

R., Eddarkaoui, S., Colin, M., Aujard, F., Deslys, J.-P., French Neuropathology

Network, Brouillet, E., Buée, L., Comoy, E., Pifferi, F., Picq, J.-L., & Dhenain,

M. (2019). Encephalopathy induced by Alzheimer brain inoculation in a non-human primate. *Acta Neuropathologica Communications*, *7*(1), 1–21.

Geula, C., & Mesulam, M. M. (1996). Systematic regional variations in the loss of cortical cholinergic fibers in Alzheimer's disease. *Cerebral Cortex (New York, N.Y. : 1991)*, *6*(2), 165–177. https://doi.org/10.1093/cercor/6.2.165

Gidyk, D., Deibel, S., Hong, N., & McDonald, R. (2015). Barriers to developing a valid rodent model of Alzheimer's disease: From behavioral analysis to etiological mechanisms. *Frontiers in Neuroscience*, *9*, 245.

Götz, J., Chen, F., van Dorpe, J., & Nitsch, R. M. (2001). Formation of neurofibrillary tangles in P301l tau transgenic mice induced by Abeta 42 fibrils. *Science (New York, N.Y.)*, *293*(5534), 1491–1495. https://doi.org/10.1126/science.1062097

Guardia-Laguarta, C., Pera, M., Clarimón, J., Molinuevo, J. L., Sànchez-Valle, R., Lladó, A., Coma, M., Gómez-Isla, T., Blesa, R., Ferrer, I., & Lleó, A. (2010). Clinical, Neuropathologic, and Biochemical Profile of the Amyloid Precursor Protein I716F Mutation. *Journal of Neuropathology & Experimental Neurology*, *69*(1), 53–59. https://doi.org/10.1097/NEN.0b013e3181c6b84d

Guo, J., & Lee, V. (2014). Cell-to-cell transmission of pathogenic proteins in neurodegenerative diseases. *Nature Medicine*, *20*(2), 130.

Hachisu, M., Konishi, K., Hosoi, M., Tani, M., Tokioka, H., Inamoto, A., Minami, S., Izuno, T., Umezawa, K., Horiuchi, K., & Hori, K. (2015). Beyond the Hypothesis of Serum Anticholinergic Activity in Alzheimer's Disease: Acetylcholine Neuronal Activity Modulates Brain-Derived Neurotrophic Factor Production and Inflammation in the Brain. *Neurodegeneration Disorders*, *15*(3), 182–187. https://doi.org/10.1159/000381531

Hamaguchi, T., Eisele, Y., Varvel, N., Lamb, B., Walker, L., & Jucker, M. (2012). The presence of Aβ seeds, and not age per se, is critical to the initiation of Aβ deposition in the brain. *Acta Neuropathologica*, *123*(1), 31–37.

Hardy, J., & Higgins, G. (1992). Alzheimer's disease: The Amyloid Cascade Hypothesis. *Science*, *256*(5054), 184–185.

Hardy, J., & Selkoe, D. (2002). The amyloid hypothesis of Alzheimer's disease: Progress and problems on the road to therapeutics. *Science*, *297*(5580), 353–356.

Harper, J., & Lansbury, P. (1997). Models of amyloid seeding in Alzheimer's disease and scrapie: Mechanistic Truths and Physiological Consequences of the Time-Dependent Solubility of Amyloid Proteins. *Annual Review of Biochemistry*, *66*(1), 385–407. https://doi.org/10.1146/annurev.biochem.66.1.385

Harris, J., Devidze, N., Verret, L., Ho, K., Halabisky, B., Thwin, M., Kim, D., Hamto, P., Lo, I., Yu, G.-Q., Palop, J., Masliah, E., & Mucke, L. (2010). Transsynaptic progression of amyloid-β-induced neuronal dysfunction within the entorhinal-hippocampal network. *Neuron*, *68*(3), 428–441.

Hatami, A., Monjazeb, S., Milton, S., & Glabe, C. (2017). Familial Alzheimer's Disease Mutations Within the Amyloid Precursor Protein Alter the Aggregation and Conformation of the Amyloid-β Peptide. *Journal of Biological Chemistry*, *292*(8), 3172–3185. https://doi.org/10.1074/jbc.M116.755264

He, Z., Guo, J. L., McBride, J. D., Narasimhan, S., Kim, H., Changolkar, L., Zhang, B., Gathagan, R. J., Yue, C., Dengler, C., Stieber, A., Nitla, M., Coulter, D. A., Abel, T., Brunden, K. R., Trojanowski, J. Q., & Lee, V. M.-Y. (2018). Amyloid-β plaques enhance Alzheimer's brain tau-seeded pathologies by facilitating neuritic

plaque tau aggregation. *Nature Medicine*, *24*(1), 29–38.

https://doi.org/10.1038/nm.4443

Heilbronner, G., Eisele, Y. S., Langer, F., Kaeser, S. A., Novotny, R., Nagarathinam, A.,
Aslund, A., Hammarström, P., Nilsson, K. P. R., & Jucker, M. (2013). Seeded
strain-like transmission of β-amyloid morphotypes in APP transgenic mice.
EMBO Reports, *14*(11), 1017–1022. https://doi.org/10.1038/embor.2013.137

Héraud, C., Goufak, D., Ando, K., Leroy, K., Suain, V., Yilmaz, Z., De Decker, R.,
Authelet, M., Laporte, V., Octave, J.-N., & Brion, J.-P. (2014). Increased
misfolding and truncation of tau in APP/PS1/tau transgenic mice compared to
mutant tau mice. *Neurobiology of Disease*, *62*, 100–112.
https://doi.org/10.1016/j.nbd.2013.09.010

Howard, R., Zubko, O., Gray, R., Bradley, R., Harper, E., Kelly, L., Pank, L., O'Brien, J.,
Fox, C., Tabet, N., Livingston, G., Bentham, P., McShane, R., Burns, A., Ritchie,
C., Reeves, S., Lovestone, S., Ballard, C., Noble, W., … Nilforooshan, R. (2020).
*Minocycline 200 mg or 400 mg versus placebo for mild Alzheimer's disease: The
MADE Phase II, three-arm RCT. 7*, 1–62. https://doi.org/10.3310/eme07020

Hsiao, K., Chapman, P., Nilsen, S., Eckman, C., Harigaya, Y., Younkin, S., Yang, F., &
Cole, G. (1996). Correlative memory deficits, Abeta elevation, and amyloid
plaques in transgenic mice. *Science*, *274*, 99–102.

Hurtado, D. E., Molina-Porcel, L., Iba, M., Aboagye, A. K., Paul, S. M., Trojanowski, J.
Q., & Lee, V. M.-Y. (2010). A{beta} accelerates the spatiotemporal progression
of tau pathology and augments tau amyloidosis in an Alzheimer mouse model.
The American Journal of Pathology, *177*(4), 1977–1988.
https://doi.org/10.2353/ajpath.2010.100346

Ittner Arne, Chua Sook Wern, Bertz Josefine, Volkerling Alexander, van der Hoven Julia, Gladbach Amadeus, Przybyla Magdalena, Bi Mian, van Hummel Annika, Stevens Claire H., Ippati Stefania, Suh Lisa S., Macmillan Alexander, Sutherland Greg, Kril Jillian J., Silva Ana P. G., Mackay Joel P., Poljak Anne, Delerue Fabien, … Ittner Lars M. (2016). Site-specific phosphorylation of tau inhibits amyloid-β toxicity in Alzheimer's mice. *Science*, *354*(6314), 904–908. https://doi.org/10.1126/science.aah6205

Iturria-Medina, Y., Sotero, R. C., Toussaint, P. J., & Evans, A. C. (2014). Epidemic spreading model to characterize misfolded proteins propagation in aging and associated neurodegenerative disorders. *PLoS Computational Biology*, *10*(11), e1003956. https://doi.org/10.1371/journal.pcbi.1003956

Jack Jr, C., Wiste, H., Weigand, S., Rocca, W., Knopman, D., Mielke, M., Lowe, V., Senjem, M., Gunter, J., Preboske, G., Pankratz, V., Vemuri, P., & Petersen, R. (2014). Age-specific population frequencies of cerebral β-amyloidosis and neurodegeneration among people with normal cognitive function aged 50–89 years: A cross-sectional study. *The Lancet*, *13*(10), 997–1105. https://doi.org/10.1016/S1474-4422(14)70194-2

Jafari, Z., Mehla, J., Kolb, B., & Mohajerani, M. (2018). Gestational Stress Augments Postpartum β-Amyloid Pathology and Cognitive Decline in a Mouse Model of Alzheimer's Disease. *Cerebral Cortex*, 1–13.

Jankowsky, J. L., & Zheng, H. (2017). Practical considerations for choosing a mouse model of Alzheimer's disease. *Molecular Neurodegeneration*, *12*(1), 89. https://doi.org/10.1186/s13024-017-0231-7

Jenkins, T. A., Nguyen, J. C. D., Polglaze, K. E., & Bertrand, P. P. (2016). Influence of Tryptophan and Serotonin on Mood and Cognition with a Possible Role of the Gut-Brain Axis. *Nutrients*, *8*(1). https://doi.org/10.3390/nu8010056

Jevtic, S., Sengar, A., Salter, M., & McLaurin, J. (2017). The role of the immune system in Alzheimer disease: Etiology and treatment. *Age Research Reviews*, *40*, 84–94.

Jin, M., Nguyen, J. D., Weber, S. J., Mejias-Aponte, C. A., Madangopal, R., & Golden, S. A. (2022). SMART: An Open-Source Extension of WholeBrain for Intact Mouse Brain Registration and Segmentation. *ENeuro*, *9*(3), ENEURO.0482-21.2022. PubMed. https://doi.org/10.1523/ENEURO.0482-21.2022

Jin, M., Shepardson, N., Yang, T., Chen, G., Walsh, D., & Selkoe, D. J. (2011). Soluble amyloid beta-protein dimers isolated from Alzheimer cortex directly induce Tau hyperphosphorylation and neuritic degeneration. *Proceedings of the National Academy of Sciences of the United States of America*, *108*(14), 5819–5824. https://doi.org/10.1073/pnas.1017033108

Joseph, J., Shukitt-Hale, B., Denisova, N. A., Martin, A., Perry, G., & Smith, M. A. (2001). Copernicus revisited: Amyloid beta in Alzheimer's disease. *Neurobiology of Aging*, *22*(1), 131–146. https://doi.org/10.1016/s0197-4580(00)00211-6

Kane, M., Lipinski, W., Callahan, M., Bian, F., Durham, R., Schwarz, R., Roher, A., & Walker, L. (2000). Evidence for Seeding of β-Amyloid by Intracerebral Infusion of Alzheimer Brain Extracts in β-Amyloid Precursor Protein- Transgenic Mice. *The Journal of Neuroscience*, *20*(10), 3606–3611.

Katzmarski, N., Ziegler-Waldkirch, S., Scheffler, N., Witt, C., Abou-Ajram, C., Nuscher, B., Prinz, M., Haass, C., & Meyer-Leuhmann, M. (2019). Aβ oligomers trigger and accelerate Aβ seeding. *Brain Pathology*, *Epub ahead of print*.

Komanduri, M., Savage, K., Lea, A., McPhee, G., Nolidin, K., Deleuil, S., Stough, C., &
Gondalia, S. (2021). The Relationship between Gut Microbiome and Cognition in
Older Australians. *Nutrients*, *14*(1). https://doi.org/10.3390/nu14010064

Kulic, L., Kurosinski, P., Chen, F., Tracy, J., Mohajeri, M. H., Li, H., Nitsch, R. M., &
Götz, J. (2006). Active immunization trial in Aβ42-injected P301L tau transgenic
mice. *Neurobiology of Disease*, *22*, 50–56.

Kumar, D., Choi, S., Washicosky, K., Eimer, W., Tucker, S., Ghofrani, J., Lefkowitz, A.,
McColl, G., Goldstein, L., Tanzi, R., & Moir, R. (2016). Amyloid-β peptide
protects against microbial infection in mouse and worm models of Alzheimer's
disease. *Alzheimer's Disease*, *8*(340), 340ra72.

Kundu, P., Stagaman, K., Kasschau, K., Holden, S., Shulzhenko, N., Sharpton, T. J., &
Raber, J. (2022). Fecal Implants From App (NL-G-F) and App (NL-G-F/E4)
Donor Mice Sufficient to Induce Behavioral Phenotypes in Germ-Free Mice.
Frontiers in Behavioral Neuroscience, *16*, 791128.
https://doi.org/10.3389/fnbeh.2022.791128

Kurkinen, M. (2021). Alzheimer's trials: A cul-de-sac with no end in sight. *Advances in
Clinical and Experimental Medicine : Official Organ Wroclaw Medical
University*, *30*(7), 653–654. https://doi.org/10.17219/acem/139501

Lamb, B. T., Call, L. M., Slunt, H. H., Bardel, K. A., Lawler, A. M., Eckman, C. B.,
Younkin, S. G., Holtz, G., Wagner, S. L., Price, D. L., Sisodia, S. S., & Gearhart,
J. D. (1997). Altered Metabolism of Familial Alzheimer's Disease-Linked
Amyloid Precursor Protein Variants in Yeast Artificial Chromosome Transgenic
Mice. *Human Molecular Genetics*, *6*(9), 1535–1541.
https://doi.org/10.1093/hmg/6.9.1535

Langer, F., Eisele, Y., Fritschi, S., Staufenbiel, M., Walker, L., & Jucker, M. (2011). Soluble Aβ seeds are potent inducers of cerebral β-amyloid deposition. *Journal of Neuroscience*, *31*(41), 14488–14495.

Latif-Hernandez, A., Sabanov, V., Ahmed, T., Craessaerts, K., Saito, T., Saido, T., & Balschun, D. (2020). The two faces of synaptic failure in AppNL-G-F knock-in mice. *ALzheimer's Research & Therapy*, *100*. https://doi.org/10.1186/s13195-020-00667-6

Latif-Hernandez, A., Shah, D., Craessaerts, K., Saido, T., Saito, T., De Stropper, B., Van der Linden, A., & D'Hooge, R. (2019). Subtle behavioral changes and increased prefrontal-hippocampal network T synchronicity in APPNL−G−F mice before prominent plaque deposition. *Behavioural Brain Research*, *364*, 431–441.

Leroy, K., Ando, K., Laporte, V., Dedecker, R., Suain, V., Authelet, M., Héraud, C., Pierrot, N., Yilmaz, Z., Octave, J.-N., & Brion, J.-P. (2012). Lack of tau proteins rescues neuronal cell death and decreases amyloidogenic processing of APP in APP/PS1 mice. *The American Journal of Pathology*, *181*(6), 1928–1940. https://doi.org/10.1016/j.ajpath.2012.08.012

Lewis, J., Dickson, D. W., Lin, W. L., Chisholm, L., Corral, A., Jones, G., Yen, S. H., Sahara, N., Skipper, L., Yager, D., Eckman, C., Hardy, J., Hutton, M., & McGowan, E. (2001). Enhanced neurofibrillary degeneration in transgenic mice expressing mutant tau and APP. *Science (New York, N.Y.)*, *293*(5534), 1487–1491. https://doi.org/10.1126/science.1058189

Lin, L., Zheng, L. J., & Zhang, L. J. (2018). Neuroinflammation, Gut Microbiome, and Alzheimer's Disease. *Molecular Neurobiology*, *55*(11), 8243–8250. https://doi.org/10.1007/s12035-018-0983-2

Liu, P., Reed, M., Kotilinek, L., Grant, M., Forster, C., Qiang, W., Shapiro, S., Reichl, J.,
Chiang, A., Jankowsky, J., Wilmot, C., Cleary, J., Zahs, K., & Ashe, K. (2015).
Quaternary structure defines a large class of amyloid-β oligomers neutralized by
sequestration. *Cell Reports*, *11*(11), 1760–1771.

Lu, D., Shaked, G., Masliah, E., Bredesen, D., & Koo, E. (2003). Amyloid β protein
toxicity mediated by the formation of amyloid-β protein precursor complexes.
Annals of Neurology, *54*(6), 781–789.

Lue, L.-F., Kuo, Y.-M., Roher, A. E., Brachova, L., Shen, Y., Sue, L., Beach, T., Kurth, J.
H., Rydel, R. E., & Rogers, J. (1999). Soluble Amyloid β Peptide Concentration
as a Predictor of Synaptic Change in Alzheimer's Disease. *The American Journal
of Pathology*, *155*(3), 853–862. https://doi.org/10.1016/S0002-9440(10)65184-X

Luna, S., Cameron, D., & Ethell, D. (2013). Amyloid-β and APP Deficiencies Cause
Severe Cerebrovascular Defects: Important Work for an Old Villain. *Plos One*,
8(9), e75052.

Maei, H., Zaslavasky, K., Teixeira, C., & Frankland, P. (2009). What is the Most
Sensitive Measure of Water Maze Probe Test Performance? *Frontiers in
Integrative Neuroscience*, *3*(4). https://doi.org/10.3389/neuro.07.004.2009

Mahler, J., Morales-Corraliza, J., Stolz, J., Skodras, A., Radde, R., Duma, C. C., Eisele,
Y. S., Mazzella, M. J., Wong, H., Klunk, W. E., Nilsson, K. P. R., Staufenbiel,
M., Mathews, P. M., Jucker, M., & Wegenast-Braun, B. M. (2015). Endogenous
murine Aβ increases amyloid deposition in APP23 but not in APPPS1 transgenic
mice. *Neurobiology of Aging*, *36*(7), 2241–2247.
https://doi.org/10.1016/j.neurobiolaging.2015.03.011

Malm, T., Magga, J., Ful Kuh, G., Vatanen, T., Koistinaho, M., & Koistinaho, J. (2008). Minocycline Reduces Engraftment and Activation of Bone Marrow-Derived Cells but Sustains Their Phagocytic Activity in a Mouse Model of Alzheimer's Disease. *Glia*, *56*, 1767–1779. https://doi.org/10.1002/glia.20726

Marzesco, A.-M., Flötenmeyer, M., Bühler, A., Obermüller, U., Staufenbiel, M., Jucker, M., & Baumann, F. (2016). Highly potent intracellular membrane-associated Aβ seeds. *Scientific Reports*, *6*(1), 28125. https://doi.org/10.1038/srep28125

Matteson, M., Linton, A., Barnes, S., Cleary, B., & Lichtenstein, M. (1996). The relationship between Piaget and cognitive levels in persons with Alzheimer's disease and related disorders. *Aging Clinical and Experimental Research*, *8*(1), 61–69. https://doi.org/10.1007/bf03340117

McAllister, B. B., Lacoursiere, S. G., Sutherland, R. J., & Mohajerani, M. H. (2020). Intracerebral seeding of amyloid-β and tau pathology in mice: Factors underlying prion-like spreading and comparisons with α-synuclein. *Neuroscience & Biobehavioral Reviews*, *112*. https://doi.org/10.1016/j.neubiorev.2020.01.026

McAllister, B., Lacoursiere, S., Sutherland, R., & Mohajerani, M. (2020). Intracerebral seeding of amyloid-β and tau pathology in mice: Factors T underlying prion-like spreading and comparisons with α-synuclein. *Neuroscience and Biobehavioral Reviews*, *112*, 1–27.

McDonald, R. (2002). Multiple Combinations of Co-Factors Produce Variants of Age-Related Cognitive Decline: A Theory. *Canadian Journal of Experimental Psychology*, *56*(3), 221–339.

McDonald, R., Craig, L., & Hong, N. (2010). The etiology of age-related dementia is more complicated than we think. *Behavioural Brain Research*, *214*(1), 3–11.

McLean, C. A., Cherny, R. A., Fraser, F. W., Fuller, S. J., Smith, M. J., Beyreuther, K., Bush, A. I., & Masters, C. L. (1999). Soluble pool of Abeta amyloid as a determinant of severity of neurodegeneration in Alzheimer's disease. *Annals of Neurology*, *46*(6), 860–866. https://doi.org/10.1002/1531-8249(199912)46:6<860::aid-ana8>3.0.co;2-m

Mehla, J., Deibel, S. H., Karem, H., Hossain, S., Lacoursiere, S. G., Sutherland, R. J., Mohajerani, M. H., & McDonald, R. J. (2022). Dramatic impacts on brain pathology, anxiety, and cognitive function in the knock-in APP(NL-G-F) mouse model of Alzheimer disease following long-term voluntary exercise. *Alzheimer's Research & Therapy*, *14*(1), 143. https://doi.org/10.1186/s13195-022-01085-6

Mehla, J., Lacoursiere, S., Lapointe, V., McNaughton, B., Sutherland, R., McDonald, R., & Mohajerani, M. (2019). Age-dependent behavioral and biochemical characterization of single APP knock-in mouse (APPNL-G-F/NL-G-F) model of Alzheimer's disease. *Neurobiology of Aging*, *75*, 25–37.

Meier-Stephenson, F. S., Meier-Stephenson, V. C., Carter, M. D., Meek, A. R., Wang, Y., Pan, L., Chen, Q., Jacobo, S., Wu, F., Lu, E., Simms, G. A., Fisher, L., McGrath, A. J., Fermo, V., Barden, C. J., Clair, H. D. S., Galloway, T. N., Yadav, A., Campágna-Slater, V., … Weaver, D. F. (2022). Alzheimer's disease as an autoimmune disorder of innate immunity endogenously modulated by tryptophan metabolites. *Alzheimer's & Dementia: Translational Research & Clinical Interventions*, *8*(1), e12283. https://doi.org/10.1002/trc2.12283

Meyer-Leuhmann, M., Coomaraswamy, J., Bolmont, T., Kaeser, S., Schaefer, C., Kilger, E., Neuenschwander, A., Ambramowski, D., Frey, P., Jaton, A., Vigouret, J., Paganetti, P., Walsh, D., Mathews, P., Ghiso, J., Staufenbiel, M., Walker, L., &

Jucker, M. (2006). Exogenous induction of cerebral β-amyloidogenesis is governed by agent and host. *Science*, *313*, 1781–1784.

Moir, R., Lathe, R., & Tanzi, R. (2018). The antimicrobial protection hypothesis of Alzheimer's disease. *Alzheimer's & Dementia*, *14*(12), 1602–1614. https://doi.org/10.1016/j.jalz.2018.06.3040

Montalvan, V., Lee, J., Bueso, T., De Toledo, J., & Rivas, K. (2020). Neurological manifestations of COVID-19 and other coronavirus infections: A systematic review. *Clinical Neurology and Neurosurgery*, *194*, 105921.

Morales, R., Bravo-Alegria, J., Duran-Aniotz, C., & Soto, C. (2015). Titration of biologically active amyloid–β seeds in a transgenic mouse model of Alzheimer's disease. *Scientific Reports*, *5*(1), 9349. https://doi.org/10.1038/srep09349

Morales, R., Duran-Aniotz, C., Castilla, J., Estrada, L. D., & Soto, C. (2012). De novo induction of amyloid-β deposition in vivo. *Molecular Psychiatry*, *17*(12), 1347–1353. https://doi.org/10.1038/mp.2011.120

Mucke, L., & Selkoe, D. J. (2012). Neurotoxicity of amyloid β-protein: Synaptic and network dysfunction. *Cold Spring Harbor Perspectives in Medicine*, *2*(7), a006338. https://doi.org/10.1101/cshperspect.a006338

Norins, L. C. (2021). Repurposing Licensed Drugs for Use Against Alzheimer's Disease. *Journal of Alzheimer's Disease : JAD*. https://doi.org/10.3233/JAD-210080

Nussbaum, J. M., Seward, M. E., & Bloom, G. S. (2013). Alzheimer disease: A tale of two prions. *Prion*, *7*(1), 14–19. https://doi.org/10.4161/pri.22118

Oakley, H., Cole, S., Logan, S., Maus, E., Shao, P., Craft, J., Guillozet-Bongaarts, A., Ohno, M., Disterhoft, J., Van Eldik, L., & Berry, R. (2006). Intraneuronal β-amyloid aggregates, neurodegeneration, and neuron loss in transgenic mice with

five familial Alzheimer's disease mutations: Potential factors in amyloid plaque formation. *Journal of Neuroscience*, *26*(40), 10129–10140.

Oddo, S., Caccamo, A., Shepherd, J. D., Murphy, M. P., Golde, T. E., Kayed, R., Metherate, R., Mattson, M. P., Akbari, Y., & LaFerla, F. M. (2003). Triple-transgenic model of Alzheimer's disease with plaques and tangles: Intracellular Abeta and synaptic dysfunction. *Neuron*, *39*(3), 409–421. https://doi.org/10.1016/s0896-6273(03)00434-3

Olsson, T., Klementieva, O., & Gouras, G. (2018). Prion-like seeding and nucleation of intracellular amyloid-β. *Neurobiology of Disease*, *113*, 1–10.

Otvos Jr, L., Szendrei, G., Lee, V., & Mantsch, H. (1993). Human and rodent Alzheimer beta-amyloid peptides acquire distinct conformations in membrane-mimicking solvents. *European Journal of Biochemistry*, *211*(1–2), 249–257. https://doi.org/10.1111/j.1432-1033.1993.tb19893.x

Palop, J. J., & Mucke, L. (2016). Network abnormalities and interneuron dysfunction in Alzheimer disease. *Nature Reviews Neuroscience*, *17*(12), 777–792. https://doi.org/10.1038/nrn.2016.141

Parhizkar, S., Arzberger, T., Brendel, M., Kleinberger, G., Deussing, M., Focke, C., Nuscher, B., Xiong, M., Ghasemigharagoz, A., Katzmarski, N., Krasemann, S., Lichtenthaler, S. F., Müller, S. A., Colombo, A., Monasor, L. S., Tahirovic, S., Herms, J., Willem, M., Pettkus, N., … Haass, C. (2019). Loss of TREM2 function increases amyloid seeding but reduces plaque-associated ApoE. *Nature Neuroscience*, *22*(2), 191–204. https://doi.org/10.1038/s41593-018-0296-9

Parker, A., Romano, S., Ansorge, R., Aboelnour, A., Le Gall, G., Savva, G. M., Pontifex, M. G., Telatin, A., Baker, D., Jones, E., Vauzour, D., Rudder, S., Blackshaw, L.

A., Jeffery, G., & Carding, S. R. (Directors). (2022, April 29). *Fecal microbiota transfer between young and aged mice reverses hallmarks of the aging gut, eye, and brain.* (Vol. 10, Issue 1). https://doi.org/10.1186/s40168-022-01243-w

Penke, B., Bogár, F., Paragi, G., Gera, J., & Fülöp, L. (2019). Key Peptides and Proteins in Alzheimer's Disease. *Current Protein & Peptide Science*, *20*(6), 577–599. https://doi.org/10.2174/1389203720666190103123434

Pignataro, A., & Middei, S. (2017). Trans-Synaptic Spread of Amyloid-β in Alzheimer's Disease: Paths to β-Amyloidosis. *Neural Plasticity*, *2017*(5281829), 6.

Pike, C., Walencewicz, A., Glabe, C., & Cotman, C. (1991). In vitro aging of β-amyloid protein causes peptide aggregation and neurotoxicity. *Brain Research*, *563*(1–2), 311–314.

Pooler, A. M., Polydoro, M., Maury, E. A., Nicholls, S. B., Reddy, S. M., Wegmann, S., William, C., Saqran, L., Cagsal-Getkin, O., Pitstick, R., Beier, D. R., Carlson, G. A., Spires-Jones, T. L., & Hyman, B. T. (2015). Amyloid accelerates tau propagation and toxicity in a model of early Alzheimer's disease. *Acta Neuropathologica Communications*, *3*(1), 14. https://doi.org/10.1186/s40478-015-0199-x

Premi, E., Garibotto, V., Gazzina, S., Grassi, M., Cosseddu, M., Paghera, B., Turla, M., Padovani, A., & Borroni, B. (2013). Beyond cognitive reserve: Behavioural reserve hypothesis in frontotemporal dementia. *Behavioural Brain Research*, *245*, 58–62.

Prokop, S., Miller, K. R., & Heppner, F. L. (2013). Microglia actions in Alzheimer's disease. *Acta Neuropathologica*, *126*, 461–477. https://doi.org/10.1007/s00401-013-1182-x

Purro, S., Farrow, M., Linehan, J., Nazari, T., Thomas, D., Chen, Z., Mengel, D., Saito,
T., Saido, T., Rudge, P., Brandner, S., Walsh, D., & Collinge, J. (2018).
Transmission of amyloid-β protein pathology from cadaveric pituitary growth
hormone. *Nature*, *564*(7736), 415–419.

Radde, R., Bolmont, T., Kaeser, S. A., Coomaraswamy, J., Lindau, D., Stoltze, L.,
Calhoun, M. E., Jäggi, F., Wolburg, H., Gengler, S., Haass, C., Ghetti, B., Czech,
C., Hölscher, C., Mathews, P. M., & Jucker, M. (2006). Abeta42-driven cerebral
amyloidosis in transgenic mice reveals early and robust pathology. *EMBO
Reports*, *7*(9), 940–946. https://doi.org/10.1038/sj.embor.7400784

Rasmussen, J., Mahler, J., Beschorner, N., Kaeser, S. A., Häsler, L. M., Baumann, F.,
Nyström, S., Portelius, E., Blennow, K., Lashley, T., Fox, N. C., Supulveda-Falla,
D., Glatzel, M., Oblak, A. L., Ghetti, B., Nilsson, K. P. R., Hammarström, P.,
Staufenbiel, M., Walker, L. C., & Jucker, M. (2017). Amyloid polymorphisms
constitute distinct clouds of conformational variants in different etiological
subtypes of Alzheimer's disease. *Proceedings of the National Academy of
Sciences*, *114*(49), 13018–13023.

Ribé, E. M., Pérez, M., Puig, B., Gich, I., Lim, F., Cuadrado, M., Sesma, T., Catena, S.,
Sánchez, B., Nieto, M., Gómez-Ramos, P., Morán, M. A., Cabodevilla, F.,
Samaranch, L., Ortiz, L., Pérez, A., Ferrer, I., Avila, J., & Gómez-Isla, T. (2005).
Accelerated amyloid deposition, neurofibrillary degeneration and neuronal loss in
double mutant APP/tau transgenic mice. *Neurobiology of Disease*, *20*(3), 814–
822. https://doi.org/10.1016/j.nbd.2005.05.027

Ridley, R. M., Baker, H. F., Windle, C. P., & Cummings, R. M. (2006). Very long term studies of the seeding of β-amyloidosis in primates. *Journal of Neural Transmission*, *113*(9), 1243. https://doi.org/10.1007/s00702-005-0385-2

Roberson, E., Scearce-Levie, K., Palop, J., Yan, F., Cheng, I., Wu, T., Gerstein, H., Yu, G., & Mucke, L. (2007). Reducing endogenous tau ameliorates amyloid ß-induced deficits in an Alzheimer's disease mouse model. *Science*, *316*(5825), 750–754.

Robinson, J. L., Lee, E. B., Xie, S. X., Rennert, L., Suh, E., Bredenberg, C., Caswell, C., Van Deerlin, V. M., Yan, N., Yousef, A., Hurtig, H. I., Siderowf, A., Grossman, M., McMillan, C. T., Miller, B., Duda, J. E., Irwin, D. J., Wolk, D., Elman, L., … Trojanowski, J. Q. (2018). Neurodegenerative disease concomitant proteinopathies are prevalent, age-related and APOE4-associated. *Brain*, *141*(7), 2181–2193. https://doi.org/10.1093/brain/awy146

Rosen, R., Fritz, J., Dooyema, J., Cintron, A., Hamaguchi, T., Lah, J., LeVine, H., Jucker, M., & Walker, L. (2012). Exogenous seeding of cerebral β-amyloid deposition in βAPP- transgenic rats. *Journal of Neurochemistry*, *120*(5), 660–666.

Rosen, R., Tomidokoro, Y., Farberg, A., Dooyema, J., Ciliax, B., Preuss, T. M., Neubert, T. A., Ghiso, J. A., LeVine, H. 3rd, & Walker, L. C. (2016). Comparative pathobiology of β-amyloid and the unique susceptibility of humans to Alzheimer's disease. *Neurobiology of Aging*, *44*, 185–196. https://doi.org/10.1016/j.neurobiolaging.2016.04.019

Ruiz-Riquelme, A., Lau, H., Stuart, E., Goczi, A., Wang, Z., Schmitt-Ulms, G., & Watts, J. (2018). Prion-like propagation of β-amyloid aggregates in the absence of APP overexpression. *Acta Neuropathologica Communications*, *6*(26).

Ryder, M. I. (2020). Porphyromonas gingivalis and Alzheimer disease: Recent findings

and potential therapies. *Journal of Periodontology*, *91 Suppl 1*(Suppl 1), S45–S49.

https://doi.org/10.1002/JPER.20-0104

Saito, T., Matsuba, Y., Mihira, N., Takano, J., Nilsson, P., Itohara, S., Iwata, N., & Saido,

T. (2014). Single App knock-in mouse models of Alzheimer's disease. *Nature*

Neuroscience, *17*(5), 661–663.

Saito, T., Matsuba, Y., Yamazaki, N., Hashimoto, S., & Saido, T. (2016). Calpain

Activation in Alzheimer's Model Mice Is an Artifact of APP and Presenilin

Overexpression. *Journal of Neuroscience*, *36*(38), 9933–9936.

https://doi.org/10.1523/JNEUROSCI.1907-16.2016

Saito, T., Mihira, N., Matsuba, Y., Sasaguri, H., Hashimoto, S., Narasimhan, S., Zhang,

B., Murayama, S., Higuchi, M., Lee, V. M. Y., Trojanowski, J. Q., & Saido, T. C.

(2019). Humanization of the entire murine Mapt gene provides a murine model of

pathological human tau propagation. *The Journal of Biological Chemistry*,

294(34), 12754–12765. https://doi.org/10.1074/jbc.RA119.009487

Salvadores, N., Moreno-Gonzalez, I., Gamez, N., Quiroz, G., Vegas-Gomez, L.,

Escandón, M., Jimenez, S., Vitorica, J., Gutierrez, A., Soto, C., & Court, F. A.

(2022). Aβ oligomers trigger necroptosis-mediated neurodegeneration via

microglia activation in Alzheimer's disease. *Acta Neuropathologica*

Communications, *10*(1), 31. https://doi.org/10.1186/s40478-022-01332-9

Sasaguri, H., Hashimoto, S., Watamura, N., Sato, K., Takamura, R., Nagata, K., Tsubuki,

S., Ohshima, T., Yoshiki, A., Sato, K., Kumita, W., Sasaki, E., Kitazume, S.,

Nilsson, P., Winblad, B., Saito, T., Iwata, N., & Saido, T. C. (2022). Recent

Advances in the Modeling of Alzheimer's Disease. *Frontiers in Neuroscience*, *16*.
https://doi.org/10.3389/fnins.2022.807473

Sasaguri, H., Nilsson, P., Hashimoto, S., Nagata, K., Saito, T., De Strooper, B., Hardy, J.,
Vassar, R., Winblad, B., & Saido, T. (2017). APP mouse models for Alzheimer's
disease preclinical studies. *EMBO J*, *36*, 2473–2487.

Saucken, V. E. von, Jay, T. R., & Landreth, G. E. (2020). The effect of amyloid on
microglia-neuron interactions before plaque onset occurs independently of
TREM2 in a mouse model of Alzheimer's disease. *Neurobiology of Disease*, *145*.
https://doi.org/10.1016/j.nbd.2020.105072

Saul, A., Sprenger, F., Bayer, T. A., & Wirths, O. (2013). Accelerated tau pathology with
synaptic and neuronal loss in a novel triple transgenic mouse model of
Alzheimer's disease. *Neurobiology of Aging*, *34*(11), 2564–2573.
https://doi.org/10.1016/j.neurobiolaging.2013.05.003

Schellenberg, G. D., & Montine, T. J. (2012). The genetics and neuropathology of
Alzheimer's disease. *Acta Neuropathologica*, *124*(3), 305–323.
https://doi.org/10.1007/s00401-012-0996-2

Schenk, D., Barbour, R., Dunn, W., Gordon, G., Grajeda, H., Guido, T., Hu, K., Huang,
J., Johnson-Wood, K., Khan, K., Kholodenko, D., Lee, M., Liao, Z., Lieberburg,
I., Motter, R., Mutter, L., Soriano, F., Shopp, G., Vasquez, N., … Seubert, P.
(1999). Immunization with amyloid-b attenuates Alzheimer- disease-like
pathology in the PDAPP mouse. *Nature*, *400*, 173–177.

Schlachetzki, C. M. J., & Hull, M. (2009). Microglial Activation in Alzheimers Disease.
Current Alzheimer Research, *6*(6), 554–563.
https://doi.org/10.2174/156720509790147179

Seilheimer, B., Bohrmann, B., Bondolfi, L., Müller, F., Stüber, D., & Döbeli, H. (1997). The toxicity of the Alzheimer's beta-amyloid peptide correlates with a distinct fiber morphology. *The Journal of Structural Biology*, *119*, 59–71.

Selkoe, D. (2000). Toward a comprehensive theory for Alzheimer's disease. Hypothesis: Alzheimer's disease is caused by the cerebral accumulation and cytotoxicity of amyloid beta-protein. *Annals of the New York Academy of Sciences*, *924*, 17–25.

Selkoe, D. J., & Hardy, J. (2016). The amyloid hypothesis of Alzheimer's disease at 25 years. *EMBO Molecular Medicine*, *8*(6), 595–608. https://doi.org/10.15252/emmm.201606210

Sengupta, U., Nilson, A., & Kayed, R. (2016). The role of amyloid-β oligomers in toxicity, propagation, and immunotherapy. *EBioMedicine*, *6*, 42–49.

Shah, D., Praet, J., Latif-Hernandez, A., Hofling, C., Anckaerts, C., Bard, F., Morawski, M., Detrez, J., Prinsen, E., Villa, A., De Vos, W., Maggi, A., D'Hooge, R., Balschun, D., Rossner, S., Verhoye, M., & Van der Linden, A. (2016). Early pathologic amyloid induces hypersynchrony of BOLD resting-state networks in transgenic mice and provides an early therapeutic window before amyloid plaque deposition. *Alzheimer's & Dementia*, *12*(9), 964–976.

Shi, N., Li, N., Duan, X., & Niu, H. (2017). Interaction between the gut microbiome and mucosal immune system. *Military Medical Research*, *4*, 14. https://doi.org/10.1186/s40779-017-0122-9

Shi, Y., & Holtzman, D. (2018). Interplay between innate immunity and Alzheimer disease: APOE and TREM2 in the spotlight. *Nature Immunology*, *18*, 759–772.

Shin, J., Yu, S.-B., Yu, U. Y., Jo, S. A., & Ahn, J.-H. (2010). Swedish mutation within amyloid precursor protein modulates global gene expression towards the

pathogenesis of Alzheimer's disease. *BMB Reports*, *43*(10), 704–709.

https://doi.org/10.5483/BMBRep.2010.43.10.704

Shipton, O. A., Leitz, J. R., Dworzak, J., Acton, C. E. J., Tunbridge, E. M., Denk, F.,

Dawson, H. N., Vitek, M. P., Wade-Martins, R., Paulsen, O., & Vargas-Caballero,

M. (2011). Tau protein is required for amyloid {beta}-induced impairment of

hippocampal long-term potentiation. *The Journal of Neuroscience : The Official*

Journal of the Society for Neuroscience, *31*(5), 1688–1692.

https://doi.org/10.1523/JNEUROSCI.2610-10.2011

Singh, S., Bermudez-Contreras, E., Nazari, M., Sutherland, R. J., & Mohajerani, M. H.

(2019). Low-cost solution for rodent home-cage behaviour monitoring. *PloS One*,

14(8), e0220751. https://doi.org/10.1371/journal.pone.0220751

Skachokova, Z., Sprenger, F., Breu, K., Abramowski, D., Clavaguera, F., Hench, J.,

Staufenbiel, M., Tolnay, M., & Winkler, D. T. (2015). Amyloid-β in the

Cerebrospinal Fluid of APP Transgenic Mice Does not Show Prion-like

Properties. *Current Alzheimer Research*, *12*(9), 886–891.

https://doi.org/10.2174/1567205012666150710115022

Soldan, A., Pettigrew, C., Cai, Q., Wang, J., Wang, M.C., Moghekar, A., Miller, M.I.,

Albert, M., & BIOCARD Research Team. (2017). Cognitive reserve and long-

term change in cognition in aging and preclinical Alzheimer's disease.

Neurobiology of Aging, *60*, 164–172.

Soscia, S., Kirby, J., Washicosky, K., Tucker, S., Ingelsson, M., Hyman, B., Burton, M.,

Goldstein, L., Duong, S., Tanzi, R., & Moir, R. (2010). The Alzheimer's Disease-

Associated Amyloid β-Protein Is an Antimicrobial Peptide. *Plos One*, *5*(3), e9505.

Spangenberg, E., Severson, P. L., Hohsfield, L. A., Crapser, J., Zhang, J., Burton, E. A.,

    Zhang, Y., Spevak, W., Lin, J., Phan, N. Y., Habets, G., Rymar, A., Tsang, G.,

    Walters, J., Nespi, M., Singh, P., Broome, S., Ibrahim, P., Zhang, C., … Green, K.

    N. (2019). Sustained microglial depletion with CSF1R inhibitor impairs

    parenchymal plaque development in an Alzheimer's disease model. *Nature*

    Communications, *10*(1), 3758. https://doi.org/10.1038/s41467-019-11674-z

Stern, Y. (2002). What is cognitive reserve? Theory and research application of the

    reserve concept. *Journal of the International Neuropsychological Society*, *8*(3),

    448–460.

Stern, Y. (2009). Cognitive reserve. *Neuropsychologia*, *47*(10), 2015–2028.

Stöhr, J., Watts, J. C., Mensinger, Z. L., Oehler, A., Grillo, S. K., DeArmond, S. J.,

    Prusiner, S. B., & Giles, K. (2012). Purified and synthetic Alzheimer's amyloid

    beta (Aβ) prions. *Proceedings of the National Academy of Sciences*, *109*(27),

    11025. https://doi.org/10.1073/pnas.1206555109

Sturchler-Pierrat, C., Abramowski, D., Duke, M., Wiederhold, K.-H., Mistl, C.,

    Rothacher, S., Ledermann, B., Bürki, K., Frey, P., Paganetti, P. A., Waridel, C.,

    Calhoun, M. E., Jucker, M., Probst, A., Staufenbiel, M., & Sommer, B. (1997).

    Two amyloid precursor protein transgenic mouse models with Alzheimer disease-

    like pathology. *Proceedings of the National Academy of Sciences*, *94*(24), 13287.

    https://doi.org/10.1073/pnas.94.24.13287

Sun, J., Xu, J., Ling, Y., Wang, F., Gong, T., Yang, C., Ye, S., Ye, K., Wei, D., Song, Z.,

    Chen, D., & Liu, J. (2019). Fecal microbiota transplantation alleviated

    Alzheimer's disease-like pathogenesis in APP/PS1 transgenic mice. *Translational*

    Psychiatry, *9*(1), 189. https://doi.org/10.1038/s41398-019-0525-3

Thaiss, C. A., Zmora, N., Levy, M., & Elinav, E. (2016). The microbiome and innate immunity. *Nature*, *535*(7610), 65–74. https://doi.org/10.1038/nature18847

Tharp, W. G., & Sarkar, I. N. (2013). Origins of amyloid-β. *BMC Genomics*, *14*(1), 290. https://doi.org/10.1186/1471-2164-14-290

Upīte, J., Kadish, I., van Groen, T., & Jansone, B. (2020). Subchronic administration of auranofin reduced amyloid-β plaque pathology in a transgenic APP(NL-G-F/NL-G-F) mouse model. *Brain Research*, *1746*, 147022. https://doi.org/10.1016/j.brainres.2020.147022

Vandersteen, A., Hubin, E., Sarroukh, R., De Baets, G., Schymkowitz, J., Rousseau, F., Subramaniam, V., Raussens, V., Wenschuh, H., Wildemann, D., & Broersen, K. (2012). A comparative analysis of the aggregation behavior of amyloid-β peptide variants. *FEBS Letters*, *586*(23), 4088–4093.

Vanderwolf, C. H. (2001). The hippocampus as an olfacto-motor mechanism: Were the classical anatomists right after all? *Behavioural Brain Research*, *127*(1), 25–47. https://doi.org/10.1016/S0166-4328(01)00354-0

Vasconcellos, L.R.C., Dutra, F.F., Siqueira, M.S., Paula-Neto, H.A., Dahan, J., Kiarely, E., Carneiro, L.A.M., Bozza, M.T., & Travassos, L.H. (2016). Protein aggregation as a cellular response to oxidative stress induced by heme and iron. *Proceedings of the National Academy of Sciences*, *113*(47), E7474–E7482.

Vogel, J., Iturria-Medina, Y., Strandberg, O., Smith, R., Evans, A., & Hansson, O. (2019). Pathological tau spreads through communicating brain regions in human Alzheimers disease. *Nature Communications*.

Vorhees, C. V., & Williams, M. T. (2006). Morris water maze: Procedures for assessing

    spatial and related forms of learning and memory. *Nature Protocols*, *1*(2), 848–

    858. PubMed. https://doi.org/10.1038/nprot.2006.116

Walker, L. C., Callahan, M. J., Bian, F., Durham, R. A., Roher, A. E., & Lipinski, W. J.

    (2002). Exogenous induction of cerebral beta-amyloidosis in betaAPP-transgenic

    mice. *Peptides*, *23*(7), 1241–1247. https://doi.org/10.1016/s0196-9781(02)00059-

    1

Walker, L. C., Lynn, D. G., & Chernoff, Y. O. (2018). A standard model of Alzheimer's

    disease? *Prion*, *12*(5–6), 261–265.

    https://doi.org/10.1080/19336896.2018.1525256

Walker, L., Schelle, J., & Jucker, M. (2016). The Prion-Like Properties of Amyloid-β

    Assemblies: Implications for Alzheimer's Disease. *Cold Spring Harbour*

    Perspectives in Medicine, *6*(7).

Watts, J. C., Condello, C., Stöhr, J., Oehler, A., Lee, J., DeArmond, S. J., Lannfelt, L.,

    Ingelsson, M., Giles, K., & Prusiner, S. B. (2014). Serial propagation of distinct

    strains of Aβ prions from Alzheimer's disease patients. *Proceedings of the*

    National Academy of Sciences, *111*(28), 10323.

    https://doi.org/10.1073/pnas.1408900111

Watts, J. C., Giles, K., Grillo, S. K., Lemus, A., DeArmond, S. J., & Prusiner, S. B.

    (2011). Bioluminescence imaging of Aβ deposition in bigenic mouse models of

    Alzheimer's disease. *Proceedings of the National Academy of Sciences*, *108*(6),

    2528–2533. https://doi.org/10.1073/pnas.1019034108

Webers, A., Heneka, M. T., & Gleeson, P. A. (2020). The role of innate immune

    responses and neuroinflammation in amyloid accumulation and progression of

Alzheimer's disease. *Immunology and Cell Biology*, *98*(1), 28–41.

https://doi.org/10.1111/imcb.12301

Webster, S. J., Bachstetter, A. D., Nelson, P. T., Schmitt, F. A., & Van Eldik, L. J.

(2014). Using mice to model Alzheimer's dementia: An overview of the clinical

disease and the preclinical behavioral changes in 10 mouse models. *Frontiers in*

Genetics, *5*, 88. https://doi.org/10.3389/fgene.2014.00088

Welander, H., Frånberg, J., Graff, C., Sundström, E., Winblad, B., & Tjernberg, L. O.

(2009). Aβ43 is more frequent than Aβ40 in amyloid plaque cores from

Alzheimer disease brains. *Journal of Neurochemistry*, *110*(2), 697–706.

https://doi.org/10.1111/j.1471-4159.2009.06170.x

Wildburger, N. C., Esparza, T. J., LeDuc, R. D., Fellers, R. T., Thomas, P. M., Cairns, N.

J., Kelleher, N. L., Bateman, R. J., & Brody, D. L. (2017). Diversity of Amyloid-

beta Proteoforms in the Alzheimer's Disease Brain. *Scientific Reports*, *7*(1), 9520.

https://doi.org/10.1038/s41598-017-10422-x

Wu, Y., Xu, X., Chen, Z., Duan, J., Hashimoto, K., Yang, L., Liu, C., & Yang, C. (2020).

Nervous system involvement after infection with COVID-19 and other

coronaviruses. *Brain, Behavior, and Immunity*, *87*, 18–22.

Xu, G., Ran, Y., Fromholt, S. E., Fu, C., Yachnis, A. T., Golde, T. E., & Borchelt, D. R.

(2015). Murine Aβ over-production produces diffuse and compact Alzheimer-type

amyloid deposits. *Acta Neuropathologica Communications*, *3*(1), 72.

https://doi.org/10.1186/s40478-015-0252-9

Yankner, B., Duffy, L., & Kirschner, D. (1990). Neurotrophic and Neurotoxic Effects of

Amyloid β Protein: Reversal by Tachykinin Neuropeptides. *Science*, *250*(4978),

279–282.

Ye, L., Fritschi, S. K., Schelle, J., Obermüller, U., Degenhardt, K., Kaeser, S. A., Eisele, Y. S., Walker, L. C., Baumann, F., Staufenbiel, M., & Jucker, M. (2015). Persistence of Aβ seeds in APP null mouse brain. *Nature Neuroscience*, *18*(11), 1559–1561. https://doi.org/10.1038/nn.4117

Ye, L., Hamaguchi, T., Fritschi, S. K., Eisele, Y. S., Obermüller, U., Jucker, M., & Walker, L. C. (2015). Progression of Seed-Induced Aβ Deposition within the Limbic Connectome. *Brain Pathology (Zurich, Switzerland)*, *25*(6), 743–752. https://doi.org/10.1111/bpa.12252

Ye, L., Rasmussen, J., Kaeser, S. A., Marzesco, A.-M., Obermüller, U., Mahler, J., Schelle, J., Odenthal, J., Krüger, C., Fritschi, S. K., Walker, L. C., Staufenbiel, M., Baumann, F., & Jucker, M. (2017). Aβ seeding potency peaks in the early stages of cerebral β-amyloidosis. *EMBO Reports*, *18*(9), 1536–1544. https://doi.org/10.15252/embr.201744067

Yrjänheikki, J., Keinänen, R., Pellikka, M., Hökfelt, T., & Koistinaho, J. (1998). Tetracyclines inhibit microglial activation and are neuroprotective in global brain ischemia. *Proceedings of the National Academy of Sciences of the United States of America*, *95 26*, 15769–15774. https://doi.org/10.1073/PNAS.95.26.15769

Zhai, Y., Yamashita, T., Nakano, Y., Sun, Z., Shang, J., Feng, T., Morihara, R., Fukui, Y., Ohta, Y., Hishikawa, N., & Abe, K. (2016). Chronic cerebral hypoperfusion accelerates Alzheimer's disease pathology with cerebrovascular remodeling in a novel mouse model. *Journal of Alzheimer's Disease*, *53*(3), 893–905.

Ziegler-Waldkirch, S., d'Errico, P., Sauer, J.-F., Erny, D., Savanthrapadian, S., Loreth, D., Katzmarski, N., Blank, T., Bartos, M., Prinz, M., & Meyer-Luehmann, M. (2018). Seed-induced Aβ deposition is modulated by microglia under

environmental enrichment in a mouse model of Alzheimer's disease. *The EMBO*

Journal, *37*(2), 167–182.

Appendix 1. Detailed Methods

A1.1. Ethics Statement. The animal study protocol was approved by the Animal Ethics Committee of the University of Lethbridge (protocol code 1810 and date of approval May 28, 2019). All Aβ seeding was done in a Biosafety Level 2+ surgical suite following approved protocols from the University of Lethbridge Biosafety Offices (protocol code BC2019-06, approved May 28, 2021).

A1.2. Experimental design. A randomized block design was used to test the factors of incubation time, genotype of mouse, and seed. The mice were grouped into cohorts based on date of birth, genotyped, and then randomly assigned to intracerebral seeding groups. The sample sizes for behaviour and immunostaining were based on previous pilot studies and during the sample size calculation where alpha = 0.05 and power = 80% and using sample sizes like previously used. Post hoc power analysis done due to the reduction in sample size between three and six months indicated that the power was sufficient to detect an existing effect with a minimum detectable effect set to 2.485 with a sample of size of 4.

A1.3. Subjects. The *App*$^{NL\text{-}G\text{-}F}$ mice (Saito et al., 2014) and their derivative littermates are a knock-in mouse model expressing three unique Aβ genes in the *App* gene without overexpressing amyloid precursor protein were previously characterized (Mehla et al., 2019) and used in this study. The mice were caged in standard housing, 2-5 mice per cage, and kept on a 12 h light/dark cycle. All testing was completed during the light cycle and done at approximately the same time each day by an experimenter blinded to the conditions. Mice were given *ad libitum* food and water. All animals were handled prior to behavioural testing. The mice were created by crossing mice from the RIKEN

institute and *C57Bl/6J* mice. The Swedish (NL) mutation increases the level of Aβ, Beyreuther/Iberian (G) increases the ratio of Aβ42 to Aβ40, and Artic mutation (F) which is in the middle of the Aβ sequence and alters binding properties of various antibodies to Aβ, as analyzed by sandwich ELISA and immunohistochemistry. The Htau mouse model (B6.Cg-*Mapt*^{tm1(EGFP)Klt} Tg(MAPT)8cPdav/J) expresses six isoforms of human tau, but does not express mouse tau (Andorfer et al., 2003) The htau mice develop age-associated tau pathology, which is most severe in the neocortex and hippocampus at nine to 15 months. Pathology includes redistribution of tau to cell bodies and dendrites, phosphorylated tau, accumulation of aggregated paired helical filaments, and thioflavin-S-positive neurofibrillary tangles.

A1.4. Genotyping. Punched mouse ear tissue was subjected to DNA extraction and PCR cycling using Millipore-Sigma's RedExtract-N-Amp Tissue PCR kit (XNAT-100RXN). PCR cycler condition: 94℃ for 3min, 94℃ for 30sec 57℃ for 45sec 72℃ for 1min x 3cycles. Stored at 4℃. Primer sequences were obtained from the Riken Institute: E16WT: 5'- ATC TCg gAA gTg AAg ATg - 3'; E16MT: 5'- ATC TCg gAA gTg AAT CTA - 3'; WT: 5'- TgT AgA TgA gAA CTT AAC - 3'; loxP: 5'- CgT ATA ATg TATgCT ATA CgA

Ag - 3'. PCR products were loaded onto agarose gel electrophoresis for visualization, with wild type band at 700bp and mutant band at 400bp.

A1.5. Aβ seed. The Aβ seeds were obtained from human HPC tissue (The National Prion Disease Pathology Disease Pathology Surveillance Center at Case Western Reserve University Medical School), assessed for purity, and stereotaxically injected. The University Hospitals Institutional Review Board (IRB) approval is for all autopsied

("discarded") human tissues and all samples are anonymized (coded) and handled in compliance with NIH policy to protect privacy. The type of seed was determined by the rate of AD progression. A control seed composed of human hippocampal tissue was also injected as a negative control (Cohen et al., 2018). All brain tissue homogenate was buffered with phosphate buffered saline (PBS) at a pH of 7.4 and kept at -80°C. The seed was 10% w/v. Prior to possession of the tissue, the tissue underwent several selection criteria steps.

1. Referral to the National Prion Disease Pathology Surveillance Centre to classify any prion disease.

2. Six or more MMSE points of decline per year.

3. Absence of autosomal dominant AD patterns

4. Absence of mutations in human prion protein.

5. Aβ and tau proteins resembling sporadic Alzheimer's Disease.

6. No other neuropathological comorbidity.

7. All results within 85% confidence interval.

Another five inclusion criteria for the classical Alzheimer's Disease tissue were used, they are as follows:

1. Clear clinical diagnosis of Alzheimer's disease

2. No autosomal dominant patterns of dementia.

3. Alzheimer's Disease based on tau and A proteins.

4. No comorbidity with other neuropathological diseases.

5. Results within 95% confidence interval.

A1.6. Stereotaxic intracerebral seeding surgery. The mice were subcutaneously injected with buprenorphine (Vetergesic; 0.05 mg/kg; concentration = 0.03 mg/ml) 30 min prior to anaesthesia induction (Isoflurane). Oxygen flow rate for induction was between 4-5 L/min and isoflurane was increased in a stepwise manner to a maximum of 5 L/min. Oxygen and anaesthesia flow rate were reduced to 0.9 L/min and 1.5-3 L/min, respectively for the duration of the surgery. After the head was shaved, the scalp was cleaned with 4% stanhexadine (Omegalab) followed by 70% isopropyl alcohol. Lidocaine (0.1 mL of 0.2%; Rafter8) was subcutaneously injected under the scalp. Bregma was used to find the stereotaxic coordinates for the medial entorhinal cortex (Allen Institute for Brain Science, 2016). The coordinates used for injection were AP: -4.48, ML: 3.00, DV: 3.44 to target the medial entorhinal cortex. A 0.5 mm diameter hole was drilled through the skull to the brain at the coordinates.

The tissue homogenate was vortexed for 30 s before being loaded into the micropipette. Each mouse received 2 µL (1 µL/hemisphere) of the A   or control tissue homogenates. Seeding was performed with a Nanoject II (Drummond Scientific Company, PA) set to slowly inject 50.6 nL. Prior to seeding, a test injection was done to ensure proper flow and the micropipette was cleaned with 70% isopropyl. The micropipette was inserted into the brain at the locations described and allowed to rest for 2 min before the first injection, with all following injections 20 seconds apart for a total of 20 injections. The micropipette stayed in place for 2 minutes after the final injection before being removed. A test injection was done again once the micropipette was removed, and the micropipette was cleaned with 70% isopropyl alcohol before the next hemisphere injection. The mice were kept on the same 12 h light/dark cycle

throughout recovery.

A1.7. Morris water task (MWT). Spatial learning and memory was tested using the MWT (Gallagher et al., 1993; Maei et al., 2009; Vorhees & Williams, 2006). The pool was 1.55 m in diameter with water temperature maintained at 21°C ± 1°C with a white, 12.5 cm submerged target platform and unobstructed distal cues surrounding the edges. At each time point following seeding, the distal cues were adjusted, and the platform was relocated to the opposing pool quadrant to create a new experimental setting. A camera fixed to the ceiling connected to a laptop with HVS Image 2100 which was used to track swim patterns of the mice. The data collected from the swim pattern was the latency, pathlength, proximity to the target, and swim speed; during the probe trial, time spent in quadrants was also collected.

The Gallagher Proximity measure was used alongside traditional measures of the MWT such as latency and pathlength, as these measurements are imprecise and a decrease in these measures does not necessarily indicate place learning (Gallagher et al., 1993). The proximity measure is the average distance from the target during the trial and is a means to identify the position of the mouse and its average search pattern with respect to the target location. Furthermore, proximity is a swim speed independent measure. But swim speed was assessed to determine if motor deficits were present. The time spent in the target quadrant during the probe trial was used to determine if the mouse learned the location of target.

A1.8. Novel Object Recognition (NOR). The NOR assessment was done in a white acrylic tub with clean mouse bedding on the bottom. Each testing time point used different object pairings to assess recognition memory over time. The objects were

cleaned with 70% isopropyl alcohol between trials.

A1.9. Filming. A camera fixed to the ceiling connected to a laptop with HVS Image 2100 was used for the MWT. For the NOR, and FC a Sony digital camera filmed the mouse behaviour from overhead. For the BB, the same digital camera filmed the mice as they crossed the beam.

A1.10. Procedure

The MWT was used to assess spatial navigation ability following seeding. As the mouse explores the pool they will come across a hidden platform. As they learn the location of the platform, there swim paths become more directed towards the target irrespective of the starting location. As a result, the time required to reach the platform and the path length swam reduce. Another result is that the average proximity the mouse is to the target also reduces. Due to mice being such poor swimmers compared to rats, using traditional measures such as latency and pathlength may not be sufficient to determine small changes in performance. Proximity however is the superior measure to assess spatial navigation in the MWT (Gallagher et al., 1993; Maei et al., 2009). The proximity is independent of swim speed and can account for smaller changes in performance.

Especially in mice where their poor ability to make sudden stops and changes in direction can increase their swim time and pathlength measures while circling the platform. The swim speed was however also measured. In chapter 2, the mice were given 4, 30 sec trials for 6 days. One the 7th day they were tested suing a no platform probe trial. In chapter 3, the mice were given 8, 30 sec trials each day for 10 days. On the 11th the mice were tested using a no platform probe trial.

Object and recognition memory were assessed using the NOR. The ratio to which a mouse investigates a pair of objects can be used to determine if the mouse was able to remember the previously investigated object and determine the other object as novel. If the mouse fails to make this distinction, it suggests impairment in object recognition memory or exploration and information gathering abilities. To test this, the mice were first habituated to an open field for 10 minutes each day for 3 days. On the fourth day two identical objects were placed in the open field and the mice were allowed to explore for 10 minutes. On the fifth day one object was replaced with a novel object and the mice were allowed to investigate for 5 minutes. Throughout the experiment the box was not cleaned as to saturate it with olfactory stimuli (Ennaceur & Delacour, 1988). The videos were filmed and scored by an experimenter blinded to seeding condition. The time the mouse spent investigating the familiar and novel object was recorded and the investigation ratio was analyzed. The investigation ratio is the amount of time investigating the novel object divided by the sum of investigating both novel and familiar objects. A value of 1 for the novel object shows the mouse spent all its time investigating the novel object, whereas a value of 0.5 shows the mouse spent equal time investigating both objects.

A1.11. Perfusions and sectioning. The mice were overdosed with an intraperitoneal injection of sodium pentobarbital and transcardially perfused with 1X phosphate buffered saline (PBS) and 4% paraformaldehyde (PFA). The brains were fixed for 24 hrs. in 4% PFA before being transferred to a solution of 30% sucrose solution for at least three days. The brains were sectioned on a frozen sliding microtome at 40 μm in a 1:6 series and stored in 1X PBS + 0.02% sodium azide solution until staining. Prior to

staining, the brain sections were mounted on super frost positively charged slides, allowed to dry up right for 30 mins and stored over night at 4°C.

A1.12. Immunohistochemistry. The slides were rinsed in 4% PFA for four minutes, washed with 1X Tris Buffer Saline (TBS), and underwent a 70% Formic Acid wash. Slides were rinsed in 1X TBS, TBS-A (1X TBS+ 0.1% Triton X), and TBS-B (TBS+ 0.1% Triton X + 2% bovine serum albumin (BSA)). The primaries used were: Anti-82E1 (Anti-β-amyloid (N), IBL,10323, mouse) 1:1000 and Anti-Iba1 (Rabbit, 019-19741, Wako) -20C 1:1000, 1ml/slide in TBS-B for 2 days at RT in a dark humid chamber, sealed in plastic wrap on the rotator at 50RPM. Following primary incubation TBS, TBS-A, and TBS-B washes were repeated. Secondaries used: Anti-mouse-alexa-488 (IgG (H+ L) goat, Abcam, ab150113) 1:1000 and anti-rabbit-alexa-594 (IgG (H+L) goat, Invitrogen, A11037) 1:1000 (1ml/slide) in TBS-B overnight in a dark humid chamber sealed in plastic wrap on the rotator at 50RPM. Secondary was washed with 1X TBS and cover slipped with Vectashield + DAPI. For ChAT and NeuN staining, sections were mounted onto slides and washed with TBS. Slides were blocked with TBS + 0.3% Triton-X + 3% goat serum (10ml – 1ml/slide) for 2h in a TBS humid chamber on a leveled rotator. Sections were inoculated with primary antibodies in TBS + 0.3% Triton-X. Slides were washed in TBS + 0.3% Triton-X before inoculated with secondary antibodies. Slides were rinsed with 1 x TBS + 0.3% Triton-X washes, TBS, and cover slipped coverslip with Vectashield (Vector Labs, H-1000).

A1.13. Imaging and pathology analysis. Full slide imaging was completed on a digital slide scanner (NanoZoomer 2.0-RS, HAMAMATSU, JAPAN) at 20X magnification. The size, number, and convexity of pathology was measured using

Ilastik (Berg et al., 2019). Convexity is a ratio of the area of the object measured and the area of its convex hull. This ratio represents a measure of how deviated the object is from a circle. In chapter 2 sections were processed from ~AP 1.7 to -4.77 and the count for each section was averaged within groups. In chapter 3, ten sections of HPC, including dorsal and ventral HPC, three sections of Substantia nigra, medial septal complex, and entorhinal cortex at 240 μm intervals were assessed. One to three brains from each seeding condition and time point were analyzed for Aβ and microglia. Percent area was calculated following methods outlined previously (Schenk et al., 1999). Briefly, the region of interest (ROI) was outlined using ImageJ and total pixel area was calculated. and the percent of the brain region occupied by the labelled pixels was calculated. ChAT+ cells were quantified through the medial septal complex using NeuroInfo Suite.

A1.14. Ilastik workflow. Prior to processing, high resolution NDPI images were exported to RGB tiff images. ImageJ was used to identify, crop, and save a standard 5000 x 5000- pixel window for each ROI – this was done to maintain consistent pixel size across all images. The pixel area for each ROI identified was measured. The pixel/μm scale was determined for each whole slide image and was used to convert pixels to $μm^2$ measurements of pathology. On average, 0.58 ± 0.01 pixels/μm was found as the ratio. The pixel and object classification workflow in Ilastik was used to segment fluorescent pathology. Ten sample images for both 82e1 and Iba1 stained sections were used to train the Ilastik classifier. Training was done to accurately identify specific fluorescent signals across each sample training image. Thresholding

was set at 0.4 for 82e1 and Iba1, with a size minimum of 10 pixels for 82e1 and 5 pixels

for Iba1.
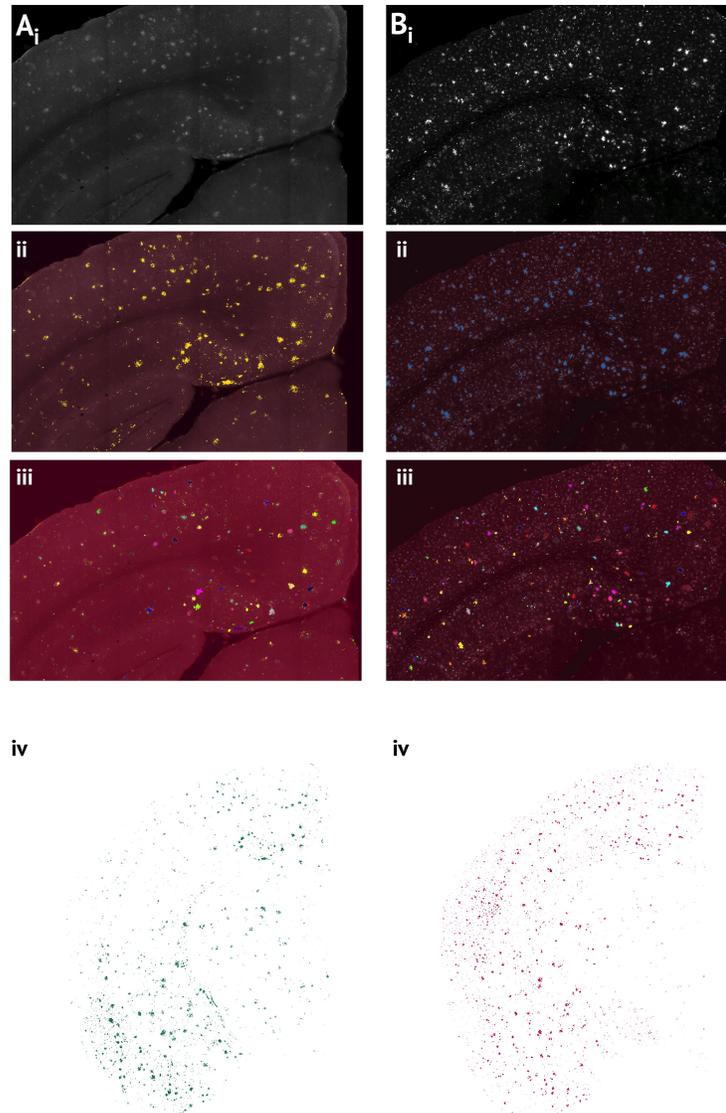
Fig. A1.1. Ilastik workflow for measuring Aβ plaque and microglia cells. A. 82e1 and **B.** Iba1 immunoreactivity training. Grey scale images (**i.**) are used to segment object from background. A prediction map of the specific plaques and microglia cells is created (**ii.**). Individual objects are created following thresholding (**iii.**). The final spatial representation for each specific object for both plaque and microglia (**iv.**).

To compare between Aβ seeds and across time, 10 sequential sections with 240 µm between

each section from the HPC, 5 from EC, 3 from RSc, 3 from MSB, and 5 from SNr, were sampled from each brain. Following processing, the sum of all pixels determined to be 82e1 or Iba1 pathology was divided by the sum of the pixel area measured for the ROI to determine the percent area covered by 82e1 and Iba1 immunoreactivity. The objects identified as Aβ plaque and microglia cells were measured, and their size and convexity (for microglia cells) were analyzed.

To assess differences in regions within seeded groups, the percent area for each sampled section was averaged and compared between regions within brains. To assess between seeds, the percent area for each region was averaged such that one percent area value for each brain was determined. These values were used to compare group differences.

A1.17. Protein analysis. Western blots were performed as by enhanced chemiluminescence as described previously by the Westaway Lab at the University of Alberta (Chishti et al., 2001; Citron et al., 1997), except ECL-Plus (Amersham Pharmacia Biotech) was used in conjunction with a "Storm" imaging system (Molecular Dynamics) for quantitative analyses. For ELISA analysis, three $App^{-/-}$ C and rpAD mice were transcardially perfused with cold 1X PBS. The entire brain was removed, cut in half, and snap-frozen. Cerebral Aβ was solubilized in a 5 m guanidine HCl, 50 mmTris-HCl, pH 8.0 buffer (Johnson-Wood et al., 1997) agitated, aliquoted, and stored at −80 °C. Thawed aliquots were diluted 10-fold or more and assessed for Aβ40 or Aβ42 using commercially available enzyme-linked immunosorbent assays (ELISAs) specific for either Aβ40 or Aβ42 and calibrated with synthetic Aβ peptides (BIOSOURCE International). The Aβ40 ELISA does not display any cross-reactivity with Aβ42 or Aβ43, and the Aβ42 ELISA does not react with either Aβ40 or Aβ43. Each brain was analyzed in duplicate or triplicate, with the average value reported for each brain. Analysis was

completed by Dr. D. Westaway's lab.

A1.18. Statistics. All statistics were done using Prism (Mac OS Version 9). Sidak's multiple comparison following when appropriate. Two-way ANOVA and mixed effect models were used to analyze behavioural and histology data.